STRUCTURAL DYNAMIC MODIFICATION USING EXPERIMENTALLY IMPROVED FINITE ELEMENT MODELS

Philip Wayne Loveday

A dissertation submitted to the Faculty of Engineering, University of the Witwatersrand, Johannesburg, in fulfilment of the requirements for the degree of Master of Science in Engineering.

Johannesburg, 1990

Declaration

I declare that this dissertation is my own, unaided work. It is being submitted for the Degree of Master of Science in Engineering in the University of the Witwatersrand, Johannesburg. It has not been submitted before for any degree or examination in any other University.

P Loveday

26th day of September 1990

Abstract

It is often desirable to predict the effect that a physical modification will have on a structure's dynamic characteristics, without the time and expense required to build a prototype.

Experimental modal models may be constructed to be more accurate than finite element models because damping and boundary conditions are difficult to model analytically. However, they do not usually contain rotational degrees of freedom which are required for beam and shell type modifications. A method for improving a finite element model's mass and stiffness matrices, using experimental results, was applied to a simple H-Frame structure. A unique mapping method was applied to expand the experimental mode shapes to the dimension of the finite element model. These mode shapes and the experimental natural frequencies were then used with the orthogonality conditions to produce an improved finite element model. The improved model reproduces the experimental natural frequencies used in the process.

The original and improved finite element models were used to predict the effect of a beam addition to the original structure. The improved model produced the better prediction when compared to experiment.

Acknowledgements

The author would like to thank the following:

- Mr. Charles P. Constancon for his technical assistance and endless enthusiasm
- Mr. Richard A. Backeberg for his supervision and encouragement during the year of 1989
- Mr. David S. Massey and Prof. E. Dokumaci for their comments on preparing this dissertation
- SDRC for allowing the use of their software for this research.

Contents

List of Figures

List of Tables

List of Symbols

MATRIX NOTATIONS

$\mathbf{E}$ Experimental mode shape matrix

$\mathbf{I}$ Unity matrix

$\mathbf{K}$ Stiffness matrix

$\mathbf{K}^{\mathrm{I}}$ Improved stiffness matrix

K Modal stiffness matrix

$\mathbf{M}$ Mass matrix

$\mathbf{M}^{\mathrm{I}}$ Improved mass matrix

M Modal mass matrix

Λ Natural frequency or spectral matrix

Φ Mass normalized mode shape matrix

Ψ Unscaled mode shape matrix

VECTOR NOTATIONS

$\mathbf{f}$ Force vector

$\mathbf{p}$ Generalized coordinate vector

$\mathbf{x}, \dot{\mathbf{x}}, \ddot{\mathbf{x}}$ Displacement, velocity, acceleration vector

ϕ Mass normalized eigenvector or mode shape vector

ϕ_a^i Generalized inverse of ϕ_a^j

SCALAR NOTATIONS

A Cross sectional area of beam

E Young's modulus of elasticity

i $(-1)^{1/2}$

I Second moment of inertia of beam cross section

G Shear modulus

K Shear coefficient

s Laplace variable

ω Natural frequency

Chapter 1

INTRODUCTION

1.1 STRUCTURAL DYNAMICS

Structural dynamics is the study of structures subjected to time-varying, or dynamic loads. These loads may cause the structure to vibrate in such a way that there is a loss in the structure's performance or a reduced fatigue life. Therefore the aim of dynamic analysis is usually to limit the structure's dynamic response to its expected operating loads.

Numerical analytical analysis and experimental modal testing are two modern methods of investigating vibration problems. The rapid development of these methods was triggered in the 1960's with the advent of the digital computer. Implementation of the finite element method and the fast Fourier transform algorithm made practical numerical and experimental vibration analysis possible.

Even though the structures are generally assumed to behave linearly, exact analytical solutions are only possible for very simple problems. For more complex problems the analytical solutions are approximated by numerical solutions such as those produced by the finite element method. Difficulties in modelling boundary conditions, damping and manufacturing defects limit the accuracy of finite element analysis. Experimental results also contain errors, but, in a well performed test, these are usually considered to be small

compared to those contained in numerical solutions. Experimental analysis of a design requires testing a prototype which can be time consuming and expensive especially if a number of designs are to be analysed to find an optimal design.

When a modification to a design or structure is proposed it is very difficult to accurately predict the effect of this modification using an experimental model of the original structure. This is because rotational degrees of freedom, which are required for moment transfers, are not usually measured. These rotational degrees of freedom are available in finite element models. It is therefore desirable to use a method which utilizes the accuracy of the experimental model and the rotational degrees of freedom of the finite element model.

The method used in this research uses the experimental results to improve the accuracy of the finite element model. This improved model is then used to predict the effects of structural modifications. The basic concept of using experimental results to produce an accurate finite element model which can be used to predict the effect of modifications is simple and has been promoted by various authors [1,2,3]. Although the method is conceptually simple, it is more difficult to apply in practice. The areas which require further consideration are the improvement of the finite element model and the modelling of the joints which are used to accomplish the modification in reality. The accuracy achieved in these steps determines the accuracy of the modification prediction.

In 1971, Berman and Flannelly [4] presented a method for improving analytical models using incomplete experimental models. The incomplete experimental models included all the analytical model degrees of freedom but only a few low frequency modes. The method uses the equations of motion and the orthogonality conditions to find an improved analytical model which is closest, in a least-squares sense, to an original analytical model. Solution of this improved model produces the experimental results.

Analytical models usually have more degrees of freedom than experimental models. It is therefore necessary to expand the experimental model to include all the degrees of freedom, including rotations, before the analytical model

can be improved. Interpolation methods have been used for this purpose [5,6]. These methods do not require the existence of an analytical model. A unique mapping method was used to expand experimental results using the results of a finite element analysis by O'Callahan [7,8].

O'Callahan *et al.* have also applied an analytical model improvement method similar to that of Berman and Flannelly which first uses the unique mapping method to expand the experimental model [9,10].

The method used here for improving the mass matrix is identical to that used by O'Callahan, however a simplified stiffness matrix improvement was formulated and applied.

1.2 OBJECTIVES

The objectives of this research are listed below in the order they were approached.

1. Apply experimental modal analysis techniques.
2. Apply finite element analysis to obtain comparative results.
3. Improve a finite element model to reproduce a set of experimental results.
4. Develop a simple model of the physical properties of a joint.
5. Use the improved finite element model and the joint properties to predict the effect of a modification and compare with experimental results.

1.3 DISSERTATION STRUCTURE

The theory relevant to this research is presented in chapters 2 and 3. Chapter 2 covers the standard topics of analytical vibration analysis, experimental modal analysis and numerical (finite element method) modal analysis. Chapter 3 presents more specialized topics which are investigated in this research. Chapter 4 presents results of experimental and finite element analyses of a H-Frame structure. These results are used in chapter 5 to produce an improved finite element model of the H-Frame structure which reproduces experimental results. The original and improved finite element models are used to predict the effects of a physical modification to the H-Frame structure. These predictions are compared to experimental results for the modified structure in chapter 6. Chapter 7 contains conclusions and recommendations for further work.

Chapter 2

REVIEW OF THEORY

Analytical vibration analysis, experimental modal analysis and numerical (finite element method) modal analysis are reviewed in this chapter. Only a brief review is presented as a number of texts and journal papers cover these topics. Although these topics are not researched here they are applied and should be understood before proceeding to the more specialized topics covered in chapter 3.

2.1 VIBRATION ANALYSIS

Linear dynamics is used to analyse the response or vibration of a linear structural system when it is subjected to a time - varying load. The responses of a linear system are related to the excitations by linear differential equations, therefore the following relations hold:

- Principle of linear superposition applies - the response to a set of excitations is equal to the sum of the responses to each excitation applied individually.
- Reciprocity - If an excitation at one point produces a response at a second point then applying the excitation at the second point would produce the identical response at the first point.

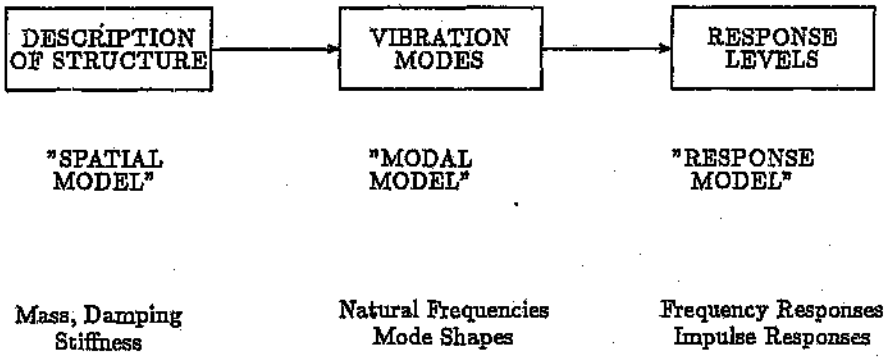

Figure 2.1: Theoretical Route to Vibration Analysis

- Frequency relations - The response to an excitation containing only certain frequencies will also contain only those frequencies.

The analytical solution of vibration problems usually follows what Ewins [11] refers to as the "theoretical route to vibration analysis." This route starts with the physical properties of the structure and proceeds to determine the response of the structure to dynamic loads. This process is illustrated in figure 2.1, taken from Ref.[11]. Experimental vibration analysis proceeds in the opposite direction, starting with measurement of the response model, followed by extraction of the modal model. It is not usually possible to form the spatial model following the experimental route. Calculating the modal model is termed analytical modal analysis or experimental modal analysis (EMA) depending on which route is taken. Analytical modal solutions which are performed numerically are termed numerical modal analysis.

Analytical modal analysis theory is described here as it forms the basis for both numerical and experimental modal analysis. There are two types of analytical models, namely continuous models and discrete-parameter models. Lumped-parameter models are a subset of discrete-parameter models.

In the analysis of continuous models, the governing differential equations and all boundary conditions must be satisfied. The exact solution of these equations is only possible for relatively simple systems and even for these simple systems the mathematical solution can become complex (see reference [12]).

In practice it is therefore generally necessary to represent a structural system as a discrete system in which the response is determined by the solution of a finite number of algebraic equations. It is therefore necessary to reduce the system to a finite number of degrees of freedom. The number of degrees of freedom is the number of independent spatial coordinates used to define the system's deflections.

Analysis of single degree of freedom systems is usually covered in detail in standard vibration texts in order to introduce the components in a vibrating system and to provide an introduction to multiple degree of freedom systems. Some civil engineering structures subjected to low frequency earthquake excitation are satisfactorily analysed by single degree of freedom models. Accurate analysis of most mechanical structural systems, however, requires the use of multiple degree of freedom models.

2.1.1 Multiple Degree of Freedom Systems

In the analysis of multiple degree of freedom systems, use is made of matrix notation to describe the physical properties (mass, stiffness and damping) of the system.

"The damping matrix is very elusive, it is hard to measure and hard to approximate analytically." [13]. For this reason it is usually neglected in the analytical analysis of lightly damped structures such as those used in this research. Neglecting damping makes the analysis far simpler and numerically more efficient. The analysis of undamped systems is presented below, followed by a brief introduction to damped system analysis.

2.1.2 Undamped Systems

The equations of motion for an undamped system are written in matrix notation as follows :

$$\mathbf{M}\ddot{\mathbf{x}} + \mathbf{K}\mathbf{x} = \mathbf{f} \tag{2.1}$$

The mass and stiffness matrices in the above equation represent the spatial (or time - domain) model of the system and are obtained by direct application of Newton's second law or by an energy method (such as the finite element method). The mass and stiffness matrices are square, symmetric and have dimension equal to the number of degrees of freedom in the model (n). $\mathbf{x}$ is the physical displacement column vector and $\mathbf{f}$ is the forcing function column vector.

The modal model comprises a set of natural frequencies and associated mode shapes often referred to as natural modes or principle modes and is the free vibration solution of equation 2.1. Solution of the homogeneous system of equations is performed by substitution of the trial solution,

$$\mathbf{x}(t) = \mathbf{x}e^{i\omega t}$$

where either the real or imaginary part of the complex exponential is assumed. This results in a linear algebraic system of equations :

$$(\mathbf{K} - \omega^2\mathbf{M})\mathbf{x} = 0 \tag{2.2}$$

To calculate the non-trivial solutions it is necessary to equate the determinant of the matrix term to zero (Cramer's Rule) i.e. $det(\mathbf{K} - \omega^2\mathbf{M}) = 0$. This produces the characteristic equation for the system which is solved to obtain n natural frequencies. These natural frequencies are then substituted into equation 2.2 to calculate the associated mode shapes. The natural frequencies and mode shapes constitute the modal model of the undamped system.

Equation 2.2 may also be written in standard eigenvalue problem form as $\mathbf{M}^{-1}\mathbf{K}\mathbf{x} = \omega^2\mathbf{x}$. Solution of this eigenvalue problem produces the n eigenvalues ω^2 (the natural frequencies squared) and eigenvectors ψ (the mode

shapes). The complete solution of the eigenproblem is usually written in matrix notation as Λ, Ψ. The eigenvalue matrix contains the eigenvalues on the diagonal and the eigenvector matrix contains the eigenvectors in columns.

It can be shown that if the system has symmetric mass and stiffness matrices, the mode shapes are orthogonal to both the mass and stiffness matrices therefore,

$$\Psi^T \mathbf{M} \Psi = M$$

$$\Psi^T \mathbf{K} \Psi = K$$

where, M and K are diagonal matrices.
The elements in M and K are referred to as the modal (or generalized) mass and stiffness for each mode. The ratio of the diagonal elements (k/m) is equal to the natural frequency of the mode squared (ω^2). Because the scaling of the mode shapes is arbitrary it is possible to scale the mode shapes so that the modal mass matrix is the unity matrix. This scaling is known as 'mass-normalisation' and the matrix of scaled mode shapes is denoted as Φ thus,

$$\Phi^T \mathbf{M} \Phi = \mathbf{I}$$

$$\Phi^T \mathbf{K} \Phi = \Lambda \tag{2.3}$$

These relations are used to decouple the equations of motion as follows :
The equations of motion for free vibration are $\mathbf{M}\ddot{\mathbf{x}} + \mathbf{K}\mathbf{x} = 0$. Premultiplication by Φ^T and insertion of $\mathbf{I} = \Phi\Phi^{-1}$ before $\ddot{\mathbf{x}}$ and $\mathbf{x}$ produces [14];

$$\Phi^T \mathbf{M} \Phi \Phi^{-1} \ddot{\mathbf{x}} + \Phi^T \mathbf{K} \Phi \Phi^{-1} \mathbf{x} = 0 \tag{2.4}$$

$$\mathbf{I} \Phi^{-1} \ddot{\mathbf{x}} + \Lambda \Phi^{-1} \mathbf{x} = 0 \tag{2.5}$$

This can be written as :

$$\mathbf{I}\ddot{\mathbf{p}} + \Lambda\mathbf{p} = \mathbf{0} \tag{2.6}$$

where, $\mathbf{p} = \Phi^{-1}\mathbf{x}$

The vector $\mathbf{p}$ is known as the system's generalized (principal or normal) coordinates as they are the set of coordinates which uncouple the equations of motion. The mode shape matrix represents the transformation from physical space to modal space and is written as $\mathbf{x} = \Phi\mathbf{p}$.

The transformation of the equations of motior from physical to modal space is used in the analysis of structural dynamic modifications and forced response analysis because solutions are numerically more efficient when the equations are uncoupled.

2.1.3 Damped Systems

The analytical models used in this research did not include damping but the curve fitting procedure used in the experimental analysis assumes either proportional or general viscous damping. For this reason only a brief description of damped system analysis is given here.

Traditionally three different forms of damping have been included in dynamic models [11]:

- Proportional Viscous Damping - damping matrix proportional to mass and stiffness matrices, i.e. $\mathbf{C} = \beta\mathbf{K} + \gamma\mathbf{M}$
  Equation of motion: $\mathbf{M}\ddot{\mathbf{x}} + \mathbf{C}\dot{\mathbf{x}} + \mathbf{K}\mathbf{x} = \mathbf{f}$
  Produces real mode shapes and complex eigenvalues.

- Structural or Hysteretic Damping - frequency dependent damping.
  Equation of motion: $\mathbf{M}\ddot{\mathbf{x}} + [\mathbf{K} + i\mathbf{H}]\mathbf{x} = \mathbf{f}$
  Produces complex mode shapes and eigenvalues.

- General Viscous Damping - damping force is assumed proportional to velocity.
  Equation of motion: $\mathbf{M}\ddot{\mathbf{x}} + \mathbf{C}\dot{\mathbf{x}} + \mathbf{K}\mathbf{x} = \mathbf{f}$

The n second - order differential equations of motion for the viscously damped system are recast into 2n first order differential equations in state space using an identity based on the mass matrix. The solution in state space produces complex mode shapes and eigenvalues.

2.2 EXPERIMENTAL MODAL ANALYSIS

Experimental modal analysis is the process of experimentally determining the free vibration natural frequencies, mode shapes and damping factors of a structure. This process is divided into three sections, namely, test setup, frequency response function measurement and parameter extraction. These three sections are discussed below.

2.2.1 Experimental Test Setup

Preparing the test involves selecting,

- suitable structure suspension,
- excitation method and
- response measurement and excitation points.

There are no standard methods for doing this and a different setup may be required for different structures.

Suspension

The suspension of the structure should be decided by considering the operating conditions of the structure and the purpose of the test.

In practice the choice of suspension is limited to two options. Either the structure can be tested in the 'freely supported' condition or it can be grounded. This 'freely supported' condition is usually achieved by suspending the structure from soft elastic bands or allowing it to lie on a soft base (foam rubber or an inflatable bag). Soft supports are selected to maintain frequencies of the structure's rigid body modes far below the structure's fundamental flexural response frequency. The soft elastic bands should be fastened to the structure at modal nodes (points that do not under go large deflections during vibration). These locations can be estimated by executing a finite element analysis of the structure. Achieving the grounded support

condition is more difficult in practice as all supports have some flexibility which is difficult to include in a finite element model. Therefore it is necessary to take precautions that the support structure is sufficiently rigid for the purposes of the test. Often the best practical solution is to test the structure supported in its operating environment. Testing in the 'freely suspended' condition produces a more general result because it is possible to determine the grounded characteristics from the free characteristics but not vice versa. This is because the free model has additional degrees of freedom.

Excitation

The structure may be excited by an impact hammer or an electrodynamic or hydraulic shaker.

The impact hammer is a simple and popular means of exciting structures. The hammer usually includes a force transducer, behind the tip, which measures the impulse transmitted to the structure. In impact testing the accelerometers remain stationary, while the location and direction of the impact changes during the test. In the time domain, an impact between two objects of infinite stiffness is represented by the Dirac delta function. Using a Fourier transform to determine the frequency content of this function produces what is known as "white noise". This is a signal which contains all frequencies (from zero to infinity) equally. In practice the contacting surfaces are not infinitely stiff. This causes the time signal to become less sharp. This signal does not contain all the high frequencies of the Dirac delta function. The frequency content is now fairly even until a certain "cut-off frequency" is exceeded after which the content of higher frequencies decreases rapidly to zero. The range of frequencies excited by an impact is therefore determined by the stiffness of the contacting surfaces. In practice hammer tips of varying stiffness are used to excite the different frequency ranges required when testing various structures. The difficulties with hammer testing involve striking the surface at the correct location normal to the surface.

A more automated test can be achieved by the use of an electrodynamic (or hydraulic) shaker. Care must be taken to ensure that the excitation force is not applied at a node of a required mode as this mode will not be excited. These shakers are connected directly to the structure with the force

transducer being as close to the structure as possible so that only the force being transmitted to the structure is measured. Thin flexible connectors called "stingers" are usually used to reduce unwanted excitations. These unwanted excitations are forces in the plane of the structure's surface and moments. The force produced by the shaker is controlled by the input signal to the shaker. One difficulty is that when a resonance of the structure is approached the excitation force level becomes very small and makes accurate measurement difficult. This problem has been addressed by the use of feedback loops which control the current (related to excitation force) supplied to the shaker's coil.

An advantage of shakers over hammers is that more than one shaker can be used simultaneously. This is termed multiple excitation testing and is used when one shaker does not supply uniform energy to all parts of the structure (due to size or damping). Multiple modes are also more easily extracted using multiple excitation testing. The disadvantages of shaker testing are that unmeasured forces are usually applied and that the accelerometers are moved around the structure during testing. The mass of the accelerometers can cause changes in the vibration of the structure when their positions are changed. This can cause inaccuracies during the parameter extraction stage.

Response Measurement

As mentioned previously, impact testing does not involve moving the accelerometers during the course of the test. It is therefore undesirable to position the accelerometers near a node of the structure, since if the accelerometer is positioned near a node the signal to noise ratio will prevent accurate measurements of that mode.

In shaker testing the locations at which responses are to be measured must be decided. This problem is equivalent to deciding the locations of impact points in an impact test. The answer to this problem lies in the fact that sufficient points must be tested so that when their deflections are plotted the mode shape is clearly recognisable. Also if the modal assurance criterion (MAC)[1] is to be used sufficient points must be tested to provide accurate results. If too few points are tested MAC values will show correlation between

[1] A popular numerical comparison of mode shapes.

mode shapes which are independent. This problem can be solved prior to the test by means of finite element model mode shapes comprising only the degrees of freedom proposed for testing. If the MAC values show correlation between these mode shapes then there are insufficient degrees of freedom to describe the mode shapes adequately.

2.2.2 Frequency Response Function Measurement

The frequency response function matrix relates the responses of a structure to the applied forces in the frequency domain. This relation is written algebraically as follows:

$$\begin{Bmatrix} X_1 \\ X_2 \\ \vdots \\ X_N \end{Bmatrix} = \begin{bmatrix} H_{11} & H_{12} & H_{13} & \cdots & H_{1N} \\ H_{21} & H_{22} & H_{23} & \cdots & H_{2N} \\ \vdots & & & & \\ H_{N1} & H_{N2} & H_{N3} & \cdots & H_{NN} \end{bmatrix} \begin{Bmatrix} F_1 \\ F_2 \\ \vdots \\ F_N \end{Bmatrix} \tag{2.7}$$

where each H is a function of frequency. This relation may be transformed to the time domain by the inverse Fourier transform. This produces the response and excitation vectors as functions of time related by the impulse response function matrix. The frequency response function matrix is symmetrical because of the structural reciprocity of linear structures. This is equivalent to the symmetry of stiffness and mass matrices (Maxwell-Betti Reciprocity theorem and the Beltrami Michele Compatibility Equations)[15]. In impact testing a single row of the frequency response function matrix is measured for each fixed accelerometer location used. In shaker testing a column of the frequency response function matrix is measured for each exciter location used.

Because the frequency response function matrix is a function of frequency it is necessary to excite the structure over the range of frequencies required in the frequency response function matrix. As was mentioned before, the frequency range excited by an impact hammer is governed by the stiffness of the hammer tip. This stiffness is varied to produce the required frequency range. Shaker testing allows more control over the frequency range. The input signal to the shaker is used to produce excitations with different characteristics.

Commonly used input signals include stepped-sinusoidal, slow sine sweep, periodic, random and transient signals. Broad band random signals are usually used with digital filters to limit the frequency range of excitation.

Obtaining frequency response functions from the signals produced by the force transducer(s) and accelerometers requires application of the principles of digital signal processing. This theory is covered in texts such as Newland[16] and only a few relevant aspects are mentioned here.

Single Excitation Response Functions

In impact testing it is possible to determine the frequency response function from the ratio of the Fourier transforms of the response and excitation as follows:

$$H(\omega) = X(\omega)/F(\omega)$$

It is however more common to determine the ratio of the average spectra of the signals. Since the signals are ergodic, frequency domain averaging will reduce the effect of noise and random disturbances.

In shaker testing with broad band random excitation the "inherent properties of random signals cause them to violate the Dirichlet condition. As a result, neither excitation nor response signals can be subjected to a valid Fourier Transform calculation and another approach must be found".[11] The alternative approach is to use the auto- and cross correlation functions of the signals. The process is illustrated in Figure 2.2.

From the figure, it is seen that two ratios for calculating $H(\omega)$ are available. Both ratios should produce the same result. The coherence (γ^2) is therefore a check on the quality of the data and the linearity of the structure.

Dual Excitation Response Functions

The principles involved in dual excitation testing can be expanded to cover multiple excitation testing with any number of excitations. Naturally the structure could be excited by each shaker sequentially but in practice it is more desirable to record the responses to all the excitations in a single excitation run and then process the data to obtain the required frequency response

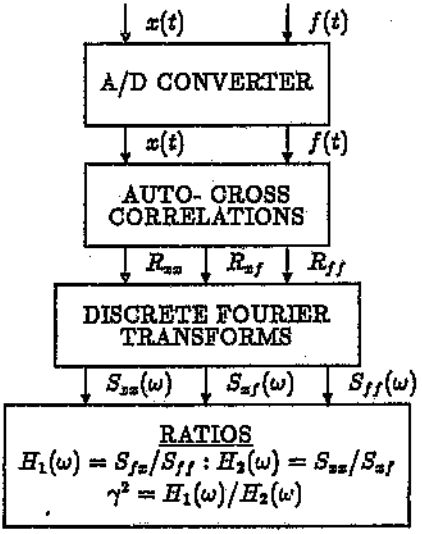

Figure 2.2: Frequency Response Function Calculation

functions. The Fourier transformed response $X(\omega)$ due to two Fourier transformed inputs $F_1(\omega), F_2(\omega)$ may be written as;

$$X(\omega) = H_{XF_1}F_1(\omega) + H_{XF_2}F_2(\omega)$$

where noise has been neglected.

According to ref.[17] the frequency response functions can be determined using auto- and cross spectra as follows (where the $_F$'s in the subscripts have been omitted):

$$S_{1X} = H_{X1}S_{11} + H_{X2}S_{12}$$

$$S_{2X} = H_{X1}S_{21} + H_{X2}S_{22}$$

These equations are then solved for H_{X_1} and H_{X_2}.

$$H_{X1} = \frac{S_{1X}S_{22} - S_{2X}S_{12}}{S_{11}S_{22} - |S_{12}|^2} = (\frac{S_{1X}}{S_{11}})\{\frac{1 - \frac{S_{2X}S_{12}}{S_{1X}S_{22}}}{1 - \gamma_{12}^2}\}$$

$$H_{X2} = \frac{S_{11}S_{2X} - S_{21}S_{1X}}{S_{11}S_{22} - |S_{12}|^2} = (\frac{S_{2X}}{S_{22}})\{\frac{1 - \frac{S_{1X}S_{21}}{S_{2X}S_{11}}}{1 - \gamma_{12}^2}\}$$

From these equations it can be seen that the coherence between the two excitations γ^2 must not be unity and should ideally be zero.

In the measurement procedure the continuous signals have been discretized and the discrete Fourier transform has been used. It is now necessary to look at some of the implications of this approximation.

Aliassing

Aliassing is a problem that occurs because a continuous signal has been sampled to produce a discretized signal. The maximum frequency that can be detected is equal to half the sampling frequency and is known as the Nyquist frequency. The existence of frequencies higher than the Nyquist

frequency distorts the frequency spectrum measured by the discrete Fourier transform analyser. The practical solution is to filter out the frequencies above the Nyquist frequency before sampling.

Leakage - Windowing

This effect results from only analysing a finite length of the signal. The finite time record is treated by the analyser as one periodic signal, or a circular function. If this record is joined into a loop there will be a discontinuity at the loop junction if the beginning and end of the time record are not equal. This causes energy to "leak" into spectral lines which are not present in the actual signal. This problem is dealt with by multiplying the time signal by a chosen function. This function is called a window. Common windows include the Hanning window, the cosine taper window and the exponential or impact window. The Hanning and cosine taper windows are zero at the beginning and end of their lengths. Therefore the resulting time signal can be looped without a discontinuity. The exponential window is used for transient vibration signals because it does not severely effect the beginning of the time record which is where most of the important information is concentrated.

2.2.3 Parameter Extraction

Parameter extraction is the process of calculating the modal model (frequencies, damping factors and mode shapes) from the measured frequency response functions or impulse response functions. This process involves curve-fitting a theoretical expression to the measured data. The form of this expression is derived from analytical modal analysis and depends on the type of damping assumed. The coefficients in the theoretical expression which best fits the measured data are the required modal properties. This curve-fitting procedure may be performed in either the frequency domain (frequency response functions) or the time domain (impulse response functions).

Analytical Expressions

The frequency response function for a system with general viscous damping may be written in series form as [18]:

$$H_{ik} = \sum_{r=1}^{N} \frac{A_{ik}^{r}}{j\omega + \zeta_r\omega_r - j\omega_r\sqrt{1-\zeta_r^2}} + \frac{A_{ik}^{r*}}{j\omega + \zeta_r\omega_r + j\omega_r\sqrt{1-\zeta_r^2}}$$

This may be written in terms of the Laplace variable s,

$$H_{ik} = \sum_{r=1}^{N} \frac{A_{ik}^{r}}{(s - s_r)} + \frac{A_{ik}^{r*}}{(s - s_r^*)} = \sum_{r=1}^{2N} \frac{A_{ik}^{r}}{(s - s_r)}$$

where,

$$s_r = -\zeta_r\omega_r \pm j\omega_r\sqrt{1-\zeta_r^2}$$

and $A_{ik}^{r} = \frac{\psi_i^r \psi_k^r}{a_r}$ is the residue at pole s_r. The equivalent impulse response function is :

$$h_{ik}(t) = \sum_{r=1}^{N} A_{ik}^{r} e^{s_r t} + A_{ik}^{r*} e^{s_r^* t} = \sum_{r=1}^{2N} A_{ik}^{r} e^{s_r t}$$

Extraction Techniques

Extraction techniques can be divided into single degree of freedom (SDOF) and multiple degree of freedom (MDOF) techniques. SDOF techniques consider only one mode at a time. It is assumed that each peak in a frequency response function is due to only one mode. This requires that the peaks be sufficiently well separated so that the effect of the surrounding modes is negligible. SDOF techniques including "second degree polynomial curve fitting', "peak-amplitude", "circle fitting" and the "inverse method" are covered in references [11,18]. According to reference [19] SDOF techniques "may provide meaningful results in some elementary cases", but MDOF techniques are recommended especially when closely spaced modes are present. MDOF techniques include the "complex exponential", "polyreference", "direct parameter" and "Ibrahim Time Domain" methods. In this research the polyreference technique was used. The Polyreference technique was developed for use with multiple exciter testing and uses all the impulse response functions from all the exciter and response locations in a global least squares manner simultaneously. Because it uses multiple exciters it is a good method for extracting close and repeated modes. The method assumes either proportional

or general viscous damping and extracts the natural frequencies and damping values in the time domain. The inverse Fourier transform can be used to obtain the required impulse response functions from averaged frequency response functions.

Extraction of the residues or mode shapes can be performed in either the time or frequency domain. [20]. The mathematical details of the technique are complicated and have been described in a number of papers. A complete theoretical explanation of the method is given in t e excellent paper by Deblauwe et al. [20]. It should be noted that if only one excitation is used the Polyreference technique reduces to the Complex Exponential technique which is described by Ewins [11].

2.3 NUMERICAL MODAL ANALYSIS

This section deals with numerical modal analysis using the displacement based finite element method. Exact, closed form, analytical solutions can most easily be found for simple problems which have uniform material properties (homogeneous), simple geometry and boundary conditions. When an analytical solution can not be found it is necessary to calculate a numerical solution which approximates the analytical solution. The finite element method is the most popular method of numerical modal analysis.

2.3.1 The Finite Element Method

The finite element method (FEM) is a versatile numerical technique which has found numerous applications in engineering analysis. Several general purpose computer codes are available and the theory has been presented in a number of books and journal papers. The purpose of this section is therefore not to give a detailed description of the finite element method but rather to present a brief introduction to some of the more important principles involved.

The finite element method can be divided into three sections [21]:

1. The formulation of the problem in variational or weighted residual form,
2. The finite element discretization of this formulation,
3. The effective solution of the resulting finite element equations.

2.3.2 Formulation of the Problem

Formulation of the problem requires consideration of the types of materials used, selection of the physical laws which will dominate the response of the system and representation of the constraints imposed on the system. All of these factors have to be modelled mathematically by systems of equations.

There are two methods of generating the governing equilibrium equations namely, direct methods and variational methods.

The direct methods use equilibrium, constitutive and compatibility requirements to generate a system of partial differential equations in the state variables.

The variational approach "can be regarded as the basis of the finite element method".[21] In the variational approach a suitable functional is minimized or maximized to produce the required system of governing equations. In elasticity problems, for example, the functional is chosen to be the total mechanical potential energy of the system and is minimized to obtain these governing equations. This method has the advantage that scalar quantities (such as energy) are used as opposed to vectors. Another advantage is that the natural boundary conditions are implicitly contained in the functional so only the essential boundary conditions need to be considered in the solution of the problem.

Additional constraints are included in the variational formulation by either the Lagrange multiplier method or the penalty method. The Lagrange multiplier method includes the constraint in the functional with an additional variable (the Lagrange multiplier). The system of equilibrium equations produced are then the system for the unconstrained problem plus an additional equation which contains the constraint. In the penalty method the constraint is again added to the functional but a constant of large magnitude is used instead of the multiplier. This results in a modified system of equilibrium equations of the same dimension as the unconstrained system of equations.

2.3.3 Finite Element Discretization

The finite element method requires that the continuum to be analysed be divided into a finite number of elements. These elements are connected at selected points called nodes. The physical quantities to be determined within an element are related to the physical quantities at the nodes by shape or interpolation functions. It is therefore only necessary to solve for the physical quantities at the nodes. The process of relating the interior of an element to

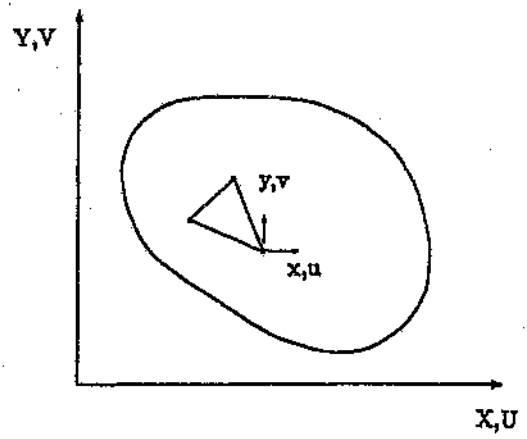

Figure 2.3: Two Dimensional Finite Element

its nodal conditions is presented below.

Derivation of Finite Element Equations

Because we are interested in dynamic analysis it is necessary to characterize the structures mass as well as stiffness. Damping characteristics are very difficult to estimate analytically and are usually determined experimentally so they are neglected here.

The following mathematical description of the displacement-based finite element method is similar to that presented by Bathe. [21] Figure 2.3 shows a two dimensional element in a plane continuum.

The first step is to relate the displacements within the finite element to the displacements at its nodes. This is done by the "displacement interpolation matrix" H.

$$u(x, y, z) = H(x, y, z)\hat{U}$$

where, u are the displacements in local coordinates, $\hat{U}$ is a vector of the

global displacement coordinates at all the node points. The vectors u and $\hat{U}$ include the coordinates v and V shown in the figure.

The strains within the elements are now related to the nodal displacements by the "strain-displacement matrix" B which is obtained by appropriately differentiating and combining rows of matrix H.

$$\epsilon(x, y, z) = \mathrm{B}(x, y, z)\hat{\mathrm{U}}$$

Next the stresses in the element are related to the strains by the "elasticity matrix" C.

$$\tau = \mathrm{C}\epsilon + \tau^I$$

where, τ^I are the initial stresses.

It is now possible to use the principle of virtual work to generate the system of equilibrium equations for the structure corresponding to the nodal point displacements. It has been shown that the principle of virtual work is equivalent to minimizing the total potential of the system. For virtual displacements the internal virtual work must be equal to the external virtual work:

$$\int_V \bar{\epsilon}^T \tau dV = \int_V \bar{\mathrm{U}}^T f^B dV + \int_S \bar{\mathrm{U}}^{S^T} f^S dS + \sum_i \bar{\mathrm{U}}^{i^T} F^i$$

where,

$\bar{\epsilon}$ represents the virtual strains,

$\bar{\mathrm{U}}$ represents the virtual displacements,

f^B, f^S are the element body and surface forces,

F^i represents a concentrated force.

Substituting the displacement, strain and stress relationships established earlier and summing the integrals for all the elements produces the following equation:

$$\begin{aligned}\bar{\hat{\mathbf{U}}}^T\left[\sum_m \int_{V^{(m)}} \mathbf{B}^{(m)T}\mathbf{C}^{(m)}\mathbf{B}^{(m)}dV^{(m)}\right]\hat{\mathbf{U}} \;=\; & \bar{\hat{\mathbf{U}}}^T\left\{\sum_m \int_{V^{(m)}} \mathbf{H}^{(m)T} f^{B(m)}dV^{(m)}\right\} \\ & +\bar{\hat{\mathbf{U}}}^T\left\{\sum_m \int_{S^{(m)}} \mathbf{H}^{S(m)T} f^{S(m)}dS^{(m)}\right\} \\ & -\bar{\hat{\mathbf{U}}}^T\left\{\sum_m \int_{V^{(m)}} \mathbf{B}^{(m)T} f^{I(m)}dV^{(m)}\right\} \\ & +\bar{\hat{\mathbf{U}}}^T F\end{aligned}$$

The integrals in this equation are evaluated over the element volumes and surfaces and can be calculated using the local element coordinate systems.

The inertial forces have been included in the formulation[2] as body forces. It is now possible to write the equilibrium equations in standard form (as was used in section 2.1) as follows:

$$\mathbf{M}\ddot{\mathbf{U}} + \mathbf{K}\mathbf{U} = \mathbf{R} \tag{2.8}$$

where,

$$\mathbf{K} = \sum_m \int_{V^{(m)}} \mathbf{B}^{(m)T}\mathbf{C}^{(m)}\mathbf{B}^{(m)}dV^{(m)}$$

$$\mathbf{M} = \sum_m \int_{V^{(m)}} \rho^{(m)}\mathbf{H}^{(m)T}\mathbf{H}^{(m)}dV^{(m)}$$

$$\mathbf{R} = \mathbf{R}_B + \mathbf{R}_S - \mathbf{R}_I + \mathbf{R}_C$$

$$\mathbf{R}_B = \sum_m \int_{V^{(m)}} \mathbf{H}^{(m)T}\left[f^{B(m)} - \rho^{(m)}\mathbf{H}^{(m)}\ddot{U}\right]dV^{(m)}$$

$$\mathbf{R}_S = \sum_m \int_{S^{(m)}} \mathbf{H}^{S(m)T} f^{S(m)}dS^{(m)}$$

[2] A Lagrangian approach may be employed to evaluate the inertia terms directly.

$$\mathbf{R}_I = \sum_m \int_{V^{(m)}} \mathbf{B}^{(m)^T} \tau^{I(m)} dV^{(m)}$$

$$\mathbf{R}_O = \mathbf{F}$$

The displacement-based finite element method is a modern variation of the Ritz analysis technique. Classical Ritz analysis is difficult to apply in practice because it requires the selection of suitable Ritz basis vectors which span the entire region of interest and satisfy the essential boundary conditions. The solution obtained is a linear combination of these vectors. To model large energy gradients a large number of basis vectors might be needed. The finite element method overcomes this problem by defining basis vectors over each element in the form of shape functions or interpolation polynomials. These displacement functions must be compatible at the element boundaries. The problem of selecting functions which can adequately describe the solution to the problem is overcome by increasing the number of elements (increasing the number of functions) in regions of high energy gradients. Polynomial functions are usually used because they are easy to differentiate. Another advantage is that where as the classical Ritz approach produces full matrices the use of node numbering schemes can significantly reduce the bandwidth of the resulting finite element matrices.

Timoshenko Beam Element

In this research, beam elements which approximate Timoshenko beam theory were used. It is therefore necessary to briefly explain the formulation of this particular element.

Linear, independent shape functions are used to represent the deflections and rotations within a linear beam element. In the two noded Timoshenko beam element, a static approximation is used to relate the rotations to the deflections. Dawe [22] used this approximation to formulate a three noded beam element which had 5th and 4th order polynomial shape functions for the deflections and rotations respectively. Using the equations of Timoshenko beam theory, he obtained the following relation, between rotations and deflections, by ignoring rotary inertia within the element.

$$EId^2\theta/dx^2 = GKA(\theta - dw/dx)$$

"This procedure means that the rotary inertia term is ignored in the moment equilibrium equation within the element but the effect of rotary inertia will nevertheless be included in 'lumped' form at the nodes."[22] By including the second derivative of deflection as a degree of freedom it is possible to obtain a 5th order polynomial shape function for the deflection of a two noded beam element.[23] If only deflections and rotations are included it is possible to use cubic and quadratic polynomial shape functions for deflection and rotation in a two noded beam element. This element will obviously outperform the simple linear beam element. The mass and stiffness matrices for a two noded Timoshenko beam element with only in plane transverse deflections and rotations are given in Appendix A.

2.3.4 Solution of Equilibrium Equations

The equilibrium equations represent the "spatial model" of the structural system. To obtain the "modal model" from the "spatial model" it is necessary to solve what is essentially an eigenvalue problem. The resulting eigenvalues are the squared natural frequencies of the undamped system and the eigenvectors are the corresponding mode shapes.

The eigenvalue problem,

$$\mathbf{K}\psi = \lambda \mathbf{M}\psi \tag{2.9}$$

is known as the generalized eigenvalue problem. Premultiplication by $\mathbf{M}^{-1}$ would result in the standard eigenvalue problem $\mathbf{A}\psi = \lambda\psi$ where $\mathbf{A} = \mathbf{M}^{-1}\mathbf{K}$. The disadvantage of this approach is that even though M and K are symmetric, the matrix A is generally nonsymmetric.[24] This loss of symmetry results in a loss of storage economy and computational efficiency. The generalized eigenvalue problem can be transformed to standard form retaining symmetry by use of either Cholesky factorization or spectral decomposition of the mass matrix. This is an efficient method only if the mass matrix is diagonal, otherwise the sparseness of the finite element matrices is destroyed and the computational advantage is lost. Therefore in practice a transformation to standard form is not always used and techniques for the

solution of the standard eigenvalue problem have been adapted to solve the generalized eigenvalue problem directly.

"It is important to realize that all solution methods must be iterative in nature, because, basically, solving the eigenvalue problem $\mathbf{K}\psi = \lambda\mathbf{M}\psi$ is equivalent to calculating the roots of the polynomial $p(\lambda)$, which has order equal to the order of K and M."[25] Available methods may be grouped into the following categories: transformation methods, vector iteration methods, polynomial iteration techniques, Sturm sequence methods and combinations of these methods. Only transformation methods, vector iteration methods and the subspace iteration method, (which is a combination of transformation and vector iterative methods), are described below.

Transformation Methods

Transformation methods use the orthogonality conditions,

$$\Phi^T\mathbf{K}\Phi = \Lambda \tag{2.10}$$

$$\Phi^T\mathbf{M}\Phi = \mathbf{I} \tag{2.11}$$

The matrix Φ which satisfies equations 2.10 and 2.11 is unique and contains the mass-normalized eigenvectors as its columns. In the transformation methods, successive pre- and postmultiplication of M and K by $\mathbf{P}_k^T$ and $\mathbf{P}_k$ is performed until the resulting matrices $\mathbf{M}_{k+1}$ and $\mathbf{K}_{k+1}$ are diagonal.

$$\mathbf{M}_{k+1} = \mathbf{P}_k^T\mathbf{M}_k\mathbf{P}_k$$

$$\mathbf{K}_{k+1} = \mathbf{P}_k^T\mathbf{K}_k\mathbf{P}_k$$

When $\mathbf{M}_{k+1}$ and $\mathbf{K}_{k+1}$ are diagonal the eigenvalues are found to be the ratios of the elements on the diagonals i.e. $\lambda_i = k_{ii}/m_{ii}$ where k_{ii} is the ith diagonal element of the matrix $\mathbf{K}_{k+1}$. The eigenvectors are found to be $\psi_i = \mathbf{P}_1\mathbf{P}_2\ldots\mathbf{P}_{k+1}m_{ii}^{-1/2}$.

Two transformation methods are considered, firstly the Generalized Jacobi method which uses both orthogonality conditions and secondly the Householder-QR-Inverse Iteration method which requires a transformation of the generalized eigenvalue problem to standard form.

Generalized Jacobi Method

In the Jacobi method for standard eigenvalue problems the matrix $\mathbf{P}_k$ is a simple rotation matrix which was used to make the elements of K zero. In the generalized Jacobi method the matrices $\mathbf{P}_k$ are chosen to simultaneously make the elements (i,j) and (j,i) in the matrices $\mathbf{K}_{k+1}$ and $\mathbf{M}_{k+1}$ zero.

The matrix $\mathbf{P}_k$ is written as follows:

$$\mathbf{P}_k = \begin{bmatrix} 1 & & & & & & & \\ & 1 & & & & & & \\ & & \ddots & & & & & \\ & & & 1 & & \alpha & & \\ & & & & \ddots & & & \\ & & & & & 1 & & \\ & & & & & & \ddots & \\ & & & \gamma & & & 1 & \\ & & & & & & & \ddots \\ & & & & & & & & 1 \end{bmatrix} \tag{2.12}$$

The constants α and γ are calculated from the elements in the (i,i),(i,j) and (j,j) locations of the $\mathbf{M}_k$ and $\mathbf{K}_k$ matrices.

It must be noted that off-diagonal elements which have been zeroed will become non-zero in subsequent transformations. Therefore when implementing this method it is necessary to decide on a value that the off-diagonal elements must not exceed and transformations must be performed to zero the largest off-diagonal elements until none exceed the preset value.

The Generalized Jacobi method is efficient for doing small eigenvalue problems but is inefficient if the problem is large and only a few eigenpairs are required. This is because the method calculates all the eigenvalues and cor-

responding eigenvectors simultaneously. The Householder-QR-inverse iteration method provides an alternative which does not have to solve for all the eigenpairs.

Householder-QR-Inverse Iteration

This method requires that the generalized eigenvalue problem first be transformed to standard form $\mathbf{A}\psi = \lambda\psi$ which may in some cases lead to ill-conditioned problems. Once the problem is in standard form the matrix A is reduced to tridiagonal form using Householder transformations. QR iteration is then applied to the tridiagonal matrix to produce the eigenvalues to high precision. Inverse iteration with shifting (see next section) is then applied to produce the eigenvectors of the matrix A of the standard eigenvalue problem. These eigenvectors must then be transformed again to produce the eigenvectors of the generalized eigenvalue problem.

Vector Iteration Methods

Power Iteration

The power iteration method is also referred to as forward iteration. In this method the generalized eigenvalue problem,

$$\mathbf{K}\psi = \lambda\mathbf{M}\psi \tag{2.13}$$

is written in the form

$$\mathbf{M}\mathbf{V}_{S+1} = \mathbf{K}\mathbf{U}_S$$

The procedure starts by assuming an initial vector $\mathbf{U}_1$ and solving for the vector $\mathbf{V}_{S+1}$. The next estimate of $\mathbf{U}$ ($\mathbf{U}_{S+1}$) is found by scaling $\mathbf{V}_{S+1}$ (setting largest element to unity or mass normalization) producing $\mathbf{U}_{S+1} = 1/\lambda\mathbf{V}_{S+1}$. The procedure converges to the highest frequency mode. For an n DOF system $\mathbf{U}_{S+1} \to \psi_n$ and $\lambda \to \omega_n^2$ as $S \to \infty$.

Inverse Iteration

Inverse iteration is very similar to power iteration. The formulation is modified so that convergence occurs towards the fundamental mode as this is usually the mode of greatest interest. In this formulation equation 2.13 is written as

$$\mathbf{K}\mathbf{V}_{s+1} = \mathbf{M}\mathbf{U}_s$$

Again a vector $\mathbf{U}_1$ is chosen as an initial estimate. $\mathbf{V}_{s+1}$ is calculated from $\mathbf{V}_{s+1} = \mathbf{K}^{-1}\mathbf{M}\mathbf{U}_s$ where the matrix $\mathbf{K}^{-1}\mathbf{M}$ is often referred to as the "dynamical matrix". $\mathbf{V}_{s+1}$ is then scaled by the factor λ, to produce $\mathbf{U}_{s+1}$ ($\mathbf{U}_{s+1} = \lambda\mathbf{V}_{s+1}$). In this method $\mathbf{U}_{s+1} \rightarrow \psi_1$ and $\lambda \rightarrow \omega_1^2$ as $S \rightarrow \infty$. According to Craig, "the most effective procedure for hand computation of a few eigenvalues and eigenvectors of a small (n less than 10) system is the method of inverse iteration." [26]

For the power method and inverse iteration method to converge to the highest and lowest frequency modes it is required that the initial vector ($\mathbf{U}_1$) is not orthogonal to the mode being calculated. Because this vector is not known at the outset it is not possible to guarantee that this condition is satisfied but the full unit vector has proven to be a good starting vector [21]. The rate of convergence of these methods can be improved by evaluating the scaling factor λ by the Rayleigh quotient method. For an example of this see reference [26].

Extensions to Power and Inverse Iteration

The iteration methods presented so far can only determine the lowest and highest frequency modes. It is therefore necessary to extend these methods to calculate the other modes. One method of producing convergence to a different mode is by applying an eigenvalue shift. This shift is performed by writing equation 2.13 as follows,

$$(\mathbf{K} - \mu\mathbf{M})\psi = (\lambda - \mu)\mathbf{M}\psi$$

The eigenvalues of this problem are now $(\lambda - \mu)$ which are the original eigenvalues λ shifted by the constant amount μ. Therefore the eigenvalues of the original problem are obtained by adding the value of the shift (μ) to

the calculated eigenvalues. The eigenvectors remain unchanged by the shift. The shift can be used with inverse iteration to find the eigenvalue (and corresponding eigenvector) closest to the shift value and is essential when the stiffness matrix is positive semidefinite. This occurs when rigid-body modes are possible and the stiffness matrix cannot be inverted. A shift is also essential in the power method when the mass matrix is diagonal with some zero diagonal elements.

Matrix deflation and Gram-Schmidt orthogonalization may also be used with power and inverse iteration to determine all the eigenvalues and eigenvectors. The matrix deflation technique operates on the eigenvalue problem after it has been transformed to standard form $\mathbf{K}\psi = \lambda\psi$. The calculated mode λ, ψ is removed from the matrix $\mathbf{K}$ resulting in matrix $\mathbf{K_1}$ which has dimension $n-1$. This is done by using the orthogonal matrix $\mathbf{P} = [\psi, \mathbf{p_2}, \mathbf{p_3}, \ldots, \mathbf{p_n}]$ where each $\mathbf{p}$ is orthogonal to ψ so that,

$$\mathbf{P}^T\mathbf{K}\mathbf{P} = \begin{bmatrix} \lambda & 0 \\ 0 & \mathbf{K_1} \end{bmatrix}$$

The matrix $\mathbf{K_1}$ has all the eigenvalues of $\mathbf{K}$ except λ and the eigenvectors of $\mathbf{P}^T\mathbf{K}\mathbf{P}$ $(\bar{\psi})$ are related to the eigenvectors of $\mathbf{K}$ by $\psi = \mathbf{P}\bar{\psi}$. This process could be repeated to find all the eigenpairs but the accumulation of errors make this method inaccurate.

A more practical procedure is to ensure that the starting iteration vector is M-orthogonal to the eigenvectors previously calculated. This is a sufficient condition to ensure that the solution will not converge to a known eigenpair. Assume that the eigenvector ψ_1 has been calculated and an arbitrary starting vector $\mathbf{U_1}$ has been selected for calculating a second eigenvector. It is necessary to ensure that the starting vector $\mathbf{U_1}$ is M-orthogonal to the calculated eigenvector ψ_1. It is possible to split $\mathbf{U_1}$ into a component $\bar{\mathbf{U}}_1$ which is M-orthogonal to ψ_1 and a multiple of ψ_1.

$$\mathbf{U_1} = \bar{\mathbf{U}}_1 + \alpha\psi_1$$

If α can be evaluated the above expression can be used to calculate $\bar{\mathbf{U}}_1$ which is a suitable starting iteration vector.

Premultiplying the terms in the above expression by $\psi_1^T \mathbf{M}$ results in $\psi_1^T \mathbf{M} \mathbf{U}_1 = 0 + \alpha \psi_1^T \mathbf{M} \psi_1$ because $\bar{\mathbf{U}}_1$ is M-orthogonal to ψ_1. Therefore α and hence $\bar{\mathbf{U}}_1$ can be calculated. This procedure can easily be extended to deal with more than one calculated eigenvector and is known as Gram-Schmidt orthogonalization.

Up till now it has been assumed that the eigenvalues are all unique. If a system has two repeated eigenvalues the power and inverse iteration methods will converge to a linear combination of the two independent eigenvectors corresponding to the repeated eigenvalues. It is not possible to determine the individual eigenvectors from this linear combination. A method of using two vectors simultaneously is presented in reference [24]. This is a particular case of simultaneous vector iteration which is mentioned as an introduction to the subspace iteration method in the next section.

Subspace Iteration

Simultaneous inverse vector iteration may be performed with p vectors as follows:

$$\mathbf{K} \bar{\mathbf{X}}_{k+1} = \mathbf{M} \mathbf{X}_k$$

$$\mathbf{X}_{k+1} = \bar{\mathbf{X}}_{k+1} \mathbf{R}_{k+1}$$

where $\mathbf{X}_k$ is a matrix containing p vectors and $\mathbf{R}_{k+1}$ is an upper-triangular matrix chosen so that $\mathbf{X}_{k+1}$ is M-orthogonal. This orthogonalization of the p vectors is required so that they do not all converge to the least-dominant eigenvector.

In this method "each iteration vector is forced to converge to a different eigenvector by orthogonalizing the ith iteration vector to the (i-1) iteration vectors that have been orthogonalized without allowing a more effective linear combination of the vectors to take place." [21]

In the subspace iteration method the subspace spanned by the iteration vectors converges to the subspace spanned by the required eigenvectors. Once

the subspace has converged the eigenvectors are obtained in one more iteration. The steps in the subspace iteration method are as follows:

$$K\bar{X}_{k+1} = MX_k$$

Calculate Reduced Matrices;

$$K_{k+1} = \bar{X}_{k+1}^T K \bar{X}_{k+1}$$

$$M_{k+1} = \bar{X}_{k+1}^T M \bar{X}_{k+1}$$

Solve The Reduced Eigenvalue Problem;

$$K_{k+1} Q_{k+1} = M_{k+1} Q_{k+1} \Lambda_{k+1}$$

The M-Orthogonality Condition is:

$$Q_{k+1}^T M_{k+1} Q_{k+1} = I$$

$$\rightarrow Q_{k+1}^T \bar{X}_{k+1}^T M \bar{X}_{k+1} Q_{k+1} = I$$

Therefore the next M-orthogonal iteration vector is:

$$X_{k+1} = \bar{X}_{k+1} Q_{k+1}$$

The generalized Jacobi method has proved to be suitable for solving the reduced eigenvalue problem because of the properties of the matrices involved. (M_{k+1} and K_{k+1} tend towards diagonal form as the method converges).

It is thus seen that the subspace iteration method is a combination of a vector iteration method and a transformation method. This method is suited to large eigenvalue problems where only a few of the eigenpairs are required.

Chapter 3

REVIEW OF RESEARCH TOPICS

This chapter reviews four areas of structural dynamics which are being researched at present. The first three topics, namely Structural Dynamic Modification, Experimental Model Expansion and Analytical Model Improvement were applied in this research while joint characterization was investigated briefly.

3.1 STRUCTURAL DYNAMIC MODIFICATION

Some authors [11,27,28] have used the term "modification" to describe a physical change to a structure when the response of the change (or addition) is considered only at the connection points. The internal characteristics of the change are therefore not included in the analysis. Analyses in which the internal degrees of freedom of the change are considered are then referred to as component mode synthesis or substructure coupling. In this dissertation however, "structural modification" is used to describe a more general selection of methods. These methods may be grouped into five categories as follows:

1. Sensitivity and Perturbation Techniques
2. Structural Modifications using Frequency Response Functions (SMURF)
3. Eigenvalue Modification
4. Eigenvalue Solution (Component Mode Synthesis)
5. Finite Element Model Predictions on a Verified Model

(Methods 2 to 5 are as listed in reference [28])

Only a brief description of the first four methods and their application is given below as only the fifth method has been applied in this research and will be described in detail in this and the following two sections.

It is important to note that any one of the five methods may be most suitable for a particular application. It is therefore necessary to have some understanding of each method and it's particular limitations in order to choose the most suitable method for a specific engineering problem.

3.1.1. Sensitivity and Perturbation Techniques

Although Lancaster [29] used perturbation theory, to add small amounts of damping to conservative systems in 1960, these techniques are more commonly used to predict the effects of mass changes to linear systems.

The sensitivity of a structure's eigenvalues and eigenvectors to changes in the structure's mass and stiffness matrices can be used in a Taylor series expansion, along with the anticipated changes, to calculate approximate eigenvalues and eigenvectors of the modified structure.

Fox and Kapoor [30] derived expressions relating the change in eigenvalues and eigenvectors to changes in the mass and stiffness matrix elements. These first derivatives of the eigenvalues and eigenvectors with respect to design changes may be used in a first order Taylor series expansion as follows:

$$\lambda_i^* \simeq \lambda_i + \Delta\delta^T \nabla\lambda_i$$

$$X_i^* \simeq X_i + [\nabla X_i]\Delta\delta$$

where,

λ_i, X_i are the ith original eigenvalue and eigenvector

λ_i^*, X_i^* are the approximations to the modified system's ith eigenvalue and eigenvector

$\Delta\delta$ is a vector of r design variables for the structure $(\Delta\delta_1, \Delta\delta_2, \ldots, \Delta\delta_r)$

$\nabla\lambda_i$ represents the vector $(\frac{\partial\lambda_i}{\partial\delta_1}, \frac{\partial\lambda_i}{\partial\delta_2}, \ldots, \frac{\partial\lambda_i}{\partial\delta_r})$

∇X_i represents the vector $(\frac{\partial X_i}{\partial\delta_1}, \frac{\partial X_i}{\partial\delta_2}, \ldots, \frac{\partial X_i}{\partial\delta_r})$

In the calculation of $\nabla\lambda_i$ and ∇X_i it is necessary to calculate the derivatives of the elements in the mass and stiffness matrices with respect to each of the design variables.

The use of a first order Taylor series expansion limits the accuracy of the approximation and places a limit on the size of modification which can be analysed. It is however, possible to calculate the terms required for higher order Taylor series expansions [31] but this becomes mathematically complex and obviously also requires greater computational effort.

Rizai and Bernard [32] used a simpler method for calculating the second derivative of the eigenvalues used in the Taylor series expansion. Their approach was to evaluate the mass and stiffness matrices (using a finite element preprocessor) for two different variations in the design parameter as well as the original mass and stiffness matrices. This gives three sets of mass and stiffness matrices for each design parameter. Simple finite difference techniques were then applied in order to evaluate the first and second derivatives of the mass and stiffness matrices with respect to each of the design parameters. These derivatives were then used to calculate first and second derivatives of the eigenvalues with respect to the design parameters.

One of the advantages of the sensitivity method is that it can not only be used to predict the effect of modifications to a structure but can also be used

to find optimal modifications to produce a required change in the dynamic characteristics of a structure. This optimization has been achieved by the implementation of a penalty function [33] and by the use of a least squares solution [31].

In the first case a penalty function is chosen which increases as any eigenvalue approaches an undesirable value or when the magnitude of the modifications increases. This penalty function is then minimized to give a solution for the optimal modifications. Because the first order Taylor expansion used is unlikely to correctly predict the effects of the modifications it is necessary to resolve the eigenproblem for the modified structure. If the results of this solution are found to be unsatisfactory it is necessary to repeat the optimization process using the modified model as the starting point. Therefore this process can be applied iteratively until convergence is obtained.

In the second case a modification to produce specific eigenvalues was presented. Two situations were treated:

- calculating the values of mass additions required given the locations,
- calculating the best locations and magnitudes of the mass additions required given the number of masses.

The least squares solutions of the systems of equations were found by the use of the Moore-Penrose generalized inverse technique (referred to as the pseudo-inverse) which is described in Appendix B. Both of these optimal modification prediction techniques can make use of experimental modal models or analytical models.

Apart from the limitation that sensitivity analysis can only be used efficiently when the required modifications are small there is also the limitation that the techniques only consider modifications at degrees of freedom present in the original model therefore modifications which have additional important degrees of freedom cannot be analysed with these techniques.

3.1.2 Structural Modifications using Frequency Response Functions

As its name implies this technique operates directly on the frequency response model and therefore the use of curve fitting techniques to extract a modal model is not required. The output from the modification process is in the form of a modified set of frequency response functions. It may then be necessary to curve fit these modified frequency response functions because a modal model gives more insight into the dynamics of the modified structure.

Only a brief outline of the process of modifying the frequency response functions and a list of the processes advantages and disadvantages are presented here. In reference [34] the simplified case of calculating the modified frequency response functions of a structure when one point is grounded was demonstrated. This example is easy to follow and is "seen to be a special case of enforcing a general multi-point rigid constraint equation" [34]. The case of calculating the constrained response of the system when subject to a general set of constraint equations is mentioned briefly followed by examples of its use and comparisons of results with modifications performed on the modal model. The application of these general constraint equations is described in slightly greater depth in reference [35]. Here it is explained that the constrained response can be found by "finding a stationary point of the constrained quadratic functional."[35] This functional represents the total "energy" of the system and therefore this analysis closely resembles the analysis of a constrained static finite element analysis which is delt with by Bathe [21]. The Lagrange multiplier method is employed to transform the functional and constraint equations into a system of linear equations which are solved to give the required modified frequency response functions. (The steps in the Lagrange multiplier method are detailed in reference [21] for the analagous problem mentioned previously.)

This approach allows connectors such as springs, dashpots and masses (with known frequency response functions) to be "tied" between points on a component or between two different components. The following applications are therefore possible: [34,35]

- connecting a point to ground
- connecting a point to ground through a spring, mass, damper
- connecting two points together
- connecting two points together through a spring, mass, damper
- attaching a spring, mass, damper to a point (tuned absorber)
- substructuring
- mass cancellation
- response ratios

Structural Modification using Frequency Response Functions has been applied to various problems and the results compared to those obtained by performing the modifications on modal models [34,36,37]. The following list of advantages and disadvantages was compiled from these references.
ADVANTAGES:

- No curve fitting required in the modification procedure.
- The effect of modes outside the frequency range of interest (including rigid body modes) is included directly.
- No linearized modal model is used therefore some degree of nonlinearity may be accommodated.
- The effects of damping are included.

DISADVANTAGES:

- Subject to computational errors due to poor quality experimental data.
- Requires driving point and cross frequency response functions at the connection points which may be inaccessible.
- Inconsistencies in frequency response functions multiply quickly as more constraints are applied therefore it should only be used for a limited number of simple constraints.

- Results are in the form of modified frequency response functions which may need to be curve fitted to gain insight from the modal model.
- Curve fitting of modified frequency response functions can be difficult if amplitude errors have been generated. (See reference [36].)

Because of these limitations it is generally recommended that the technique be used only for troubleshooting applications, where a simple modification must be analysed quickly, and for validation of experimentally derived modal models.

3.1.3 Eigenvalue Modification

The eigenvalue modification process was pioneered by Weissenburger [38] who predicted the effects of the addition of lumped masses and discrete springs on continuous linear systems. Weissenburger used the original systems eigensolution to transform the problem (including modification) from physical space to modal space.

This produces a new eigenvalue problem in modal space. If a number of modifications are included, this new eigenvalue problem requires computational work equal to that of solving the original problem. This situation is avoided by performing only a single modification at a time requiring "the solution of a one dimensional eigenvalue problem in order to determine the modified modal properties" [39]. The modified modal properties are then used for successive modifications.

When the full set of eigenvalues is available the method produces exact results but good approximations can be achieved with incomplete original modal models (as is more common in practice).

Weissenburger's method was extended by Pomazal and Snyder [40] who applied the method to discrete systems with linear viscous damping (in the original system and the modification). To include the effects of general viscous damping the second order equations of motion were transformed into twice as many first order equations by the use of an identity based on the mass matrix.

At this stage the method did not allow a modification which required additional degrees of freedom. This shortcoming was addressed by Hallquist and Snyder [41,42] who extended the method to permit the synthesis of two discrete viscously damped systems and the connection of viscously damped multi-dimensional continuous systems with discrete springs or viscous dampers.

Because this method uses the modal model of a system to perform modifications it may be applied directly to experimental modal models. Unfortunately the lack of rotational degrees of freedom in experimental models makes it difficult to model real engineering modifications such as the addition of beams and plates.

This problem has been investigated by O'Callahan [43] who used modal expansion techniques (see section 3.2) to provide the rotational degrees of freedom necessary for addition of three dimensional beam elements.

A more practical approach was suggested in reference [44] where the experimental model is used only to validate the finite element model. The finite element modes (which include rotational degrees of freedom) are then used in the modification process.

In 1976 Arora [45] stated the following limitation of the process, "Since the procedure permits only one modification or tie, it must be applied successively if multiple ties or modifications are required. Therefore, it is sometimes more efficient to seek a direct solution to the problem of connected systems. Also, when mass on a damped system is modified, the procedure uses three successive modifications."

Recent research has resulted in a method known as "Simultaneous Structural Dynamics Modification (S^2DM)".[39] In this method all the required modifications are transformed into modal space simultaneously. The resulting eigenvalue problem then has dimension equal to the number of modes (of the original model) included in the modification process. The size of the eigenvalue problem is therefore independent of the number of modifications being made. This method has been shown to become more efficient than successive modifications when the number of modifications required increases.

In conclusion the eigenvalue modification method is a powerful and efficient structural modification tool. In practice the modifications should be applied simultaneously to a set of experimentally validated finite element modes which span the frequency range required. The validation of the finite element model might require altering the original finite element model to produce better correlation with the experimental results. Methods for improving finite element models using experimental models are presented in section 3.3.

3.1.4 Eigenvalue Solution (Component Mode Synthesis)

Component Mode Synthesis is an energy method for calculating the dynamic characteristics of a structural system from the dynamic characteristics of its components. It was originally developed to reduce the size of the eigenvalue problem which has to be solved for a large structural system and is also useful when the components of the system are being designed and analysed by different groups working separately.

This method is regarded as a Rayleigh-Ritz analysis in which the difficulty of selecting appropriate Ritz basis vectors is overcome by using what Hurty called "component modes."

The complete system's modes are then synthesized from modes of the individual components (or subsystems) by the application of constraint equations. These constraint equations are derived from the conditions of force equilibrium and displacement compatibility at the junctions between the components.

Hurty [46] initially developed the method to analyse undamped structural systems whose components are connected with redundant connections and later extended the method to include linear viscous damping [47]. Hurty used the following three component modes (displacement functions) to define independent categories of generalized co-ordinates for each component :

- Rigid-body modes - describe rigid body displacements without deformation. There can be a maximum of six or less if external constraints are present.
- Constraint modes - a set of displacements defined by applying a static unit displacement to each redundant constraint in turn with all the other constraints fixed. Number of modes equal to number of redundant constraints.
- Fixed-interface normal modes - normal modes of vibration of the component with all constraints fixed.

The system equations of motion were obtained by applying Lagrange's equation (Hamilton's principle) with the constraint equations being included by the method of Lagrange multipliers.

Bamford introduced a fourth type of component mode :

- Attachment modes - for a restrained system this is the static deflection of the component when a unit force is exerted on one coordinate of the component with the remaining attachment coordinates free. "For an unrestrained structure, attachment modes are defined by the response of a uniformly accelerating system ."[48]

When attachment modes are used free-interface and hybrid-interface modes are employed. These modes are normal modes of the component when none or part of the interface coordinates are restrained when the eigenvalue problem is solved for the component.

Craig and Bampton [49] simplified the treatment of rigid-body modes by showing that it is unnecessary to separate the rigid-body modes from the redundant constraint modes.

Interface loading was investigated [50] by the use of a static reduction (Guyan reduction [51]) to constrain the motions of a component's interior coordinates to move only with respect to the motion of the interface coordinates.

Klosterman [52] studied the combination of experimental modal models and finite element models by the component mode synthesis method. Both unconstrained and constrained modal models were considered.

The effect of using a truncated set of component modes has been investigated and reduced by the method of Kuhar and Stahle. [53]

Numerous combinations of the types of component modes have been formulated and applied to various problems. A recent, detailed review of component-mode synthesis and SMURF (which is referred to as "Frequency Domain Component-Mode Synthesis Methods") has been presented by Craig. [54]

3.1.5 Finite Element Model Predictions

It is a fairly simple matter to add a physical modification to the finite element model of a structural system. The solution of this modified finite element model then produces the dynamic characteristics of the modified structural system. For this method to produce accurate results it is obviously necessary that the original finite element model be accurate and for the modification to the model to be representative of the actual modification to the physical structural system.

The accuracy of the original finite model is usually determined by comparison with the results of an experimental modal analysis. This is a vital step in the procedure as it is extremely difficult to model boundary conditions, joint mechanics and damping accurately when using the finite element method. Also in some cases the exact properties of materials might be unavailable. Although there are errors in experimentally determined modal models (measurement errors, nonlinearities, etc.) these models are usually judged to be more accurate than the finite element models. If the correlation between the two models is unsatisfactory it is necessary to improve (update, correct, optimize) the finite element model until agreement with the experimental model is obtained.

The modification to be applied to the original structural system must be modelled correctly. If the modifications are simple, such as discrete mass, stiffness or damping additions, modelling is simple. But if the modification involves the attachment of beams, plates or indeed another complete structural system, it is to be expected that the properties of the connections or joints between the original model and the modification will effect the dynamics of the new structural system. Therefore, in these cases it is necessary to include the characteristics of the joints as well as the modifications in the modified finite element model.

The procedure involved in this method has been outlined in the literature, [1,2,3] and is summarized in Fig. 3.1 This figure illustrates the procedure when a prescribed modification is made as well as when an optimal modification has to be determined to produce a required change in the dynamic characteristics of the system.

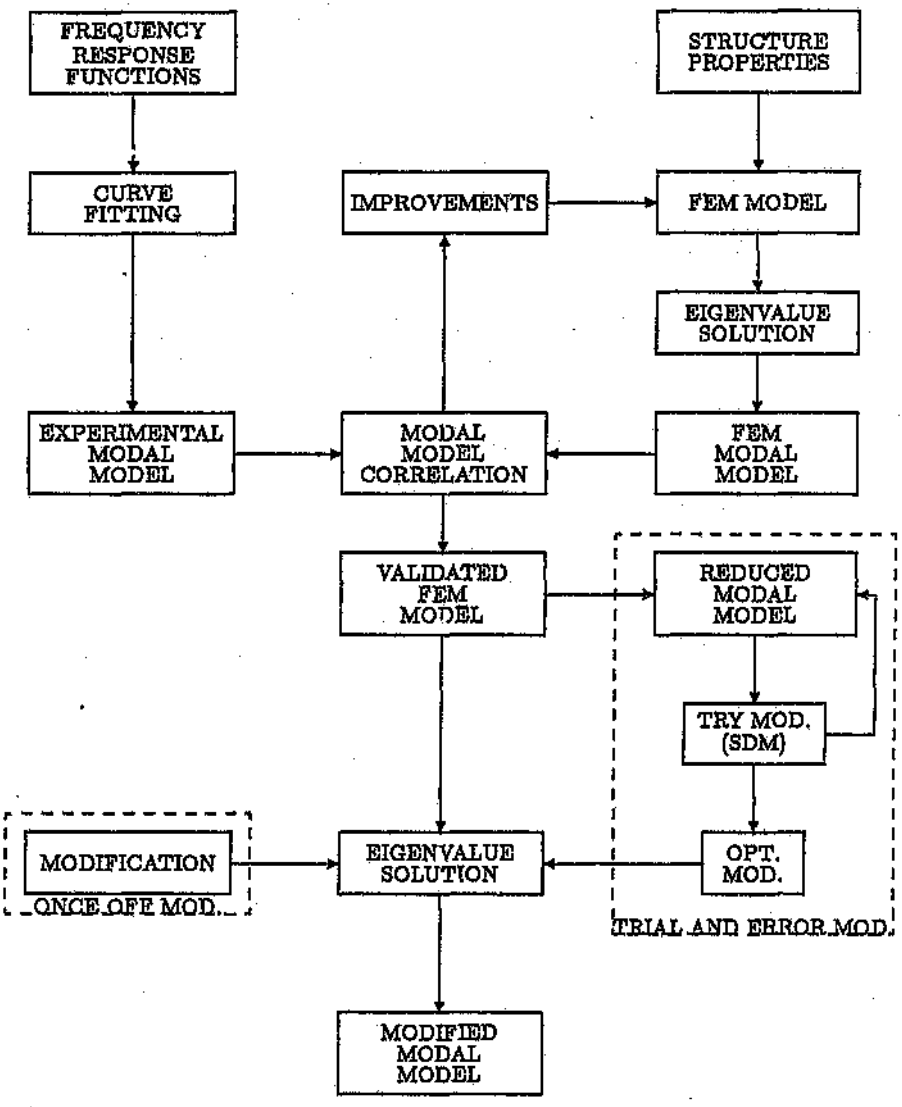

Figure 3.1: Finite Element Model Prediction Procedure

Although this procedure is conceptually simple, two areas require further description. Firstly, the method of improving the finite element model requires careful consideration if the resulting model is to represent the structure accurately. This is the topic of sections 3.2 and 3.3. Secondly, modifications in which joint properties are important must naturally incorporate these joint properties. Modelling of joints is discussed in section 3.4.

This method is sometimes not considered a "Structural Modification Method" but it cannot be ignored as "in many cases it is the best engineering solution." [28]

3.2 EXPERIMENTAL MODEL EXPANSION

In practice, angular motion is difficult to measure, so experimental modal models do not usually include rotational degrees of freedom (RDOF). In addition to this, parts of a structure may be inaccessible, thus translational degrees of freedom (TDOF) at these points will also be absent from the experimental modal model. If the experimental model is to be used for predicting structural dynamic modifications which include moment transfers (beams and plate additions) it is necessary that the RDOFs at the attachment points are present in the modal model. Also if the model is to be used to improve a finite element model, using the orthogonality conditions (see section 3.3), it is necessary to have all the finite element model degrees of freedom in the modal model. Essentially three methods of approximating the unmeasured degrees of freedom have been used:

1. Polynomial Interpolation methods
2. Analytical reduction/expansion methods
3. Unique mapping methods

3.2.1 Polynomial Interpolation Methods

As the name implies these methods fit polynomial displacement functions to measured degrees of freedom. These polynomials are then used directly to approximate translational displacements at unmeasured degrees of freedom. Rotational degrees of freedom are determined by differentiating the displacement polynomials and evaluating the rotations at the required degrees of freedom. These methods use each mode shape independently of the others and do not require a finite element model of the structure.

Lagrange polynomials and cubic spline functions have been used to approximate rotational degrees of freedom at connection points in modal models [5]. Finite element shape functions have also been used to approximate unmeasured rotations from measured translations [6].

The limitations of these methods are that they require good experimental measurements and require the measurement points to be fairly close together so that the polynomial can approximate the deformation accurately.

3.2.2 Analytical Reduction/Expansion Methods

Methods to reduce the number of degrees of freedom in finite element models were developed primarily to reduce the amount of computation required for the analysis of complex structures. The simplest and most widely used method is Guyan reduction [51]. This is a static reduction technique and can produce inaccurate results if insufficient degrees of freedom are used to represent a structure's mass distribution.

The dynamic reduction/expansion method requires more computation but does produce an exact transformation at the natural frequencies of the structure. The mathematical formulation of this method is presented below:

The equations of motion for a full undamped model can be partitioned to separate the DOFs (x_t) included in the reduced (test) model and the omitted DOFs (x_o).

$$\begin{bmatrix} M_{tt} & M_{to} \\ M_{ot} & M_{oo} \end{bmatrix} \begin{Bmatrix} \ddot{x}_t \\ \ddot{x}_o \end{Bmatrix} + \begin{bmatrix} K_{tt} & K_{to} \\ K_{ot} & K_{oo} \end{bmatrix} \begin{Bmatrix} x_t \\ x_o \end{Bmatrix} = \begin{Bmatrix} f_t \\ f_o \end{Bmatrix} \tag{3.1}$$

The free vibration eigenvalue problem for the ith mode is then written as:

$$-\omega_i^2 \begin{bmatrix} M_{tt} & M_{to} \\ M_{ot} & M_{oo} \end{bmatrix} \begin{Bmatrix} \psi_{it} \\ \psi_{io} \end{Bmatrix} + \begin{bmatrix} K_{tt} & K_{to} \\ K_{ot} & K_{oo} \end{bmatrix} \begin{Bmatrix} \psi_{it} \\ \psi_{io} \end{Bmatrix} = \begin{Bmatrix} 0 \\ 0 \end{Bmatrix} \tag{3.2}$$

where the ith eigenvector has been partitioned into reduced and omitted DOFs. The second equation can now be used to relate the omitted part of the mode shape to the reduced part as follows:

$$\psi_{io} = [-\omega_i^2 M_{oo} + K_{oo}]^{-1} [\omega_i^2 M_{ot} - K_{ot}] \psi_{it} \tag{3.3}$$

or $\psi_{io} = t_i \psi_{it}$

It is now possible to relate the complete mode shape to the reduced part by defining the partitioned transformation matrix $T_i = [I : t_i]^T$ so that,

$$\psi_i = T_i \psi_{it}$$

This transformation matrix includes the natural frequency of the ith mode and is therefore only correct at the frequency ω_i. It is therefore necessary to calculate a transformation matrix for each mode shape which is to be expanded.

It should be noted that if the natural frequency ω_i is set equal to zero the frequency-independent Guyan reduction/expansion is obtained.

The effectiveness of the dynamic reduction/expansion scheme depends on the accuracy of the original finite element mass and stiffness matrices. "A severe drawback of this approach is that errors in the analytical representation are introduced into the test modes by the expansion technique, thus contamination of the test data can lead to errors during system identification." [55]

3.2.3 Unique Mapping Methods

The Unique Mapping Method provides an alternative scheme for using a finite element model to expand experimental mode shapes. A unique transformation matrix which maps the reduced (partitioned) finite element mode shapes, containing only the test DOFs, to the full finite element mode shapes, is calculated. This unique mapping is then applied to the experimental mode shapes to produce the expanded experimental mode shapes (containing the full set of analytical degrees of freedom).

This method has been applied by O'Callahan et al. [7,8] and Kammer [55] and is described mathematically below:

The mode shapes (eigenvectors) represent a transformation from physical to modal space.

$$\mathbf{X}_n = \mathbf{\Phi}_n \mathbf{p} \tag{3.4}$$

$\mathbf{p}$ is a column vector of the generalized coordinates in modal space, with dimension equal to the number of modes included in mode shape matrix $\mathbf{U}_n$. Therefore, considering the reduced model (the same number of modes but fewer degrees of freedom), the equivalent expression,

$$\mathbf{X}_a = \mathbf{\Phi}_a \mathbf{p} \tag{3.5}$$

contains the same vector $\mathbf{p}$. Because the mode shape matrices are not square it is necessary to use the Moore-Penrose generalized inverse (see Appendix B) to formulate a mapping between the full and reduced displacement vectors. Writing equation 3.5 as $\mathbf{p} = \mathbf{\Phi}_a^{\dagger}\mathbf{X}_a$, where $\mathbf{\Phi}_a^{\dagger}$ is the Moore-Penrose generalized inverse of $\mathbf{\Phi}_a$, and substituting it into equation 3.4 gives:

$$\mathbf{X}_n = \mathbf{\Phi}_n \mathbf{\Phi}_a^{\dagger} \mathbf{X}_a \tag{3.6}$$

In the case where the number of DOFs exceed the number of modes available the unique generalized inverse is, $\mathbf{\Phi}_a^{\dagger} = (\mathbf{\Phi}_a^T \mathbf{\Phi}_a)^{-1} \mathbf{\Phi}_a^T$. Therefore,

$$\mathbf{X}_n = \mathbf{T}_a \mathbf{X}_a \tag{3.7}$$

where $\mathbf{T}_a$ is the transformation matrix required to map the experimental mode shapes to the expanded set of experimental mode shapes as follows:

$$\mathbf{E}_n = \mathbf{T}_a \mathbf{E}_a \tag{3.8}$$

3.3 ANALYTICAL MODEL IMPROVEMENT

In vibration analysis the finite element method (see section 2.3) is widely used to create analytical models of structures. However, in linear structural dynamics, inaccurate modelling of geometry, boundary conditions, joints and damping may severely limit the accuracy of these finite element models. Therefore, before a finite element model can be used for the purpose of predicting the effects of design changes or modifications to an existing structure, it is necessary to validate the model. This validation is usually obtained by comparison of the results with the results of an experimental modal analysis of the structure or a prototype. Although inaccuracies such as approximations in curve fitting techniques, masses of accelerometers, unintentional excitations and modal truncation are present in experimental models, these models are usually assumed to be accurate. If the correlation between the two models is found to be unsatisfactory for the purpose intended, it is necessary to improve the finite element model to produce natural frequencies and mode shapes which agree better with the experimental results. The improvement process will therefore use the original finite element model and the experimental model to produce an improved finite element model.

Model improvement is often referred to as "analytical model optimization" and has been separated into two classes [56]:

1. methods using sensitivity analysis techniques.
2. methods based essentially upon equations of motion and upon orthogonality conditions.

The sensitivity analysis techniques will be discussed briefly, followed by a more detailed description of a particular method using orthogonality conditions.

3.3.1 Sensitivity Analysis Techniques

The problem of improving a finite element model using sensitivities is very similar to using sensitivities to predict the optimal structural modifications

required to cause prescribed changes in the structure's vibration characteristics. (see section 3.1.1)

Again a first or second order Taylor series expansion is used to relate "design changes", sensitivities to changes and the magnitude of the required changes in vibration characteristics. In this case the "design changes" include changes in design variables or direct changes to elements of the mass and stiffness matrices. Therefore, a greater flexibility in choice of variables is available compared to the structural dynamic modification situation.

Usually variables describing areas of modelling uncertainty are chosen so that the improvement process can produce a model which is a better physical representation of the structure. This requires the analyst to exercise a certain amount of judgement.

The system of equations established using the Taylor series expansion are then solved by an optimization technique such as least squares analysis.

Because of the nature of the sensitivity analysis method it will only produce accurate results when only small changes are required to improve the model. If larger changes are required it may be necessary to use the method iteratively (resolving the predicted model and then improving again). Large changes may also become unrealistic (see reference [57]) and it may be necessary to apply constraints to the magnitudes of the changes. [58]

These methods in general are inefficient use of the computational effort required to calculate all the sensitivities required. They have however, been applied to the problem of identifying material properties of solid rocket fuel by Kammer et al. [59], where the number of variables was not excessive.

These methods usually only use the experimental frequencies in the improvement process, therefore the information contained in the experimental mode shapes is usually wasted.

3.3.2 Methods Based on the Equations of Motion and Orthogonality Conditions

Berman and Flannely [4] presented a method which utilizes orthogonality conditions, the equations of motion and the theory of the Moore-Penrose generalized inverse to improve the finite element model's mass and stiffness matrices using an incomplete experimental modal model. Because the experimental model is incomplete, (fewer modes than degrees of freedom) there are an infinite number of analytical models which can reproduce the incomplete model. In this method the generalized inverse technique is used to determine the analytical model, which is the closest (in a least squares sense) to the original analytical model, and reproduces the incomplete experimental modal results. It is therefore important that the original model does represent the physical structure adequately. This method also includes the use of weighting factors which allow the analyst to limit the regions of the matrices to be modified (regions of modelling uncertainty).

A similar method which uses Lagrange multipliers instead of the generalized inverse has also been researched [60,61]. In this approach a function containing the corrections to the spatial matrices is minimized. The advantage over the generalized inverse technique however, is not clear.

It has been shown that techniques using the equations of motion, orthogonality conditions and the generalized inverse can be used to identify the regions of a structure which have been modelled inaccurately [62,63]. Therefore corrections to the analytical model made by this method should occur where they are necessary and not simply at random.

In recent years O'Callahan *et al.* [9,10] have researched this method and included a model expansion process for expanding the experimental mode shapes to the number of degrees of freedom used in the finite element model. The method described below uses the same mass matrix improvement as O'Callahan but the formulation of the stiffness matrix improvement has been simplified. This section is taken from reference [64].

Mass Matrix Improvement

The mass matrix improvement process involves modifying the original mass matrix so that it satisfies the condition.

$$\mathbf{E}_n^T \mathbf{M}_n^I \mathbf{E}_n = \mathbf{I} \tag{3.9}$$

Since the improved mass matrix, $\mathbf{M}_n^I$, is not unique, the solution closest to the original mass matrix must be found. To achieve this, the change in the mass matrix is minimized via the generalized inverse procedure. Also weighting factors may be included so that certain elements in the matrix are more sensitive to changes than others. The procedure is outlined below [9]. It is required to minimize the Euclidean norm of:

$$\mathbf{M}_W = \mathbf{N}_A^{-1}(\mathbf{M}_N^I - \mathbf{M}_n)\mathbf{N}_A^{-1}. \tag{3.10}$$

This implies the minimization of the change to the original mass matrix with the weighting factors ($\mathbf{N}_A^{-1}$) applied. In order to make the sensitivity of the mass matrix elements proportional to their magnitudes, $\mathbf{N}_A^{-1}$ is chosen such that $\mathbf{N}_A^2 = \mathbf{M}_n$. Substituting $\mathbf{M}_N^I$ from equation 3.10 into equation 3.9 gives:

$$\mathbf{E}_n^T(\mathbf{N}_A\mathbf{M}_W\mathbf{N}_A + \mathbf{M}_n)\mathbf{E}_n = \mathbf{I} \tag{3.11}$$

which can be rewritten in the form of equation (B.1) in Appendix B.

$$\mathbf{E}_n^T\mathbf{N}_A\mathbf{M}_W\mathbf{N}_A\mathbf{E}_N = \mathbf{I} - \mathbf{E}_n^T\mathbf{M}_n\mathbf{E}_n \tag{3.12}$$

From Appendix B the minimum-norm least-squares solution to the above equation is,

$$\mathbf{M}_W = (\mathbf{E}_n^T\mathbf{N}_A)^\dagger(\mathbf{I} - \mathbf{E}_n^T\mathbf{M}_n\mathbf{E}_n)(\mathbf{N}_A\mathbf{E}_n)^\dagger \tag{3.13}$$

Construction of the generalized inverses and application of equation 3.10 gives the expression for the improved mass matrix.

$$\begin{aligned}\mathbf{M}_n^I \;=\; & \mathbf{M}_n + \mathbf{M}_n\mathbf{E}_n(\mathbf{E}_n^T\mathbf{M}_n\mathbf{E}_n)^{-1} \\ & (\mathbf{I} - \mathbf{E}_n^T\mathbf{M}_n\mathbf{E}_n)(\mathbf{E}_n^T\mathbf{M}_n\mathbf{E}_n)^{-1}\mathbf{E}_n^T\mathbf{M}_n\end{aligned} \tag{3.14}$$

Stiffness Matrix Improvement

The formulation of the stiffness matrix improvement used in this paper differs from that used by O'Callahan [9], but produces very similar results. The improved stiffness matrix must satisfy the equations of motion $\mathbf{K}_n^I \mathbf{E}_n = \omega^2 \mathbf{M}_n^I \mathbf{E}_n$. Pre-multiplication by E_n^T gives:

$$\mathbf{E}_n^T \mathbf{K}_n^I \mathbf{E}_n = \omega^2 \tag{3.15}$$

Following the same procedure as was used for the mass matrix improvement but using $\mathbf{N}_\lambda^2 = \mathbf{M}_n^I$ gives the following result:

$$\begin{aligned} \mathbf{K}_n^I &= \mathbf{K}_n + \mathbf{M}_n^I \mathbf{E}_n \\ &\quad (\omega^2 - \mathbf{E}_n^T \mathbf{K}_n \mathbf{E}_n) \mathbf{E}_n^T \mathbf{M}_n^I \end{aligned} \tag{3.16}$$

3.4 JOINT CHARACTERIZATION

When a modification to a structure involves the attachment of a mass, spring or component to the original structure by a flexible connection it may be necessary to include the characteristics of the connection or joint in the modification prediction process. The presence of the joint may add mass, stiffness and damping to the modified structure. Apart from the effect the linear stiffness of the joint has on the natural frequencies of the system, the joint may be a significant source of damping and nonlinearity. According to reference [65] joints are the dominant sources of damping and nonlinearities in aircraft and space structures but play a lesser role in earth - based structures.

There are a number of variables which effect the dynamic characteristics of a joint and may make joints which appear to be identical respond differently to dynamic loads. These include :

- Manufacturing tolerance
- Contacting surface finish and lubrication
- Alignment during assembly
- Static load level
- Local thermal deformations

"Therefore the detailed calculation of joint characteristics from first principles is unproductive." [65] It is thus necessary to experimentally determine the characteristics of the joint and to adapt a relatively simple analytical model to obtain agreement with the experimental model.

Various methods of joint characterization have been documented. These methods vary in complexity depending on the application, the most complex being the "Force-State Mapping Procedure" developed by Crawley which has been used to identify strong nonlinearities in joints of space structures using extensive testing [65,66]. A method which has been termed the "residual force technique" has also been used for solving nonlinear analytical models of joints [67]. In this method the linear characteristics are grouped on the

left hand side of the equation of motion and the nonlinear characteristics appear on the right hand side. The terms on the right hand side may be considered as "residual forces" which represent nonlinear corrections to the linear structure to produce the nonlinear response. Modal analysis of the linear terms then reduces the size of the integration problem which has to be solved to determine the joint's transient response. This technique was not validated experimentally.

It is also possible to avoid some of the complexities of nonlinear analysis by using an approximate linear model. This approach allows the construction of a simpler model but the model can only be used near the conditions (amplitude and frequency of vibration) at which it was constructed. This approach was adopted by Foelsche *et al.* [68] for the design of joint-dominated space structures. Analytical nonlinear models were approximated by equivalent linear models which have constant parameters over the expected range of transient response. The method used was referred to as amplitude averaging. The resulting linear models can then be used in design optimization, subject to verification by time integration.

Linear stiffness and damping properties of joints have also been extracted from experimental modal results. This has been done by using an inverse substructure coupling technique to uncouple the components of a structure [69,70,71]. The joint properties are found iteratively by determining the parameters which separate the original modal model into uncoupled models.

Chapter 4

MODAL ANALYSIS OF ORIGINAL STRUCTURE

4.1 THE TEST STRUCTURE

A small, mild steel structure resembling an H was chosen for this research. The structure was machined from a single piece of steel and had mortice joints at the ends to facilitate future modification. The structure was very lightly damped and could therefore be analysed accurately by the finite element method with damping neglected. The structure's dimensions are shown in figure 4.1.

4.2 FINITE ELEMENT MODAL ANALYSIS

4.2.1 The Finite Element Model

The test structure is simple to model using the finite element method if certain assumptions are made. The first of these assumptions is that damping is negligible. For this structure this simplification is valid but is not applicable

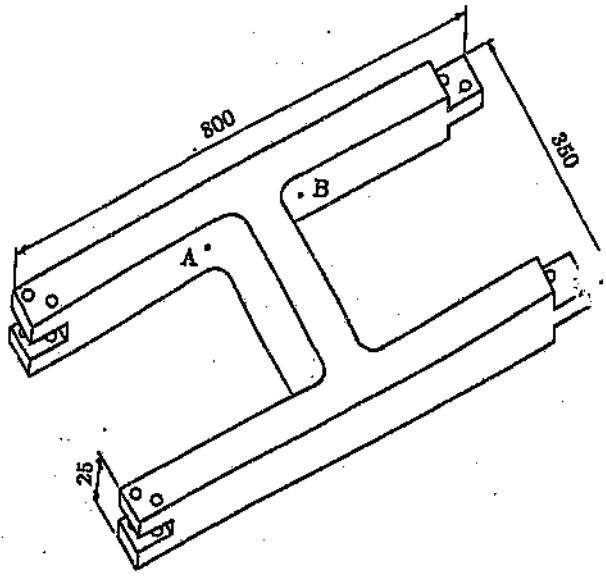

Figure 4.1: Test Structure Dimensions

to all structures. Next the fillets and bolt holes were completely ignored. This simplification means that the structure could be modelled as an assemblage of beam elements. A vast number of solid elements would be required to model this structure's bending behaviour, therefore the use of beam elements greatly reduces the size of the finite element model. The structure was adequately modelled with 46 nodes (276 degrees of freedom) connected by two noded beam elements. The formulation of the beam elements used approximates Timoshenko beam theory [72]. This formulation is described in chapter 2. The first 38 nodes were positioned at locations which were to be tested experimentally. The mortice joints were modelled by assigning the correct physical properties to the elements at the ends. Because the structure was tested in the freely supported condition the finite element model contained six rigid body modes. The SDRC I-DEAS[1] package makes use of "kinematic degrees of freedom" to eliminate the rigid body modes. The user is required to select "kinematic degrees of freedom" in such a way that

[1]Integrated Design Engineering Analysis Software supplied by Structural Dynamics Research Corporation.

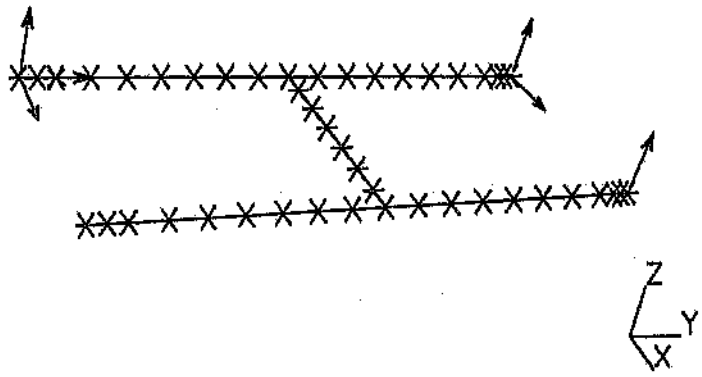

Figure 4.2: The Finite Element Model

if those degrees of freedom were restrained no rigid body motion would be possible. Six translational degrees of freedom were chosen which would eliminate all six rigid body modes. Figure 4.2.1 shows the finite element model's nodes and kinematic degrees of freedom.

4.2.2 Equilibrium Equation Solution

The SDRC "Simultaneous Vector Iteration" method was used to solve the eigenvalue problem. This is the subspace iteration method described in section 2.3.4. This method was chosen because only the low frequency modes were required. The alternative method was a generalized Jacobi method with the option of Guyan reduction. The first twenty modes (including the six rigid body modes) were calculated to a frequency accuracy of six significant digits. Six iterations were required to obtain this accuracy.

4.3 EXPERIMENTAL MODAL ANALYSIS

4.3.1 Test Setup

The test structure was suspended by two soft elastic cords, at points A and B in figure 4.1. Three Structcell accelerometers were used to measure the responses (accelerations) to impulses supplied by a PCB impact hammer. The accelerometers measured translations in orthogonal directions and were positioned at separate locations on the structure to avoid measurement at a modal node (see figure 4.1). Impacts were applied at 38 different locations on the structure in each of the three directions.

4.3.2 Modal Analysis Procedure

A Genrad 2515 computer aided test system was used to record the transducer output signals in the form of frequency response functions over the range 0 to 640 Hz. These frequency response functions were then transferred to a MicroVax minicomputer where they were analysed using the I-DEAS Test Data Analysis package. The reference (impact location and direction) and response (accelerometer location and measurement direction) positions were swapped when the frequency response functions were stored. This is possible because of the reciprocity of linear structures. This resulted in effectively three "exciter" locations and a number of "response measurement" points. The Polyreference parameter extraction technique was used to extract the modal model from all the data simultaneously. Single degree of freedom techniques would however have also produced satisfactory results for this structure. The structure is very lightly damped and proportional viscous damping was assumed in the parameter extraction process resulting in real modes. The option of a general viscous damping model was also available but was considered excessively complex for this lightly damped structure. Eleven modes were extracted over the frequency range 0 to 640 Hz.

MODE NO	NATURAL FREQ. (Hz)	
	FEM	EXP.
1	59.29	58.10
2	65.36	68.19
3	137.81	144.17
4	154.43	167.70
5	193.31	198.07
6	195.31	203.65
7	208.48	214.24
8	584.12	591.43
9	595.79	601.19
10	598.26	604.69
11	626.55	630.94
12	680.08	
13	833.39	
14	1018.30	

Table 4.1: Original Model Frequencies

4.4 MODAL ANALYSIS RESULTS

The natural frequencies obtained from the finite element analysis and the experimental test are listed in table 4.4.

Only two finite element and experimental mode shapes are presented in figures 4.4 and 4.4. The remainder of the mode shapes may be found in Appendix E.

4.5 DISCUSSION OF RESULTS

In practice experimentally obtained natural frequencies are usually more accurate than the finite element natural frequencies. In this research the

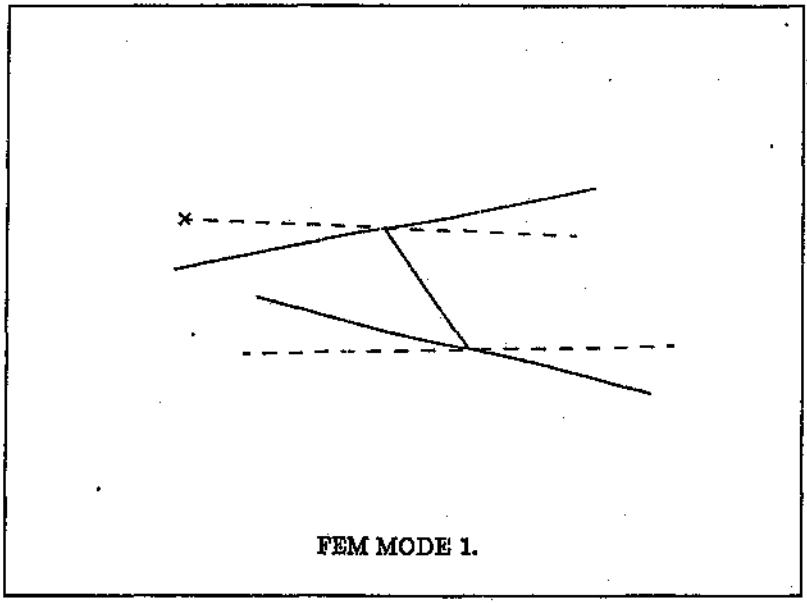

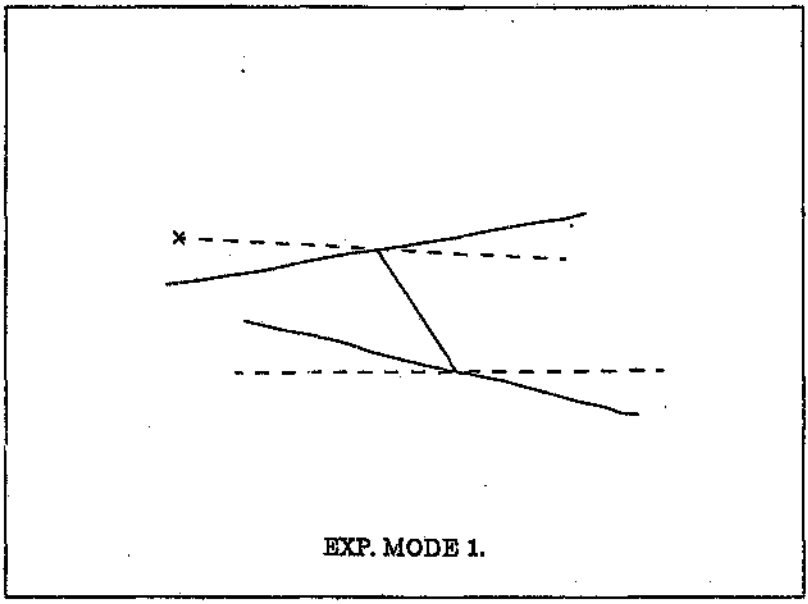

Figure 4.3: Original Mode Shape No. 1

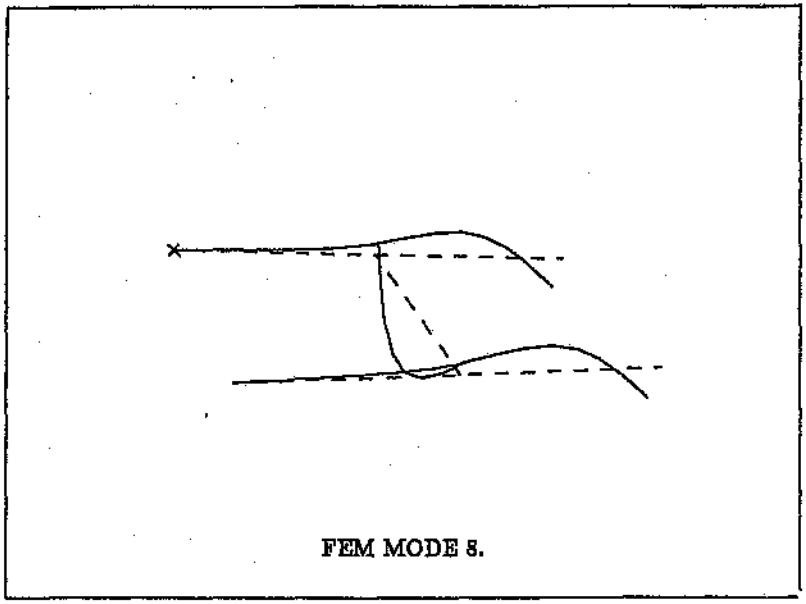

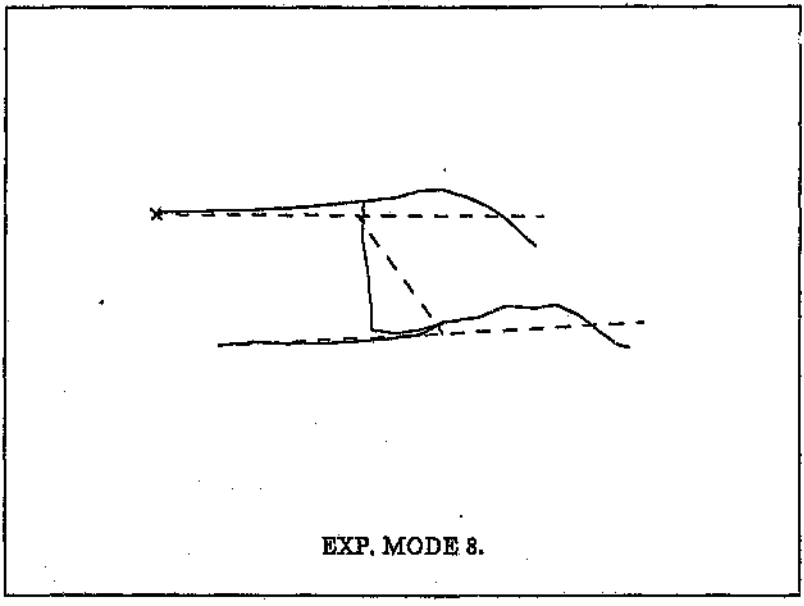

Figure 4.4: Original Mode Shape No. 8

experimental frequencies are assumed to be correct and the finite element frequencies are compared to the experimental frequencies.

Because the structure was simple it was expected that the finite element frequencies would not differ substantially from the experimental frequencies. This was found to be the case with the maximum difference being 7,8% of the frequency (mode no. 4). On average the first eight finite element frequencies are approximately 3% less than the experimental frequencies.

The experimental mode shapes have sufficient degrees of freedom to give a good visual representation of the deflections of the lower frequency modes. If the frequency range was increased more points would have been required to represent the greater deflection gradients of the higher frequency mode shapes. The experimental mode shapes show slight irregularities which are attributed to experimental errors. These irregularities appear to be most pronounced at the accelerometer locations suggesting that the mass of the accelerometers may affect the shapes. This structure was previously tested by the multiple shaker method [64]. The poor quality of the mode shapes thus obtained was largely attributed to the moving of the accelerometers during testing.

Identifying which experimental mode shapes correspond to the finite element mode shapes was simple for this structure and can be achieved by visual inspection. Nevertheless a MAC matrix was computed to measure the correlation between the mode shapes. This MAC matrix is included in Appendix E. The diagonal terms in the matrix ranged from a maximum of 0,993 to a minimum of 0,738 with the maximum off diagonal term being 0,069. It is therefore clear that no modes have been overlooked in the experimental analysis. This is important as all the modes in the frequency range of interest are necessary in the finite element model improvement process if the improved model is to accurately describe the structure's behaviour over the frequency range.

It is interesting to note that if the mortice joints are neglected, the symmetric finite element model produces a symmetric mode no.8 at a frequency of 579.47 Hz. This gives an indication of the structure's sensitivity to mass changes at the ends.

Chapter 5

MODEL EXPANSION AND IMPROVEMENT

The expansion of the experimental mode shapes and the subsequent improvement of the original finite element model was carried out in the I-DEAS hypermatrix pack environment. This environment is described briefly, in Appendix C, as its limitations made the procedure more complicated than necessary. The limitations however do not effect the accuracy of the results of the expansion and improvement process.

5.1 EXPANSION AND IMPROVEMENT PROCEDURE

The steps involved in the expansion and improvement procedure, which were included in the standard I-DEAS "simultaneous vector iteration" program, are illustrated in figure 5.1. A more detailed explanation of the steps follows.

The first step of the procedure is the input of the original mode shapes. The experimental mode shapes were extracted and the finite element mode shapes were calculated previously (Chapter 3) and written to separate I-DEAS universal files. These universal files have a different format to those used in the hypermatrix environment. A Fortran program was used to reformat the

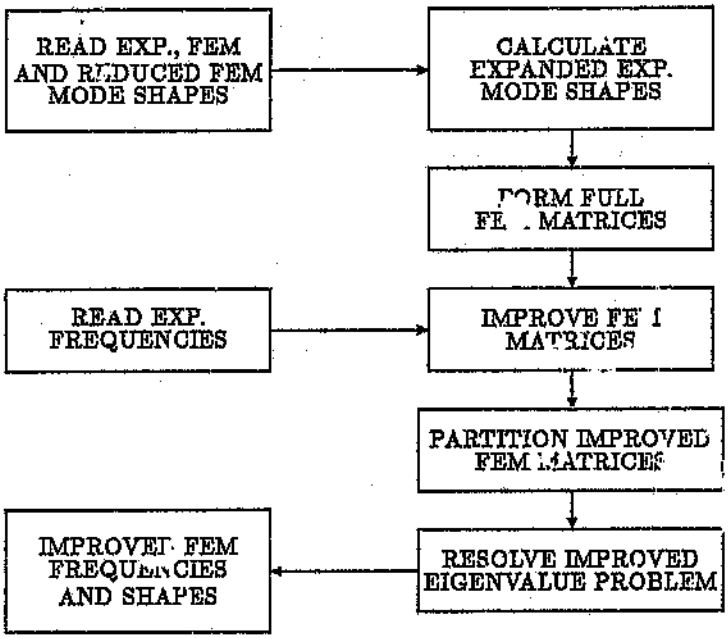

Figure 5.1: Model Expansion and Improvement Procedure

information and to scale the mode shapes. The finite element mode shapes were scaled by I-DEAS so that the magnitude of the largest element was unity and the modal masses were included in the universal file. These modal masses were used to mass normalise the finite element mode shapes as required in the procedure. The experimental mode shapes were scaled so that the largest element in each shape was equal to the corresponding element in the equivalent mass normalized finite element mode shape. This ensures that the experimental shapes show deflections in the same directions as the finite element shapes.

The scaled experimental and finite element mode shapes were then written to a universal file which could be read into the hypermatrix database. A matrix containing the finite element mode shapes truncated to include only test degrees of freedom was also written.

The Fortran program was also used to convert the experimental natural frequencies from Hertz to rad/s and to square them before writing them to a universal file for reading into the hypermatrix environment during the improvement process.

Once the mode shapes were contained in the hypermatrix database the theory described in section 3.2.3 was applied to calculate the expanded experimental mode shapes. Because the matrix could not be written to a universal file without corruption it was printed to the log file as six digit accuracy is sufficient to obtain visual illustration of the mode shapes. This matrix was later reformatted to the standard universal file format by a second Fortran program. This universal file was read and the expanded mode shapes were plotted at a later stage.

Once the expanded experimental mode shapes were available in the hypermatrix database the mass and stiffness matrices were required for the improvement process. In the standard I-DEAS "simultaneous vector iteration" program the complete mass and stiffness matrices are never formed. Instead they are formed in partitioned form to separate the kinematic degrees of freedom from the independent degrees of freedom. The full (unpartitioned) mass and stiffness matrices therefore had to be formed for the improvement process. After the experimental eigenvalues and a unity matrix, of dimension

equal to the number of modes being used, were read the mass and stiffness matrices were improved using the method described in section 3.3.2.

The full improved mass and stiffness matrices were then partitioned by pre- and post multiplication by matrices formed outside I-DEAS for this purpose. The partitioned matrices were then checked by resolving the improved eigenvalue problem using the standard "simultaneous vector iteration" algorithm.

5.2 RESULTS

5.2.1 Expansion Procedure Results

The expansion procedure was used to expand the first eight experimental mode shapes to contain all the finite element model degrees of freedom (including rotational degrees of freedom). Only the X and Z directions were included in the original experimental shapes to illustrate the expansion of the Y components. The first and eighth expanded mode shapes and the corresponding original mode shapes are shown in figures 5.2 and 5.3. The remaining six pairs of mode shapes are included in Appendix E.

5.2.2 Improvement Procedure Results

Resolving the improved eigenvalue problem resulted in the experimental natural frequencies for the first eight modes. The frequencies of the higher frequency modes is unaltered by the improvement process. These results are shown in table 5.1.

Examination of the improvements at matrix element level has proved to be unproductive except for simple cases [64]. It was therefore decided not to include such information here.

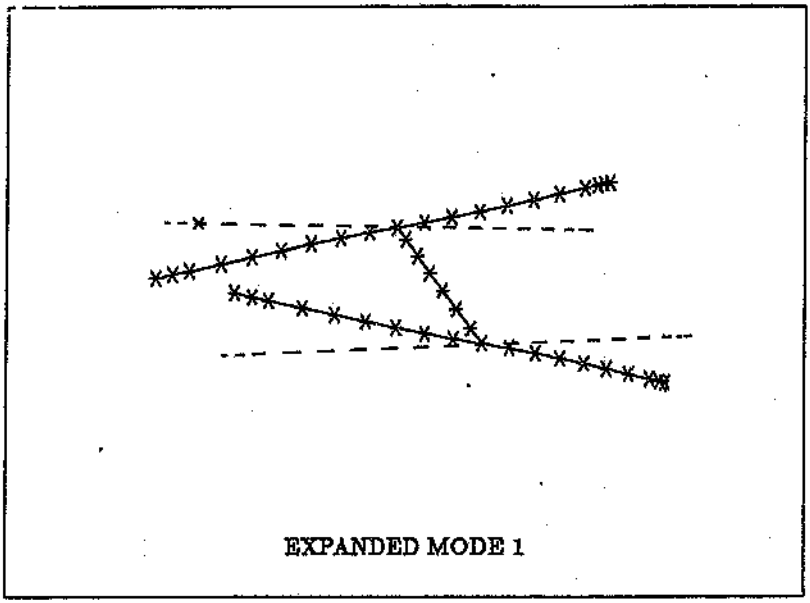

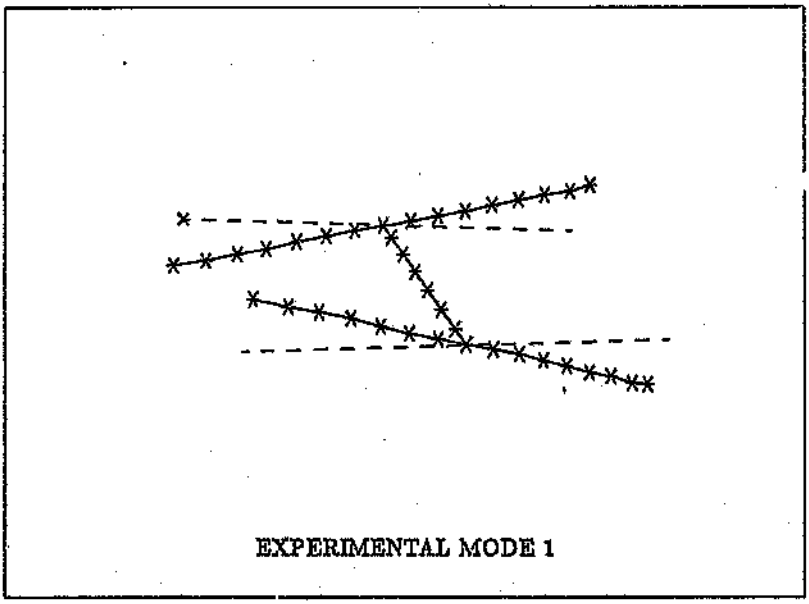

Figure 5.2: Expansion of Mode 1

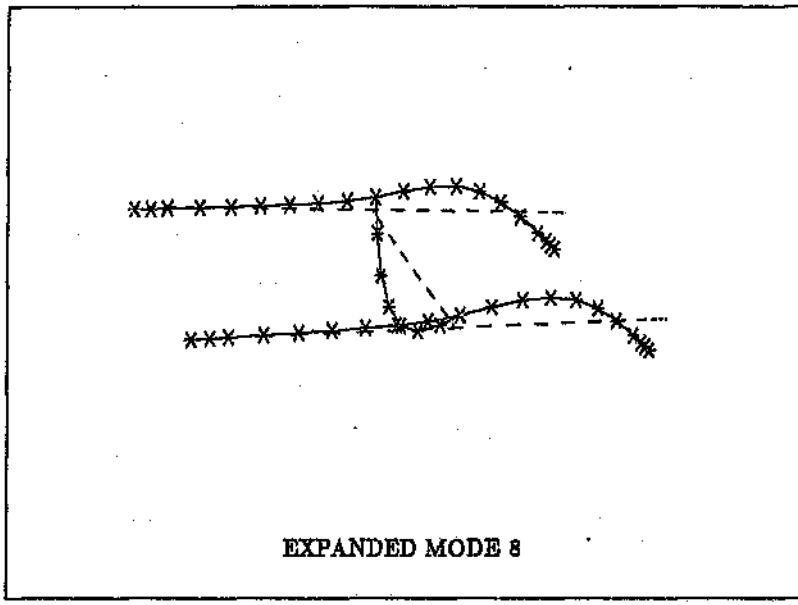

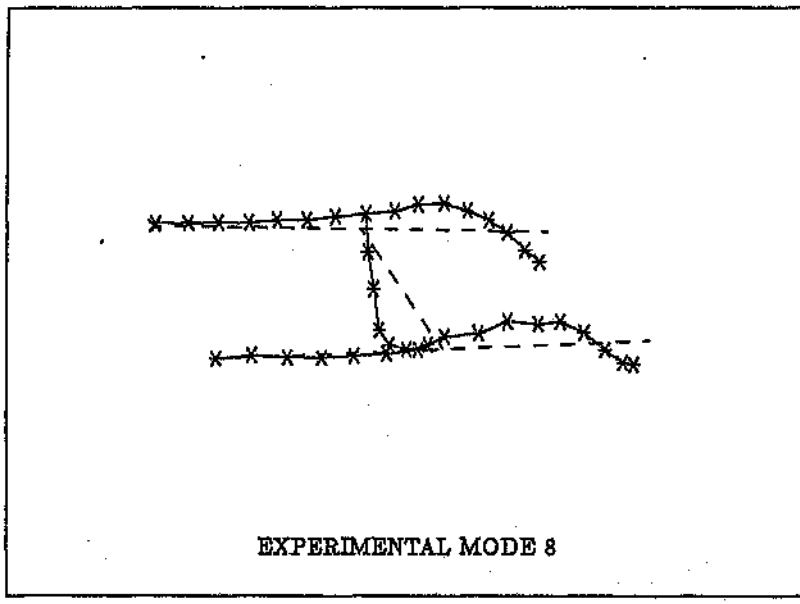

Figure 5.3: Expansion of Mode 8

MODE NO	NATURAL FREQ.(Hz)		
	FEM	EXP.	IMP.
1	59.29	58.10	58.10
2	65.36	68.19	68.1'
3	137.81	144.17	144.17
4	154.43	167.70	167.70
5	193.31	198.07	198.07
6	195.31	203.65	203.65
7	208.48	214.24	214.24
8	584.12	591.43	591.43
9	595.79	601.19	595.79
10	598.26	604.69	598.26
11	626.55	630.94	626.55
12	680.08		680.08
13	833.39		833.39
14	1018.30		1018.30

Table 5.1: Comparison of Improved Frequencies

5.3 DISCUSSION

The hypermatrix environment proved to be a powerful tool for performing matrix operations. The errors encountered during output are expected to be corrected in later versions of the package. Therefore further use of this tool is recommended once the output error has been overcome.

Inspection of the expanded mode shapes shows that they are very similar to the original finite element mode shapes. The expansion process has not only increased the degrees of freedom in the mode shapes but has also smoothed the experimental irregularities. The Y direction degrees of freedom were not present in the original experimental shapes. Modes 2 and 4 show that these degrees of freedom have been expanded correctly along the cross member.

These qualitative observations are not surprising if the expansion process is studied in more depth. The equation $E_n = T_u E_a$ was used to expand the experimental mode shapes to the finite element degrees of freedom. More insight into the nature of this equation is obtained by re-writing it as:

$$E_n = U_n (U_a^T U_a)^{-1} U_a^T E_a$$

This equation may be simplified to $A = BC$ where, $B = U_n$. Column r of A is computed as follows:

$$\begin{Bmatrix} a_{11} \\ a_{12} \\ \vdots \\ a_{1n} \end{Bmatrix} = \begin{Bmatrix} b_{11}c_{1r} + b_{12}c_{2r} + b_{13}c_{3r} \cdots b_{1n}c_{nr} \\ b_{21}c_{1r} + b_{22}c_{2r} + b_{23}c_{3r} \cdots b_{2n}c_{nr} \\ \vdots \\ b_{n1}c_{1r} + b_{n2}c_{2r} + b_{n3}c_{3r} \cdots b_{nn}c_{nr} \end{Bmatrix}$$

therefore,

$$\begin{Bmatrix} a_{11} \\ a_{12} \\ \vdots \\ a_{1n} \end{Bmatrix} = c_{1r} \begin{Bmatrix} b_{11} \\ b_{21} \\ \vdots \\ b_{n1} \end{Bmatrix} + c_{2r} \begin{Bmatrix} b_{12} \\ b_{22} \\ \vdots \\ b_{n2} \end{Bmatrix} + c_{3r} \begin{Bmatrix} b_{13} \\ b_{23} \\ \vdots \\ b_{n3} \end{Bmatrix} + \cdots + c_{nr} \begin{Bmatrix} b_{1n} \\ b_{2n} \\ \vdots \\ b_{nn} \end{Bmatrix}$$

From this it is clear that each expanded mode shape is a linear combination of the finite element mode shapes used in the expansion procedure. The coefficient a_{ir} represents the contribution of finite element mode shape i to the expanded mode shape r. Therefore the expanded mode shapes are confined to the matrix space spanned by the finite element mode shapes included in the expansion procedure. Because the expanded shapes are linear combinations of the finite element shapes they are smooth because of the "continuous" nature of finite element mode shapes. If the original finite element model contains gross errors or deficiencies the matrix space spanned by it's low frequency modes will not include the true (experimental) mode shapes. This means that important information will be lost in the expansion process.

Because the eight experimental and finite element mode shapes used in the expansion process appear to be well correlated it is expected that each expanded mode shape has as its major contribution the corresponding finite element mode shape. This was validated during the expansion process. For mode 1 the contribution coefficients were, 1,0235E+0, -6,1088E-3, 7,9242E-3, 2,9630E-2, -1,2837E-3, -4,0644E-3, 6,7545E-3 and -3,0130E-3 showing that the major contribution came from finite element mode shape 1.

The finite element model improvement process uses the expanded experimental mode shapes. Therefore it is essential that the mode shapes are realistic the improvement process is to produce a good model of the actual structure. The improved finite element model was resolved to check it's accuracy. The resolve reproduced the expanded experimental mode shapes at the experimental frequencies. This indicates that the improvement process was completed successfully. It is interesting to note that the higher frequency modes, which were not included in the improvement process, are not affected by the process. In the improvement process the mass matrix was used to weight the changes. This has the effect of making the changes to a region of the matrix proportional to the mass in this region. This ensures that the mass and stiffness of regions having small mass do not become unrealistically large and vice versa. Direct physical interpretation of the change was not possible. If the original model was known to have regions which were inadequately modelled, weighting matrices could have been chosen to concentrate the changes in those regions.

The improvement process was seen to destroy the sparseness of the finite element matrices. Eigenvalue solution of the improved matrices required approximately twice the time required for the original matrices.

The ability of the improved model to represent the structure was investigated in chapter 6 where it is used to predict the effect of a modification to the structure.

Chapter 6

STRUCTURAL DYNAMIC MODIFICATION

In this chapter the effect of a physical modification to the H-Frame structure is predicted. The prediction was performed using two different models of the H-Frame structure. The first model was the original finite element model described in chapter 4 while the second was the improved finite element model described in chapter 5. The predictions were compared to an experimental model of the modified structure.

6.1 MODIFICATION DETAILS

The physical modification consisted of bolting a cross beam between two ends of the existing H-Frame structure. These details are shown in figure 6.1.

A pre-stress existed in the modified structure due to poor tolerances in the manufacture of the test pieces.

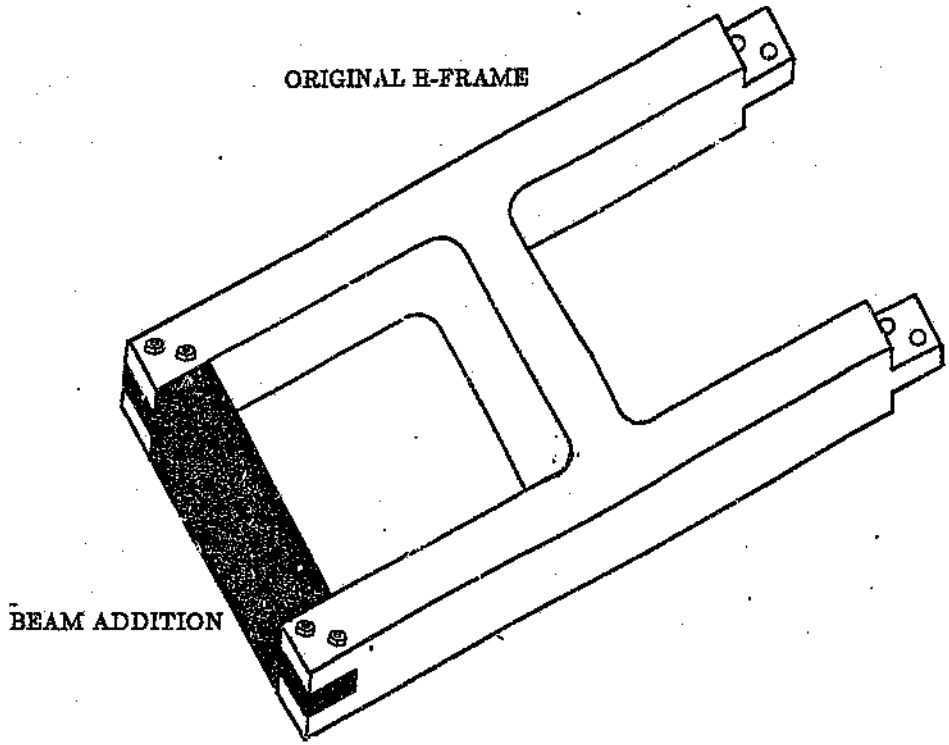

Figure 6.1: Modification Details

6.2 FE MODEL ADDITIONS

The beam modification was modelled using ten two noded Timoshenko beam finite elements. Translational and rotational spring elements were used to connect the beam modification to the H-Frame finite element models. Ideally the stiffness of these springs should be equal to the stiffness of the actual bolted joint. Because these joint stiffnesses are impossible to determine analytically a simple structure containing a single joint was tested experimentally and modelled with finite elements. The spring stiffnesses used in the simple model were changed by trial and error until reasonable agreement between the two models' natural frequencies and mode shapes was obtained. Results are included in Appendix E. The spring stiffness values thus obtained were used in the modification of the H-Frame.

6.3 MODIFICATION RESULTS

Table 6.1 shows the results of the modification process. Frequencies obtained using the original H-Frame model and the improved H-Frame model are compared to experimental results for the modified structure. Mode shapes are included in Appendix E.

6.4 DISCUSSION OF RESULTS

The finite element model prediction using the original H-Frame model produced frequencies similar to the experimental results. The magnitude of the first ten frequencies differ on average by 5,54 Hz or 2,68 % of the frequency. These errors are fairly small and would probably be acceptable in practice. The major sources of error in this prediction are the inaccuracies in the original H-Frame model and inaccuracies in the characteristics of the joints. The first of these sources of error was addressed by using the improved H-Frame finite element model for the prediction. The magnitude of the first ten frequencies then differed on average by 4,12 Hz or 1,70 % of the frequency.

MODE NO	NATURAL FREQ.(Hz)		
	EXP	FEM	IMP.
1	85.90	90.16	91.23
2	111.42	106.66	112.18
3	164.69	160.58	163.34
4	181.17	169.55	181.26
5	224.81	219.15	223.47
6	250.85	257.31	262 62
7	483.81	474.12	470.12
8	484.94	479.86	483.52
9	618.95	621.29	621.63
10	629.35	630.84	632.17
11		667.06	667.14
12		733.23	733.01
13		878.92	876.92
14		918.73	932.40

Table 6.1: Comparison of Modified Structure Frequencies

This global comparison does show a slightly better prediction using the improved H-Frame model. It is however necessary to compare the results on a mode by mode basis to gain further insight and to investigate why some frequencies moved further from the experimental results. This sort of comparison can only be made qualitatively as it is not known how much each H-Frame mode contributes to the modified structure's modes.

The modes in which the predicted frequencies showed large changes when the improved H-Frame model was used were considered. Modes 2,3 and 4 showed better agreement with experimental frequencies while modes 6 and 7 showed poorer agreement. By comparing the mode shapes of the H-Frame and the modified structure it is in general possible to identify which H-Frame mode shapes contribute to the modified mode shapes. For example the first mode of the modified structure can be seen to be governed by the first mode of the H-Frame. If mode 2 is considered it can be seen that this mode is governed by mode 2 and possibly mode 3 of the H-Frame. In the improvement process the frequencies of these two modes were increased by 2,83 Hz and 6,36 Hz respectively. The effect of these increases is seen on the modification as an increase of 5,52 Hz for mode 2.

Modes 3 and 4 of the modified structure show similar features. The frequency of mode 5 of the H-Frame was increased by 4,76 Hz contributing to an increase of 2,76 Hz in mode 3 of the modified structure. The frequency of mode 4 of the H-Frame increased by 13,27 Hz contributing to the 11,71 Hz increase in the modified structure's 4th mode.

Using the improved H-Frame model causes poorer agreement with the experimental results for modes 6 and 7. The H-Frame's 7th frequency increased by 5,76 Hz while the modified structure's 6th frequency increased by 4,00 Hz. It is possible that inaccuracies in the joint properties caused the prediction, using the original H-Frame model, to be too high and that if the correct joint properties were known the original model might have produced a frequency less than the experimental frequency. This error would then have been decreased by using the improved H-Frame model. The joint mode shapes (in Appendix E) show greater displacements across the joint in the experimental shapes than in the finite element shapes. Also, the finite element frequencies are on average higher than the experimental frequencies (see table E.2). This

suggests that the springs used in the finite element models are indeed too stiff. Decreasing the stiffness of the springs in the finite element model of the modified structure would tend to reduce the finite element frequencies.

The predicted frequency of mode 7 is also seen to be further from the experimental frequency when the improved H-Frame model is used. Mode 9 of the H-Frame is expected to be the major contribution to mode 7 of the modified structure. Mode 9 was not included in the H-Frame improvement process but it is evident that the improvement process does have an effect on this mode when it is used in a modification even though it does not effect the corresponding mode of the H-Frame. Some of this effect may also have been caused by other modes which were used in the improvement process. Considering the higher frequency modes it does appear that the improvement process has an effect on the performance of the modes which were not used in the improvement process.

Unfortunately modelling of the joint was not performed successfully (see Appendix D). If accurate stiffness had been obtained for the joint when used in the simple structure it is expected that a better prediction of the modified structure's properties would have been obtained. One limitation of this method is that the joints in the modified structure were subjected to a pre-stress, due to poor tolerances, which did not exist in the simple jointed structure. The effect of these pre-stresses on the properties of the joint would be very difficult to quantify. Although further work is required on joint characterization the trail and error procedure used here may be adequate for a number of practical applications.

Chapter 7

CONCLUSIONS

Experimental and analytical (finite element method) modal models were produced for a simple H-Frame structure. Good correlation between the models was observed. On average the first eight finite element model natural frequencies were approximately three percent less than the experimental frequencies. A MAC matrix showed reasonable correlation between the mode shapes. The diagonal terms of the matrix varied between 0,738 and 0,993 while the maximum off diagonal term was 0,069.

The first eight experimental mode shapes were expanded up to the finite element model's degrees of freedom. A limitation of the expansion process was observed. This limitation is that the expanded experimental mode shapes are limited to the matrix space spanned by the finite element mode shapes used in the expansion process. This means that good finite element mode shapes are required if the experimental mode shapes are to be expanded accurately.

The expanded experimental mode shapes and the experimental natural frequencies were used to improve the finite element model. The improved finite element model reproduced the first eight natural frequencies and expanded mode shapes, while the higher frequency modes remained unchanged. Because the original finite element model is used to 'seed' the improvement process it is important that it is a good representation of the structure. Direct physical interpretation of the changes to the finite element model matrices was not possible.

A bolted joint was characterized by testing a simple structure containing a joint and then varying the joint stiffness in a finite element model until reasonable agreement was obtained.

The original and improved finite element models were used to predict the effect of the addition of a beam between two ends of the H-Frame structure. These predictions were compared to experimental results for the modified structure. The prediction using the improved model was found to be better than the prediction using the original model. The average error in the first ten frequencies was reduced from 2,68% to 1,70%. The effect of the improvement process on the individual modes was visible. It is believed that better results would have been obtained if the joint properties were known more accurately.

Recommendations for Further Work

It is believed that the model improvement process could be used to obtain matrices describing joint properties (see Appendix D). This would be achieved by concentrating the improvements to a finite element model of a jointed structure to the joint region by the use of weighting matrices. The expansion process used in this work would not be suitable as the displacements across the joint would be lost if the original finite element model did not have these displacements. In order to obtain displacements across the joint, the stiffness of the original joint model would have to be low, but a low stiffness would introduce local modes and make correlation with the experimental model very difficult. If a suitable expansion process could be found, the improvement process could provide an efficient method for obtaining a linearized model of a joint.

REFERENCES

[1] Ramsey, K.A. Firmin, A. Experimental Modal Analysis, Structural Modifications and FEM Analysis - Combining Forces on a Desktop Computer, *Proceedings of the First International Modal Analysis Conference*, Orlando, Florida, 1982, p443-455.

[2] McDonald, P.R. Wiley, G.H. A Methodology for Integrating Test with Design and Analysis Using I-DEAS, *Proceedings of the 6th International Modal Analysis Conference*, Kissimmee, Florida, 1988, p456-463.

[3] Pal, T.G. Schmid'oerg, R.A. Combining Analytical and Experimental Modal Analysis for Effective Structural Dynamic Modelling, *Proceedings of the 1st International Modal Analysis Conference*, Orlando, Florida, 1982, p265-271.

[4] Berman, A., Flannelly, W.G. Theory of Incomplete Models of Dynamic Structures, *AIAA Journal*, Vol. 9, No. 8, August 1971, p.1481-1487.

[5] Hermanski, M. Ostholt, H. Linking Finite Elements With Experimental Modal Analysis, *International Journal of Modal Analysis*, July 1987, p144-147.

[6] Mitchell-Dignan, M. Pardoen, G.C. The Estimation of Rotational Degrees-of-Freedom Using Shape Functions, *Proceedings of the 6th International Modal Analysis Conference*, Kissimmee, Florida, 1988, p566-571.

[7] O'Callahan, J.C. Avitable, P. Lieu, I-W. Madden, R. An Efficient Method of Determining Rotational Degrees of Freedom From Analytical and Experimental Modal Data, *Proceedings of the 4th International Modal Analysis Conference*, Los Angeles, 1986, p50-58.

[8] O'Callahan, J.C. Avitable, P. Riemer, R. System Equivalent Reduction Expansion Process (SEREP), *Proceedings of the 7th International Modal Analysis Conference*, Las Vegas, 1989, p29-37.

[9] O'Callahan, J.C., Le .. ,R.K. Optimization of Mass and Stiffness Matrices Using a Generali.. Inverse Technique on the Measured Modes, *Proceedings of the 3rd International Modal Analysis Conference*, 1985, p.75-79.

[10] Avitabile, P., O'Callahan, J., Milani, J., Dong-Rong Pan, E. System Model Development Using Analytically Enhanced Experimental Data, *Proceedings of the 7th International Modal Analysis Conference*, 1989, p.589-595.

[11] Ewins, D.J. *Modal Testing: Theory and Practice*, Research Studies Press Ltd, England, 1984.

[12] Love, A.E.H. *A Treatize on the Mathematical Theory of Elasticity*", 4th edition, Dover Publications, Inc, New York, 1944.

[13] Snyder, V.W. Review of Matrix Formulations Used in Modal Analysis, *Proceedings of the 7th International Modal Analysis Conference*, Las V.. s, 1989, p313-316.

[14] Timoshenko, S. Young, D.H. Weaver, W,Jr. *Vibration Problems in Engineering*, 4th edition, John Wiley & Sons, Inc., New York, 1974.

[15] Lang, G.F. *Modal Testing Principles*, Technical report No.023/87, Solartron Instruments.

[16] Newland, D.E. *An Introduction to Random Vibrations and Spectral Analysis*, 2nd edition, Longman Scientific & Technical, 1984.

[17] Zaveri,K. *Modal Analysis of Large Structures-Multiple Exciter Systems*, Bruel & Kjuer,1985.

[18] SDRC *I-DEAS - Test Data Analysis User Guide*, Level 4.

[19] Snoeys, R. SAS, P. Heylen, W. Van der Auweraen, H. Trends in Experimental Modal Analysis, *Mechanical systems and Signals Processing*, 1(1), 1987, p.5-27.

[20] Deblauwe,, F. Brown, D.L. Allemang, R.J. The Polyreference Time Domain Technique, *Proceedings of the 5th International Modal Analysis Conference*, London, England, 1987, p.832-845.

[21] Bathe, K-J. *Finite Element Procedures in Engineering Analysis*, Prentice-Hall, New Jersey, 1982

[22] Dawe, D.J. A Finite Element for the Vibration Analysis of Timoshenko Beams, *Journal of Sound and Vibration*, Vol.60, No.1, 1978, p11-20.

[23] Dawe, D.J. *Matrix and Finite Element Displacement Analysis Of Structures*, Oxford University Press, New York, 1984.

[24] Carey, G.F. Oden, J.T. *Finite Elements-Computational Aspects-Vol.III*, Prentice-Hall, Inc. USA, 1984.

[25] Bathe, K-J. Wilson, E.L. *Numerical Methods in Finite Element Analysis*, Prentice-Hall, NJ, 1976.

[26] Craig, R.R. Jr. *Structural Dynamics-An Introduction to Computer Methods*, John Wiley & Sons, USA, 1981.

[27] Jetmundsen, B. *On Frequency Domain Methodologies for Prescribed Structural Modification and Subsystem Synthesis* PhD Thesis, 1986, p6.

[28] Brown, D.L. Course Notes, *7th International Modal Analysis Conference*, Las Vegas, Nevada, 1989.

[29] Lancaster, P. Free Vibrations of Lightly Damped Systems by Perturbation Methods, *Quart. J. Mech. App. Math.* Vol 13, 1960, p138-155.

[30] Fox, R.L. Kapoor, M.P. Rates of Change of Eigenvalues and Eigenvectors, *AIAA Journal*, Vol. 6, No. 12, 1968, p2426-2429.

[31] Zhang, Q. Wang, W. Allemang, R.J. Brown, D.L. Prediction of Mass Modification for Desired Natural Frequencies, *Proceedings of the 6th International Modal Analysis Conference*, Kissimmee, Florida, 1988, p1026-1032.

[32] Rizai, M.N. Bernard, J.E. An Efficient Method for Predicting the Dynamic Effects of Redesign, *Proceedings of the First International Modal Analysis Conference*, Orlando, Florida, 1982, p436-442.

[33] Starkey, J.M. Bernard, J.E. Optimal Redesign Based - Modal Data, *Proceedings of the 1st International Modal Analysis Conference*, Orlando, Florida, 1982, p591-597.

[34] Crowley, J.R. Rocklin, G.T. Klosterman, A.L. Vold, H. Direct Structural Modification using Frequency Response Functions, *Proceedings of the 2nd International Modal Analysis Conference*, Orlando, Florida, 1984, p58-65.

[35] *I-DEAS Test Data Analysis Manual*, V4.1, SDRC, p20.1-20.3.

[36] Crowley, J.R. Crowley, S.M. Rocklin, G.T. Gorman, T.E. A Comparison of SMURF and Modal Modeling, *Proceedings of the 3rd International Modal Analysis Conference*, Orlando, Florida, 1985, p1053-1059.

[37] Jones, R. Iberle, K. Structural Modification: A Comparison of Techniques, *Proceedings of the 4th International Modal Analysis Conference*, Los Angels, CA., 1986, p59-65.

[38] Weissenburger, J.T. Effect of Local Modifications on the Vibration Characteristics of Linear Systems, *Journal of Applied Mechanics*, June 1968, p327-332.

[39] Wallack, P. Skoog, P. Richardson, M. Simultaneous Structural Dynamics Modification (S^2DM), *Proceedings of the 6th International Modal Analysis Conference*, Kissimmee, Florida, 1988, p1033-1038.

[40] Pomazal, R.J. Snyder, V.W. Local Modifications of Damped Linear Systems, *AIAA Journal*, Vol. 9, No. 11, 1971, p2216-2221.

[41] Hallquist, J. Snyder, V. Synthesis of Two Discrete Vibratory Systems Using Eigenvalue Modification, *AIAA Journal*, Vol.11, No.2, 1973, p247-249.

[42] Hallquist, J. Snyder, V. On the Connection of Viscously Damped Continuous Vibratory Systems, *Journal of Sound and Vibration*, Vol.32, No.1, 1974, p131-142.

[43] O'Callahan, J.C. Chou, C-M. Study of a Structural Modification Procedure with Three Dimensional Beam Elements Using a Local Eigenvalue

Modification Procedure, *Proceedings of the 2nd International Modal Analysis Conference*, Orlando, Florida, 1984, p945-952.

[44] Wallack, P. Skoog, P. Richardson, M. Comparison of Analytical and Experimental Rib Stiffener Modifications to a Structure, *Proceedings of the 7th International Modal Analysis Conference*, Las Vegas, Nevada, 1989, p965-973.

[45] Arora, J.S. Survey of Structural Reanalysis Techniques, *Journal of the Structural Division ASCE*, Vol.102, No. ST4, 1976, p783-802.

[46] Hurty, W.C. Vibrations of Structural Systems by Component Mode Synthesis, *Proc. ASCE*, Vol.85, No.EM4, Aug.1960, p51-69.

[47] Hurty, W.C. Dynamic Analysis of Structural Systems Using Component Modes, *AIAA Journal*, Vol.3, No.4, April 1965, p678-685.

[48] Hintz, R.M. Analytical Methods in Component Modal Synthesis, *AIAA Journal*, Vol.13, No.8, Aug.1975, p1007-1016.

[49] Craig, R.R. Bampton, M.C.C. Coupling of Substructures for Dynamic Analysis, *AIAA Journal*, Vol.6, No.7, July 1968, p1313-1319.

[50] Benfield, W.A. Hruda, R.F. Vibration Analysis of Structures by Component Mode Substitution, *AIAA Journal*, Vol.9, No.7, July 1971, p1255-1261.

[51] Guyan, R.J. Reduction of Stiffness and Mass Matrices, *AIAA Journal*, Vol.3, No.2, Feb. 1965, p380.

[52] Klosterman, A.L. *On the Experimental Determination and Use of Modal Representations of Dynamic Characteristics*, Ph.D. dissertation, University of Cincinnati, 1971.

[53] Kuhar, E.J. Stahle, C.V. Dynamic Transformation Method for Modal Synthesis, *AIAA Journal*, Vol.12, No.5, May 1974, p672-678.

[54] Craig, R.R. A Review of Time-Domain and Frequency-Domain Component-Mode Synthesis Methods, *Journal of Modal Analysis*, Vol.2, No.2, April 1987, p59-72.

[55] Kammer, D.C. Test-Analysis-Model Development Using an Exact Modal Reduction, *International Journal of Modal Analysis*, October 1987, p174-179.

[56] Heylen, W. Optimization of Model Matrices by Means of Experimentally Obtained Dynamic Data, *Proceedings of the 1st International Modal Analysis Conference*, 1982.

[57] Loveday, P.W. *Analytical Model Optimization and Structural Dynamic Modification of a H-Frame Structure*, 2nd Progress Report, University of the Witwatersrand, 1989.

[58] Wei, M.L. Janter, T. Optimization of Physical Model via Selected Physical Parameters, *Proceedings of the 6th International Modal Analysis Conference*, 1988.

[59] Kammer, D.C. Test-Analysis Correlation of the Space Shuttle Solid Rocket Motor Centre Segment, *Journal of Spacecraft and Rockets*, Vol.26, No.4, 1989, p266-273.

[60] Berman, A. Mass Matrix Correction using Incomplete Set of Measured Modes, *AIAA Journal*, Vol.17, No.10, October 1979.

[61] Wei, F-S. Stiffness Matrix Correction from Incomplete Test Data, *AIAA Journal*, Vol.18, No.10, October 1980.

[62] Dobson, B.J. Modification of Finite Element Models using Experimental Modal Analysis, *Proceedings of the 2nd International Modal Analysis Conference*, 1984.

[63] Sidhu, J. Ewins, D.J. Correlation of Finite Element and Modal Test Studies of a Practical Structure, *Proceedings of the 2nd International Modal Analysis Conference*, 1984.

[64] Loveday, P.W Constancon, C.F. Analyt'cal Model Improvement Using Experimental Modal Results, submitted to *R & D Journal*, 1990.

[65] Crawley, E.F. Nonlinear Characteristics of Joints as Elements of Multi-Body Dynamic Systems, *NASA CP 3094*, Part 2, 1989. p543-569.

[66] Ikegami, R. Church, S.M. Kleinholz, D.A. Fowler, B.L. Experimental Characterization of Deployable Trusses and Joints, *NASA CP 2467*, Part 1, 1987, p1271-1287.

[67] Chapman, J.M. Shaw, F.H. Russel, W.C. Dynamics of Trusses Having Nonlinear Joints, *NASA CP 2467*, Part 1, 1987, p539-565.

[68] Foelsch, G.A. Griffin, J.H. Bielak, J. Transient Response of Joint Dominated Space Structures: A New Linearization Technique, *AIAA Journal*, Vol.26, No.10, 1988, p1278-1285.

[69] Gray, S.D. Starkey, J.M. Dynamic Substructure Separation Using Physical and Modal Models, *Proceedings of the 6th International Modal Analysis Conference*, Kissimmee, Florida, 1988, p1119-1123.

[70] Gray, S.D. Starkey, J.M. Mount Property Identification an Optimizational Approach to Dynamic Substructuring, *Proceedings of the 7th International Modal Analysis Conference*, Las Vegas, 1989, p38-44.

[71] Lawrence, C. Huckelbridge, A.A. Characterization of Structural Connections for Multicomponent Systems, *NASA CP 3003*, Vol.1, 1988, p337-352.

[72] SDRC I-DEAS *Model Solution Manual*, V4.1.

[73] Ben-Israel, A. Greville, T.N.E. *Generalized Inverses-Theory and Applications*, John Wiley & Sons, Inc., 1974.

[74] Penrose, R. A Generalized Inverse for Matrices, *Proc. Cambridge Philos. Soc.*, Vol.51, 1955, p406-413.

[75] Przemieniecki, J.S. *Theory of Matrix Structural Analysis*, Dover Publications, Inc., New York, 1985.

APPENDIX A:TIMOSHENKO BEAM ELEMENT MATRICES

The mass and stiffness matrices for a two noded beam element with only in plane deflections and rotations approximating Timoshenko beam theory are given below.

The stiffness matrix is a reduced form of the twelve degree of freedom matrix presented in reference [75].

$$k = \begin{bmatrix} \frac{12EI_z}{l^3(1+\phi_y)} & & & \\ \frac{6EI_z}{l^2(1+\phi_y)} & \frac{(4+\phi_y)EI_z}{l(1+\phi_y} & & \\ -\frac{12EI_z}{l^3(1+\phi_y} & -\frac{6EI_y}{l^2(1+\phi_y)} & \frac{12EI_z}{l^3(1+\phi_y)} & \\ \frac{6EI_z}{l^2(1+\phi_y)} & \frac{(2-\phi_y)EI_z}{l(1+\phi_y)} & -\frac{6EI_z}{l^2(1+\phi_y} & \frac{(4+\phi_y)EI_z}{l(1+\phi_y)} \end{bmatrix}$$

where, the shear parameter $\phi_y = \frac{12EI_z}{GA_{S_y}l^2}$ and A_s is the cross-sectional area effective in shear. The mass matrix is as presented in reference [75].

$$m = \frac{\rho Al}{(1+\phi_s)^2}$$

$$\begin{bmatrix} \frac{13}{35}+\frac{7}{10}\phi_s+\frac{1}{3}\phi_s^2 & & & \\ (\frac{11}{210}+\frac{11}{210}\phi_s+\frac{1}{24}\phi_s^2)l & (\frac{1}{105}+\frac{1}{60}\phi_s+\frac{1}{120}\phi_s^2)l^2 & & \\ \frac{9}{70}+\frac{3}{10}\phi_s+\frac{1}{6}\phi_s^2 & (\frac{13}{120}+\frac{3}{40}\phi_s+\frac{1}{24}\phi_s 02)l & \frac{13}{35}+\frac{7}{10}\phi_s+\frac{1}{3}\phi_s^2 & \\ -(\frac{13}{420}+\frac{3}{40}\phi_s+\frac{1}{24}\phi_s^2)l & -(\frac{1}{140}+\frac{1}{60}\phi_s+\frac{1}{120}\phi_s^2)l^2 & -(\frac{11}{210}+\frac{11}{120}\phi_s+\frac{1}{24}\phi_s^2)l & (\frac{1}{105}+\frac{1}{60}\phi_s+\frac{1}{120}\phi_s^2)l^2 \end{bmatrix}$$

$$+\frac{rhoAl}{(1+\phi_s)^2}\left\{\frac{r}{l}\right\}^2$$

$$\begin{bmatrix} \frac{6}{5} & & & \\ (\frac{1}{10}-\frac{1}{2}\phi_s)l & (\frac{2}{15}+\frac{1}{6}\phi_s+\frac{1}{3}\phi_s^2)l^2 & & \\ -\frac{6}{5} & (-\frac{1}{10}+\frac{1}{2}\phi_s)l & \frac{6}{5} & \\ (\frac{1}{10}-\frac{1}{2}\phi_s)l & (-\frac{1}{60}-\frac{1}{6}\phi_s+\frac{1}{6}\phi_s^2)l^2 & (-\frac{1}{10}+\frac{1}{2}\phi_s)l & (\frac{2}{15}+\frac{1}{6}\phi_s+\frac{1}{3}\phi_s^2)l^2 \end{bmatrix}$$

where, $\phi_s = \frac{12EI}{GA_s l^2}$.

APPENDIX B:THE MOORE-PENROSE GENERALIZED INVERSE

Introduction

A theoretical N degree of freedom linear system can be solved to produce a modal database containing N natural frequencies (eigenvalues) and their associated N dimensional mode shape vectors (eigenvectors). The experimental modal analysis of a practical engineering structure, however, usually produces far fewer natural frequencies than the number of degrees of freedom measured during the test (due mainly to accelerometer frequency limits). It is also not usually practical to solve a finite element model for its full set of natural frequencies. Therefore, when using experimental mode shape matrices to improve finite element models, linear equations containing non-square matrices have to be solved. The Moore-Penrose generalized inverse is a powerful tool when correctly applied to this problem.

This appendix presents a brief discussion of the theory of the generalized inverse. The interested reader requiring a more comprehensive mathematical description is referred to the text by Ben-Israel and Greville [73].

E.H. Moore made the first publication on the subject, (then called "the reciprocal of the general algebraic matrix") in 1920. In this paper he defined a unique inverse for all matrices. It was, however, only in the 1950's that the least-squares properties were discovered and extended by Bjerhammar and Penrose respectively.

Penrose Conditions

E.H. Moore showed that there exists a unique inverse for any general nonzero matrix. Penrose presented four conditions for the calculation of the unique inverse. "The four equations:

- $AXA = A$,
- $XAX = X$,
- $(AX)' = AX$,

- $(XA)^* = XA$

have a unique solution for any A." - Penrose [74].

This unique solution is often denoted by $A^\dagger$ and is known as the Moore - Penrose generalized inverse. Other non-unique generalized inverses which do not satisfy all of the above four conditions can be constructed. These inverses have useful least-squares properties which will be mentioned later. The notation used for these inverses is that used in reference[74]. A generalized inverse satisfying the first and third conditions, for example, will be denoted as $A^{(1,3)}$ and is an element of $A\{1,3\}$ the set of all generalized inverses satisfying the first and third Penrose conditions.

Construction of Generalized Inverses

As only the unique generalized inverse $A^\dagger$ is used in this report the construction of non-unique inverses is not covered here.

"G.C. MacDuffee apparently was the first to point out, about 1959, that the full rank factorization of a matrix A leads to an explicit formula for its Moore-Penrose inverse, $A^\dagger$. However, he did so in private communications, and there is no published work that can be cited." [73]. If matrix A is a mxn matrix of rank r, $(r > 0)$ then there exists a factorization $A = FG$ such that F is a mxr matrix of rank r and G is a rxn matrix also of rank r. This is known as the full-rank factorization of matrix A. This full-rank factorization is related to the Moore-Penrose generalized inverse by the following formula:

$$A^\dagger = G^*(F^*AG^*)^{-1}F^*$$

Note that if A is a real matrix the Hermitian transpose (denoted by *) reduces to the normal transpose.

A.4 Least-Squares and Minimum-Norm Properties

If $Ax = b$ is an inconsistent linear system of equations, with A of size mxn and b of size mx1, a residual vector $r = b - Ax$ can be defined. It is often desirable to find the solution x which will make the Euclidean norm of the

residual vector a minimum. ie. To make $\sum_{i=1}^{n} | r |^2 = \| b - Ax \|^2$ a minimum. It was shown in reference[73]. that this condition is satisfied by choosing $x = A^{(1,3)}b$. In other words the Euclidean norm of the residual vector is minimized by using any generalized inverse of A which satisfies the first and third Penrose conditions. Because this is not a unique generalized inverse there are infinite solutions (x) which satisfy the imposed condition. These solutions may be written as:

$x = A^{\dagger}b + (I - A^{(1,3)}A)y,$
where y is an arbitrary nx1 vector. Note that if A is of full column rank then the above expression produces a unique solution.

If there are an infinite number of solutions it is necessary to impose additional constraints on the solution in order to achieve a unique solution. For example, it is possible to find a minimum norm solution, (a solution which makes $\| x \|^2$ a minimum). It can be shown that such a solution is found by $x = A^{(1,4)}b$.

"The least-squares solutions of $Ax = b$ coincide with the solutions of $Ax = AA^{(1,3)}b$" [73]. The minimum-norm solution of the latter equation is therefore $x = A^{(1,4)}AA^{(1,3)}b$.
It was shown by Urquhart that $A^{(1,4)}AA^{(1,3)} = A^{\dagger}$, therefore $x = A^{\dagger}b$ is the minimum-norm least-squares solution to the inconsistent linear system of equations $Ax = b$.

From this result it is a simple matter to show that the minimum-norm least-squares solution to the inconsistent matrix equation $AXB = D$ is,
$X = A^{\dagger}DB^{\dagger}.$ (B.1)

APPENDIX C: HYPERMATRIX ENVIRONMENT

The standard I-DEAS finite element solution routines are performed in the hypermatrix environment. The finite element model's spatial matrices are calculated here and subsequent equilibrium equation solutions are performed by various algorithms.

he standard routines are available to the user in the form of program files which can be inspected or modified. The program files consist of commands which are used to perform powerful matrix manipulations. Apart from executing standard or user written program files the matrix manipulations can be performed interactively using menus. Matrix input and output is achieved by reading and writing "universal" files. These universal files contain the matrix name, format control cards, and the matrix elements to twenty digit accuracy. Unfortunately it was found that writing matrices larger than a certain dimension was not done correctly. For example it was found that a mode shape matrix of dimension 276x8 was corrupted in the 3rd, 4th,7th and 8th columns in a repeatable manner. It is suggested that such an error may be caused by an insufficient dimension statement in the Fortran source code. This source code is not available to the user and SDRC were unaware of the problem, but promised to investigate it further. They also suggested printing large matrices to the log file. This worked satisfactorily but only gives six significant figure accuracy. It was possible to prove that the error only occurred on writing and not on reading. It was therefore possible to read large matrices into the hypermatrix environment accurately.

APPENDIX D: JOINT CHARACTERIZATION

To obtain the properties of the joint to be used in the modification a simple structure containing an "identical" joint was tested and modelled using finite elements. In the finite element model the joint was represented by three translational and three rotational springs. The stiffnesses of the springs were varied by trial and error until reasonable correlation with the experimental model was obtained. The two models' frequencies and mode shapes are included in Appendix E.

The possibility of using the finite element model improvement process for joint characterization was investigated briefly.

The improvement process used on the H-Frame structure relies on an expansion technique to expand the experimental mode shapes to the finite element model's dimension prior to improvement. It was shown that this expansion process produces expanded mode shapes which are linear combinations of the finite element modes shapes used in the expansion process. Therefore if the finite element mode shapes do not include displacements across the joint these displacements in the experimental modes shapes will be lost in the expansion process. These displacements are obviously very important in the joint characterization process, therefore an alternate expansion process would have to be employed.

The use of weighting matrices to concentrate the improvements in the joint region was investigated by using two finite element models with different joint properties. The first model was used to produce natural frequencies and mode shapes to simulate an experimental modal model. This eliminated the need for expansion. The second model was assumed to be the original finite element model and was improved using the simulated experimental modal model. The joint properties for the two models are listed in table D.1.

The first eight modes were used in the expansion process. The results of the improvement process are presented in table D.2.

The results show that a significant improvement has been achieved. The results, do however, differ from those achieved in the H-Frame expansion

DEGREE OF FREEDOM	MODEL 1	MODEL 2
STIFFNESS		
X	1.0E+08	5.0E+07
Y	1.0E+08	5.0E+07
Z	1.0E+09	5.0E+06
RX	1.0E+06	5.0E+05
RY	1.0E+06	5.0E+05
RZ	1.0E+07	5.0E+06
MASS		
X	1.0E-02	2.0E-02
Y	1.0E-02	2.0E-02
Z	1.0E-02	2.0E-02
RX	5.0E-03	1.0E-02
RY	5.0E-03	1.0E-02
RZ	5.0E-03	1.0E-02

Table D.1: Finite Element Joint Properties

MODE NO.	"EXPERIMENTAL"	ORIGINAL	IMPROVED
1	42.73	42.66	42.63
2	145.32	135.40	145.23
3	158.14	151.25	157.93
4	180.92	152.13	180.76
5	237.78	236.36	237.10
6	381.52	319.87	381.25
7	383.04	342.25	382.23
8	441.58	387.01	441.14
9	624.01	612.91	616.24
10	693.51	647.15	691.63
11	774.90	697.31	771.86
12	790.94	755.14	786.73
13	1049.55	1037.35	1046.75
14	1058.72	1046.20	1056.45

Table D.2: Joint Improvement Results

process. The improved frequencies do not agree exactly with the experimental results and the modes not included in the improvement process have been effected. There are two possible reasons for these differences. Firstly, the "experimental" mode shapes are no longer in the matrix space spanned by the corresponding finite element mode shapes and secondly the number of variables in the improvement process has been severely limited.

APPENDIX E: ADDITIONAL RESULTS

Original Modal Models

0.992	0.000	0.000	0.001	0.000	0.000	0.031	0.000	0.001	0.000	0.006	0.000
0.004	0.993	0.028	0.001	0.000	0.000	0.000	0.000	0.008	0.000	0.000	0.000
0.000	0.023	0.975	0.002	0.000	0.000	0.007	0.000	0.025	0.000	0.000	0.000
0.000	0.000	0.000	0.983	0.000	0.015	0.000	0.001	0.000	0.001	0.000	0.005
0.000	0.001	0.000	0.018	0.960	0.003	0.000	0.010	0.000	0.024	0.000	0.000
0.000	0.000	0.001	0.001	0.027	0.938	0.000	0.001	0.001	0.000	0.000	0.032
0.028	0.001	0.004	0.002	0.000	0.000	0.974	0.000	0.001	0.000	0.033	0.000
0.001	0.002	0.003	0.000	0.016	0.000	0.000	0.929	0.009	0.022	0.000	0.000
0.000	0.006	0.013	0.015	0.000	0.000	0.000	0.000	0.910	0.000	0.004	0.000
0.000	0.000	0.001	0.003	0.016	0.000	0.001	0.009	0.001	0.738	0.001	0.002
0.013	0.000	0.001	0.069	0.000	0.000	0.035	0.000	0.000	0.000	0.840	0.003

Table E.1: Modal Assurance Criteria Matrix

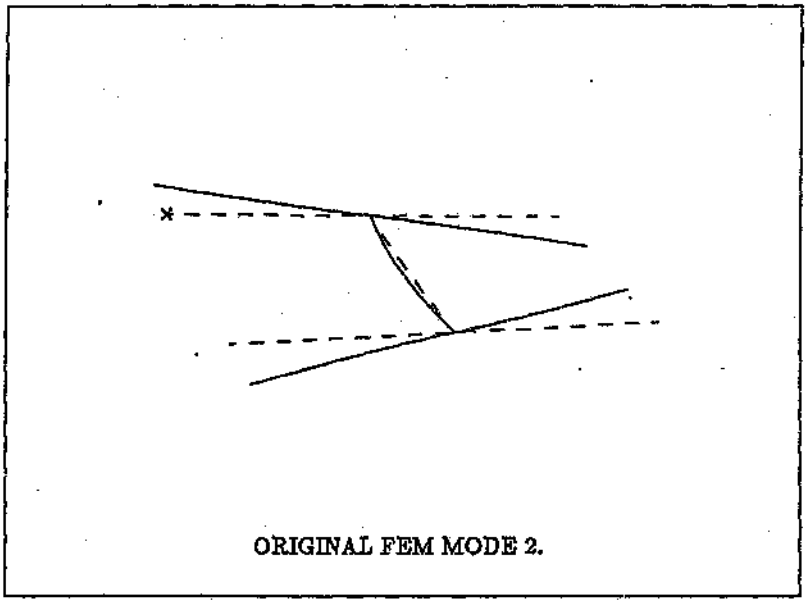

Figure E.1: H-frame Mode 2

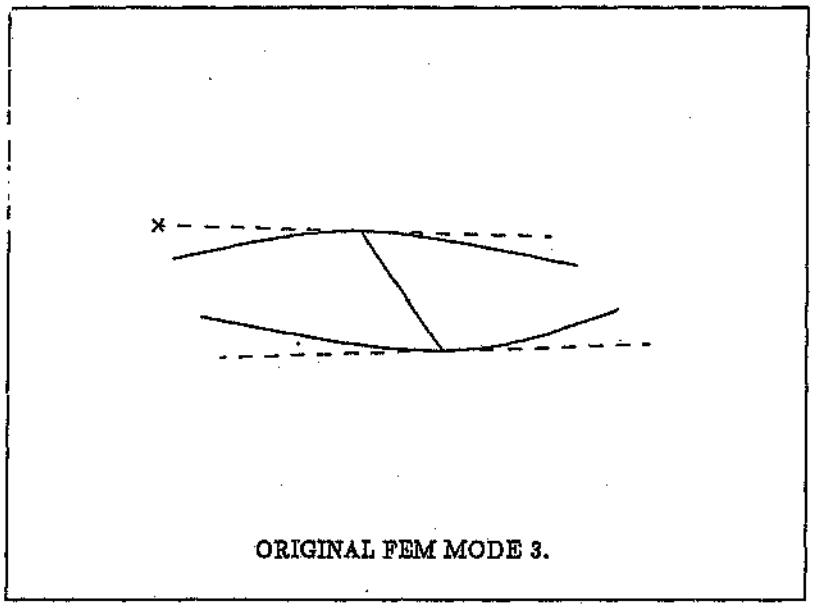

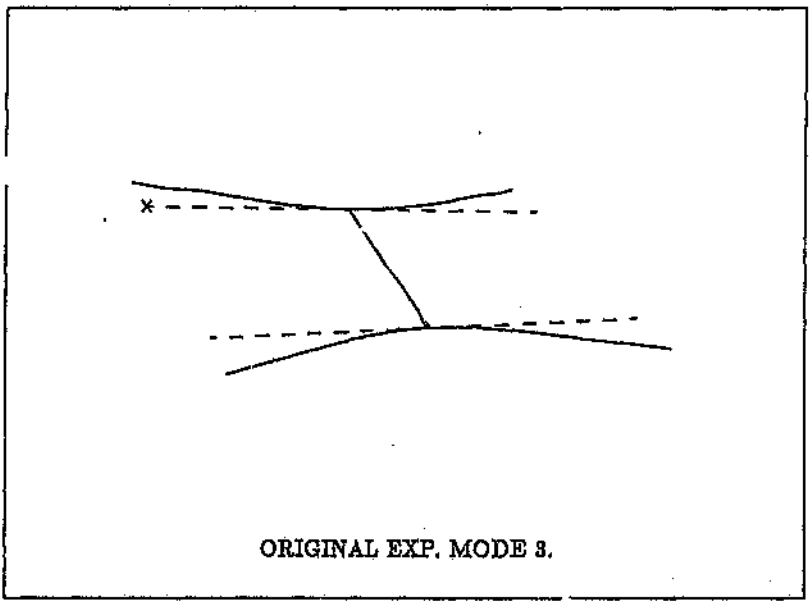

Figure E.2: H-frame Mode 3

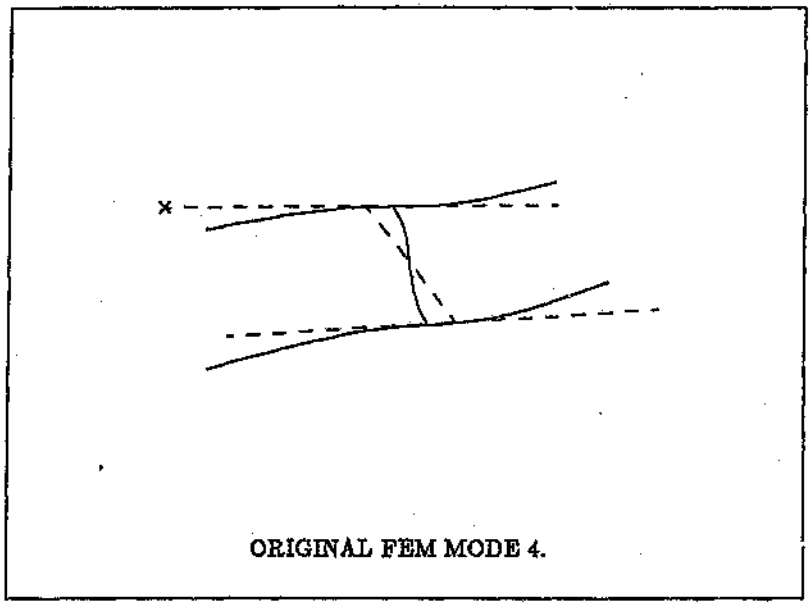

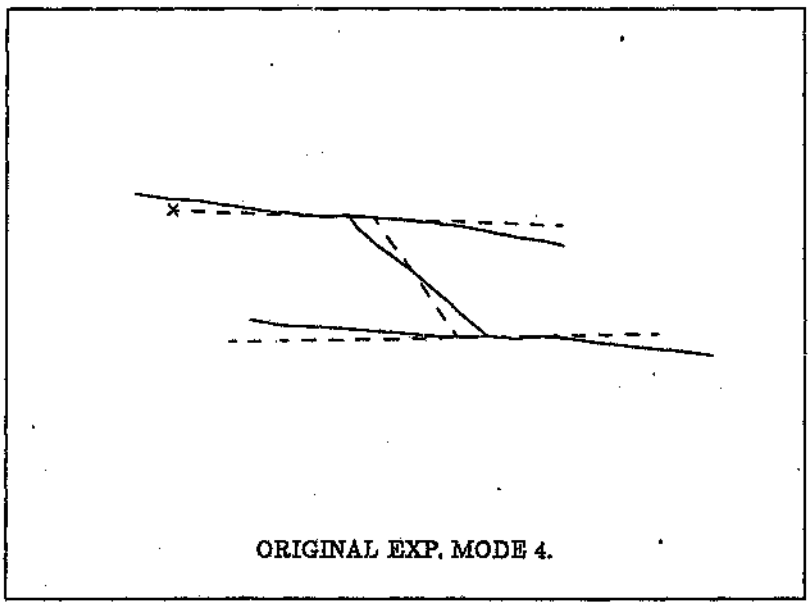

Figure E.3: H-frame Mode 4

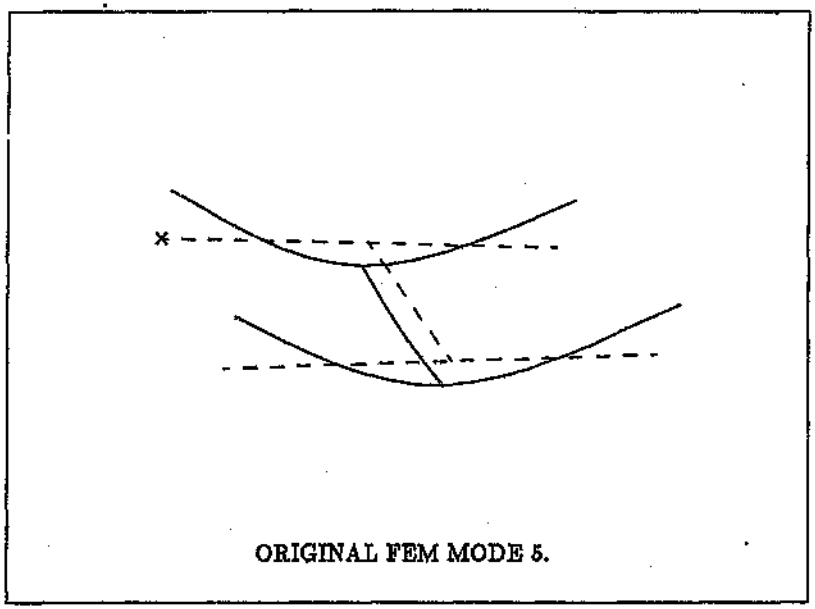

ORIGINAL FEM MODE 5.

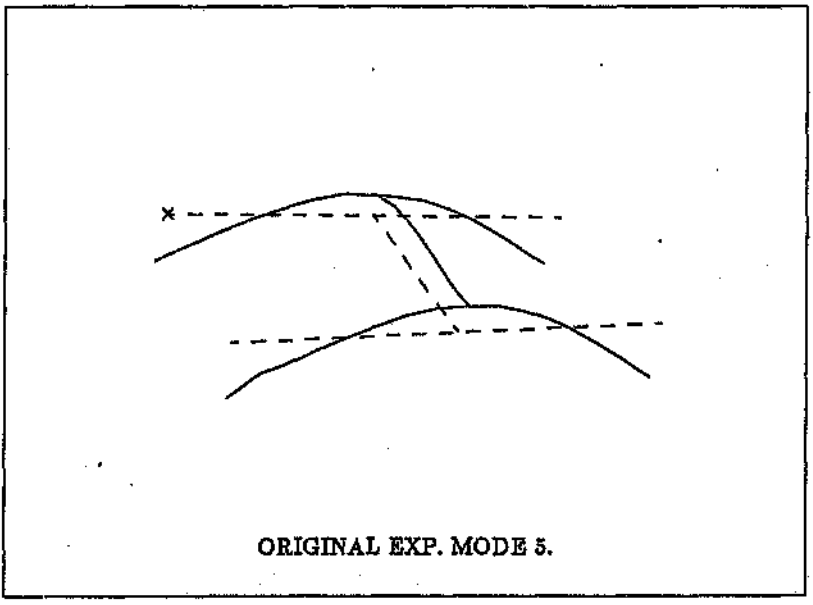

ORIGINAL EXP. MODE 5.

Figure E.4: H-frame Mode 5

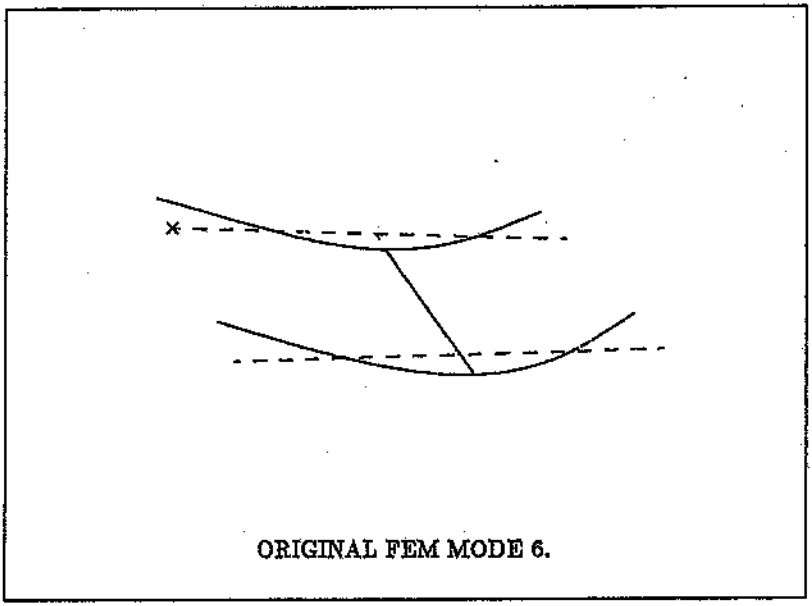

ORIGINAL FEM MODE 6.

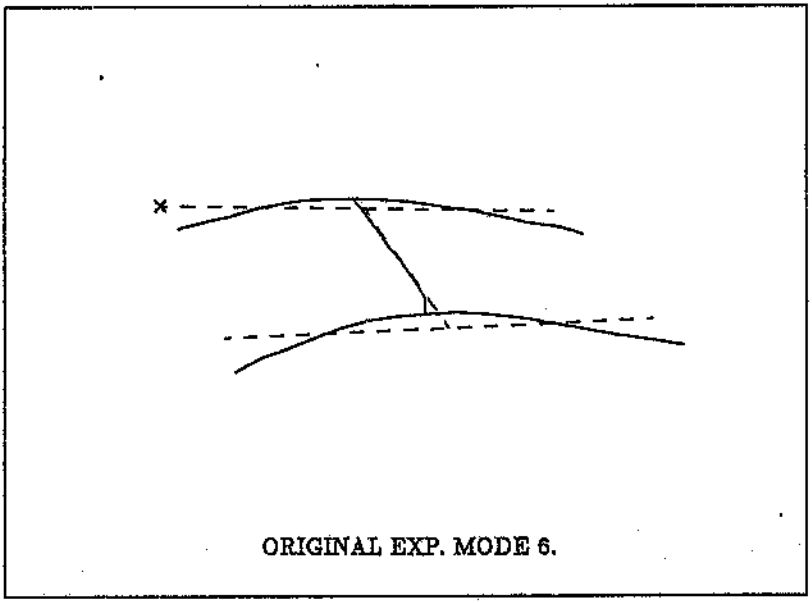

ORIGINAL EXP. MODE 6.

Figure E.5: H-frame Mode 6

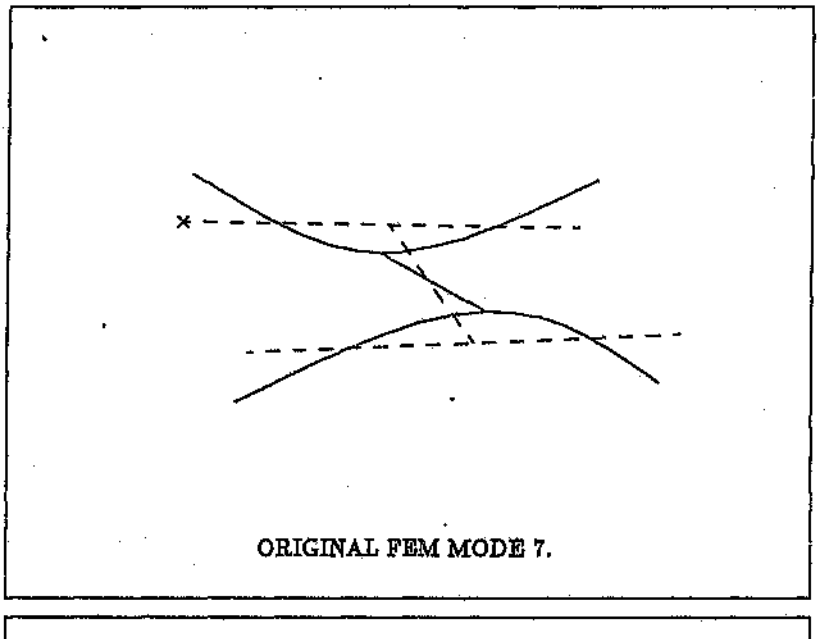

Figure E.6: H-frame Mode 7

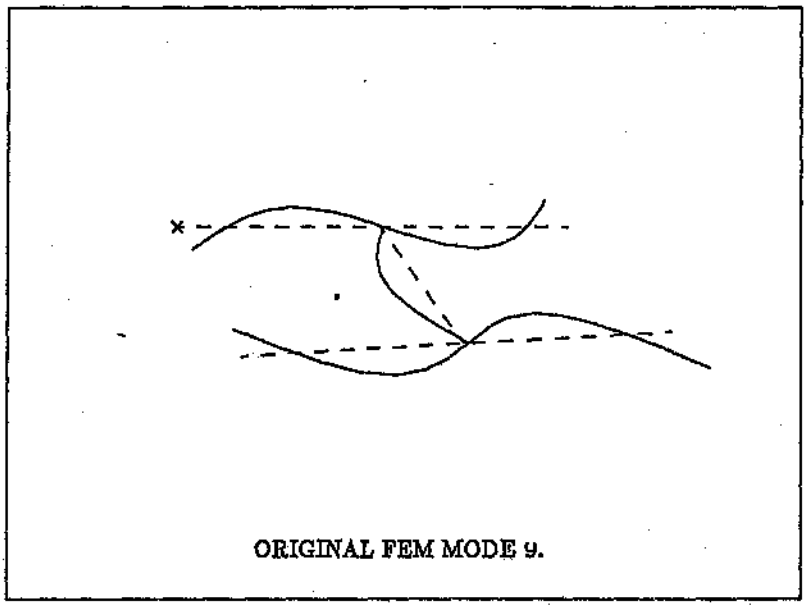

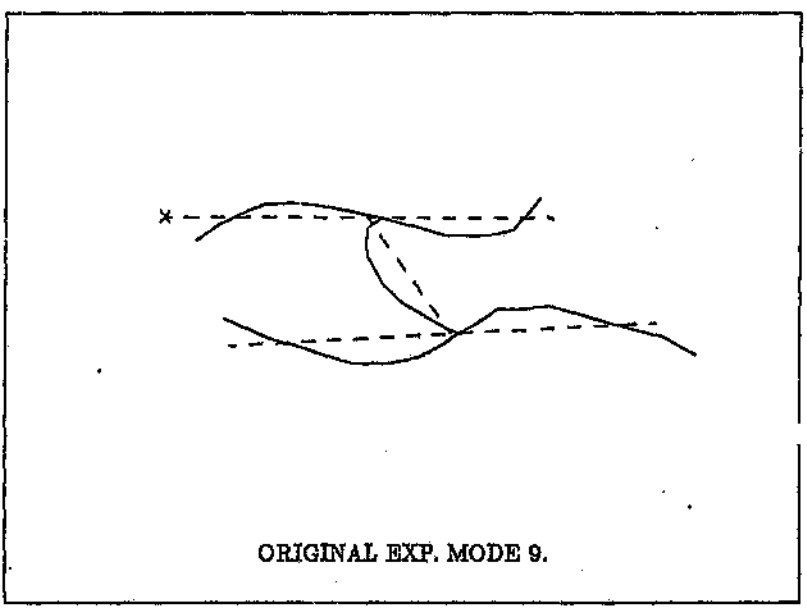

Figure E.7: H-frame Mode 9

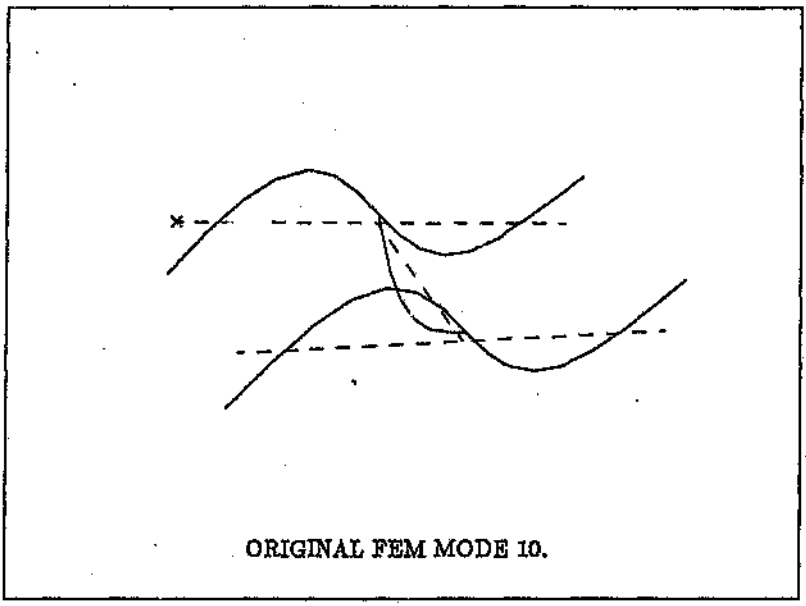

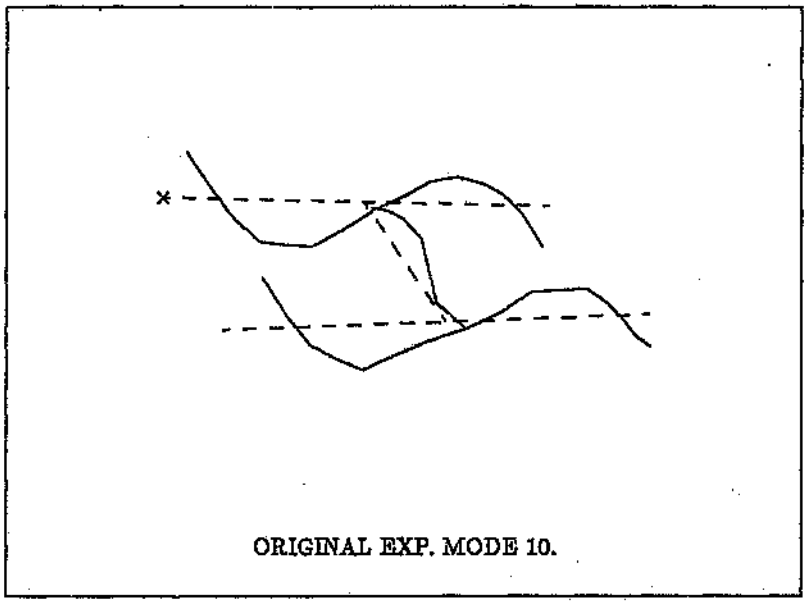

Figure E.8: H-frame Mode 10

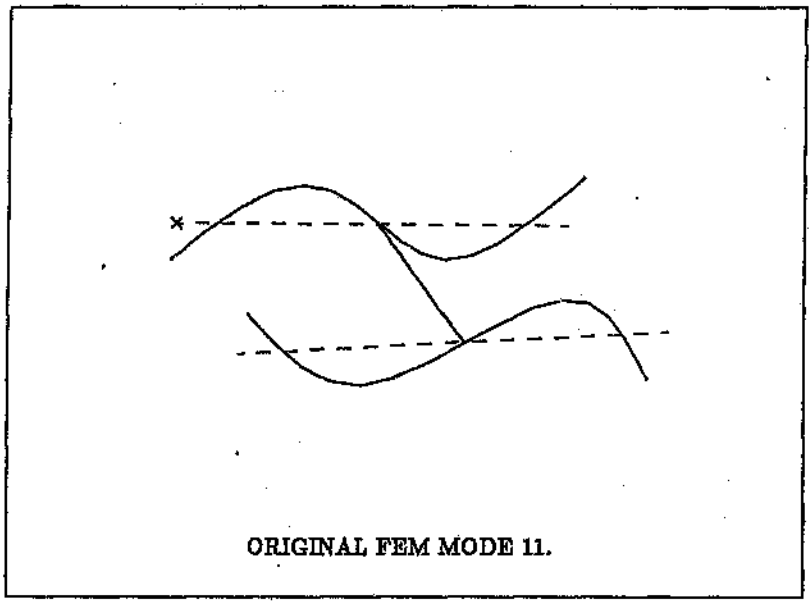

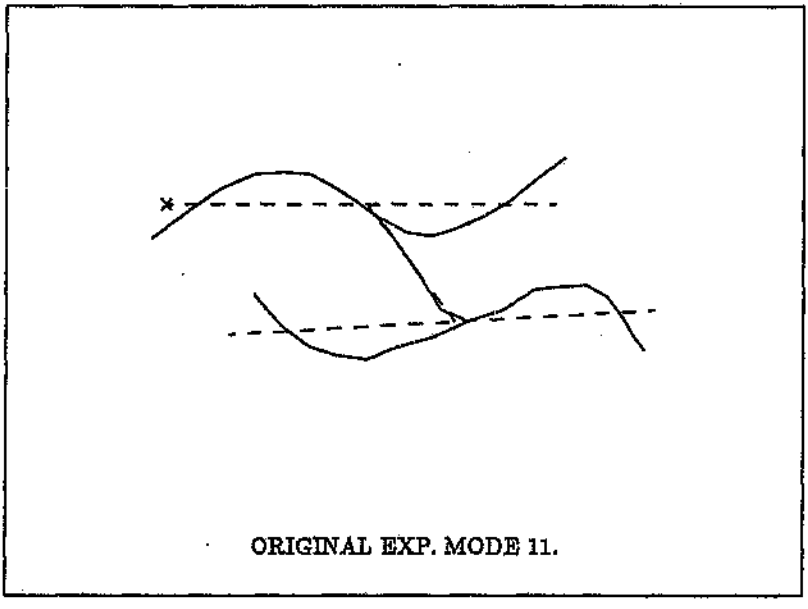

Figure E.9: H-frame Mode 11

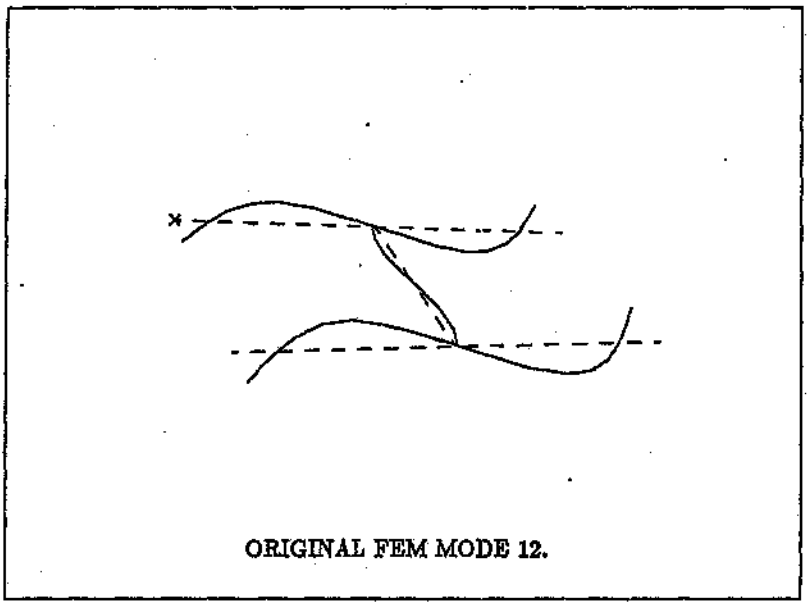

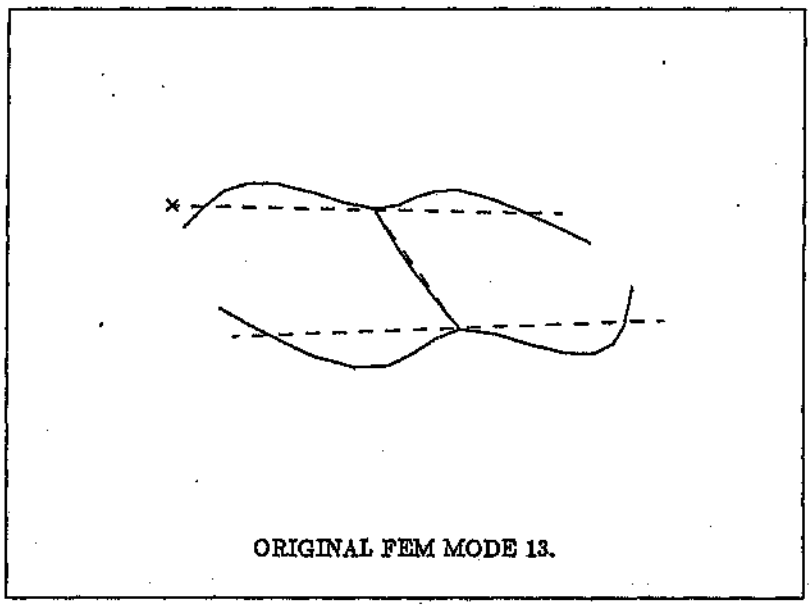

Figure E.10: H-frame Modes 12 and 13

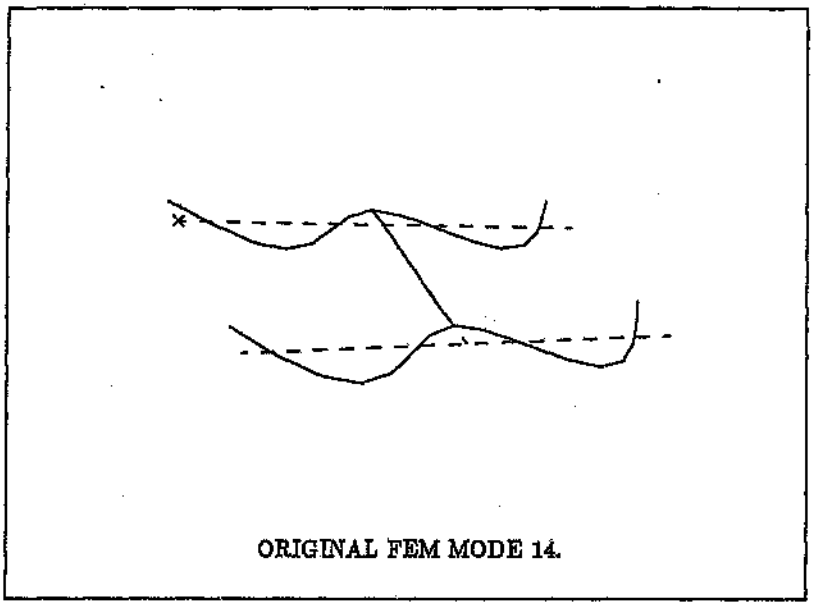

Figure E.11: H-frame Mode 14

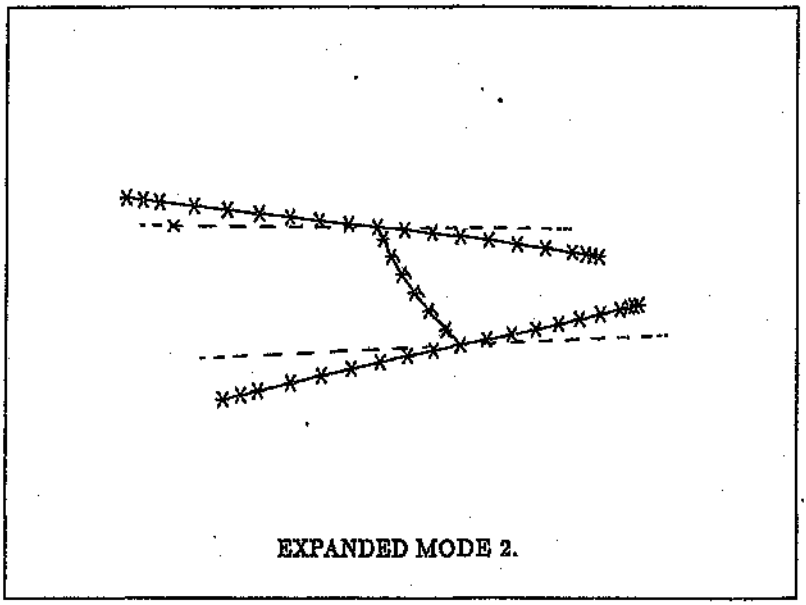

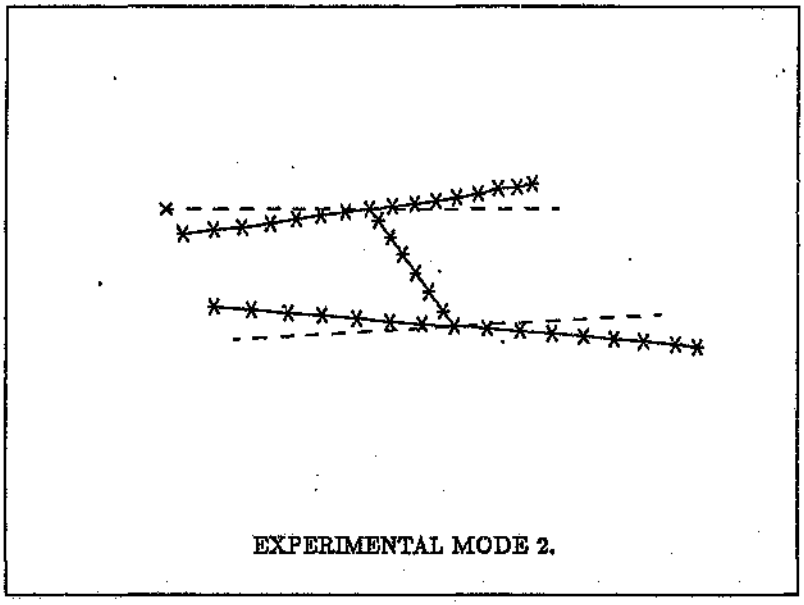

Figure E.12: Expansion of Mode 2

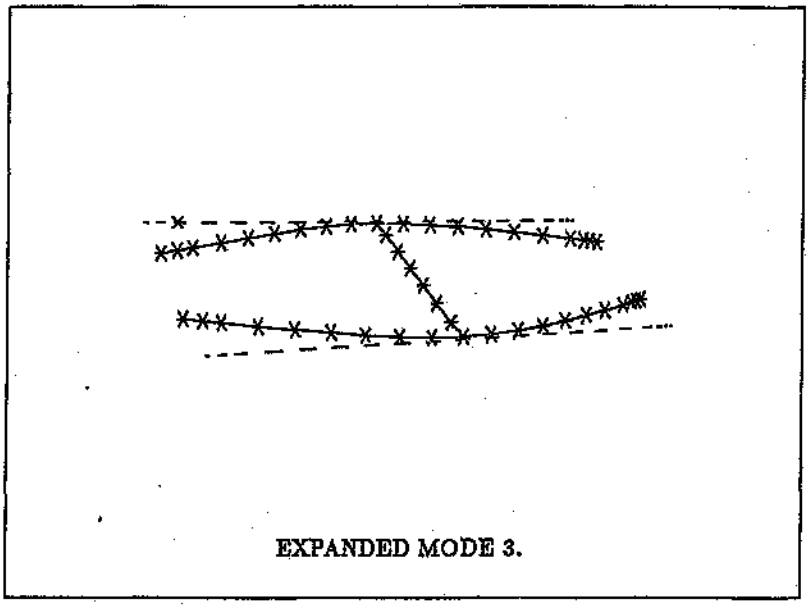

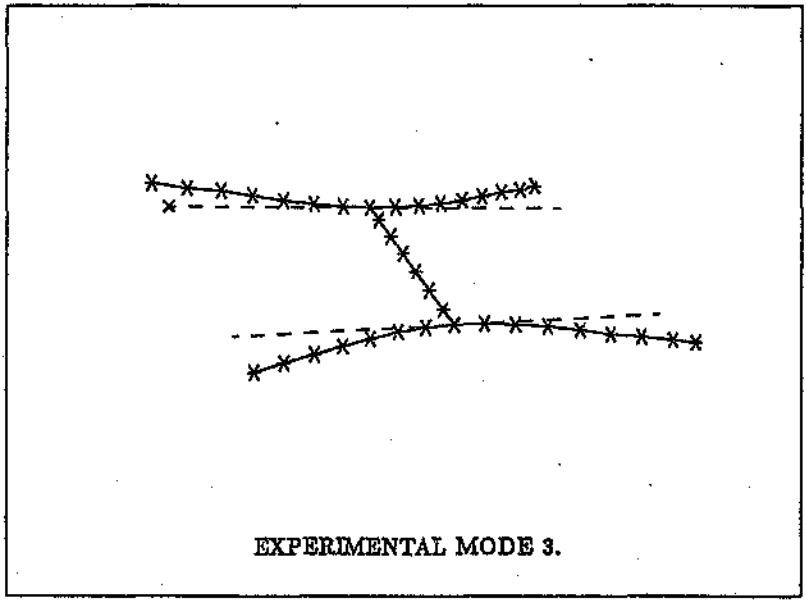

Figure E.13: Expansion of Mode 3

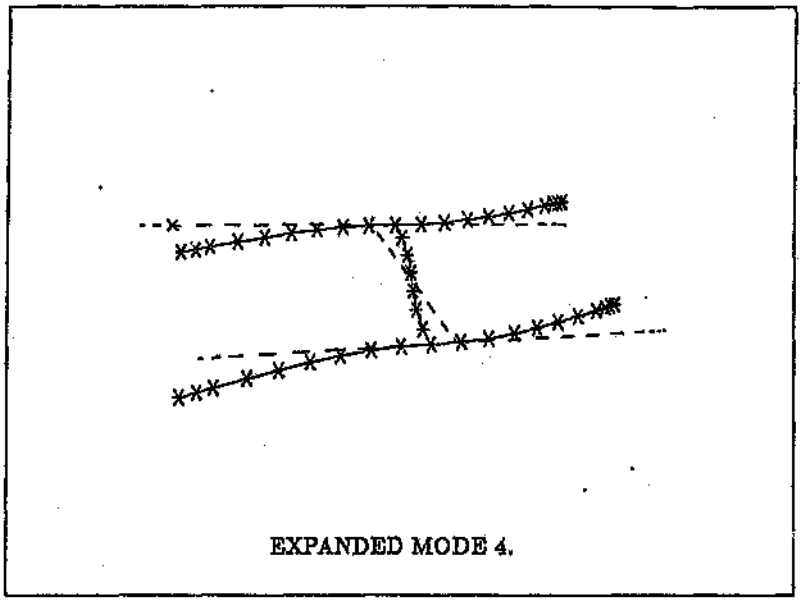

EXPANDED MODE 4.

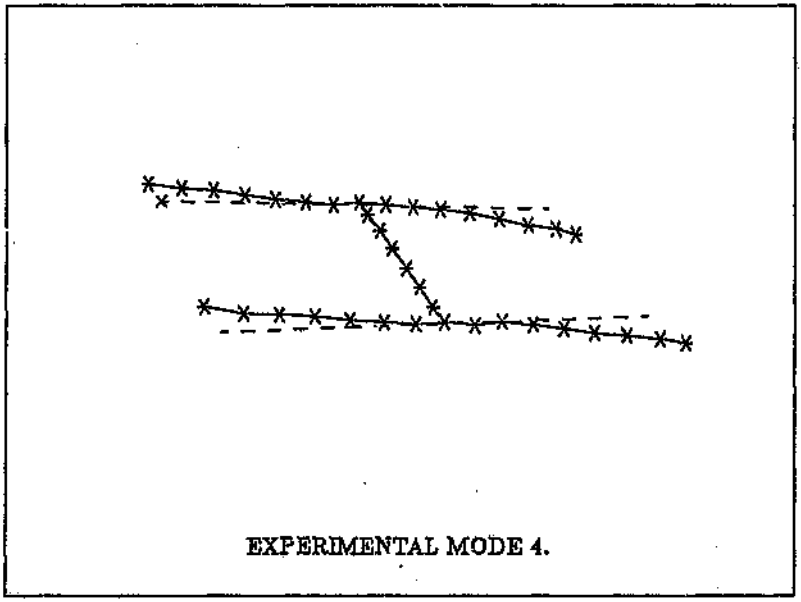

EXPERIMENTAL MODE 4.

Figure E.14: Expansion of Mode 4

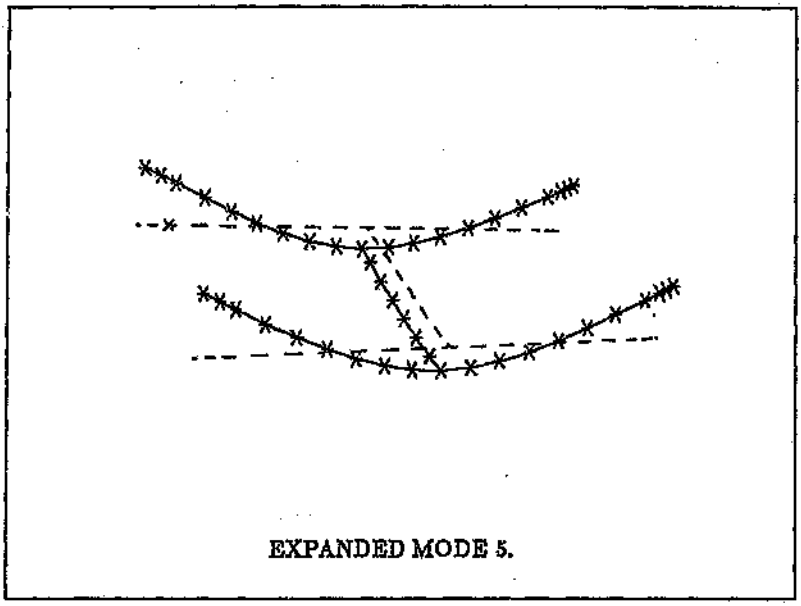

Figure E.5: Expansion of Mode 5

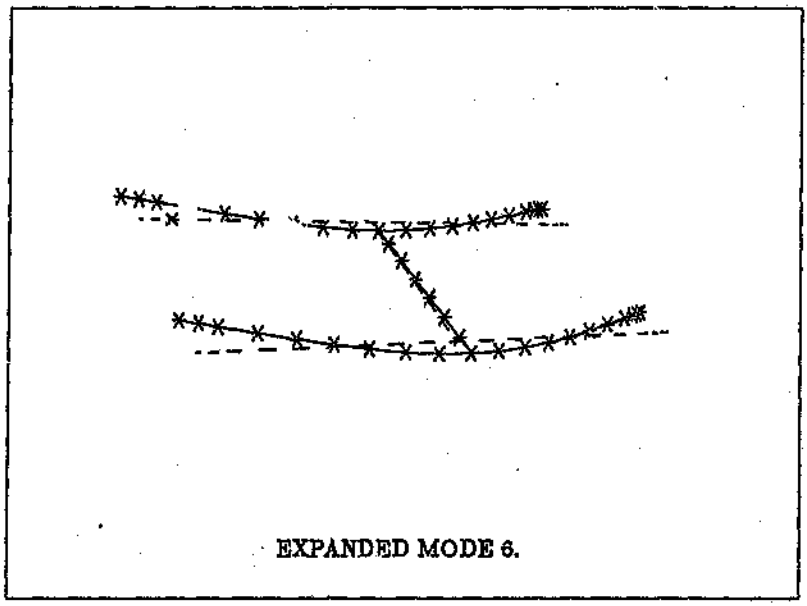

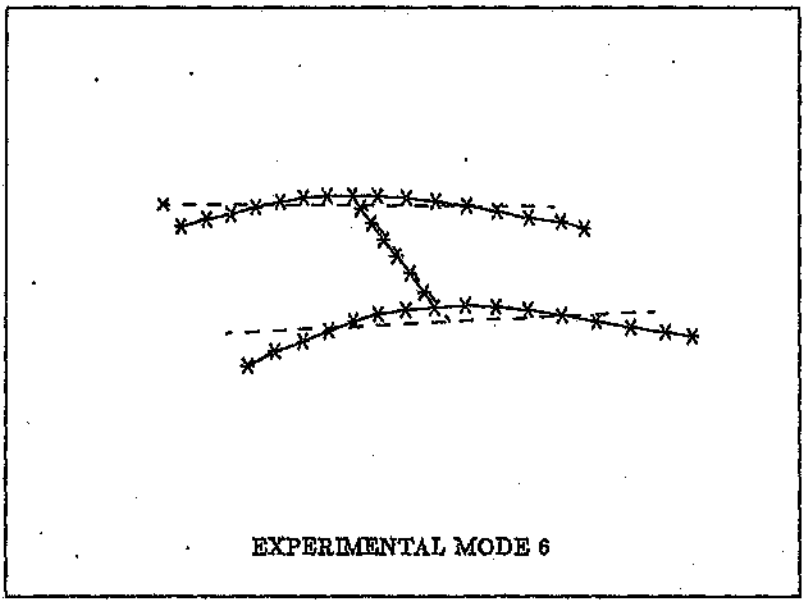

Figure E.16: Expansion of Mode 6

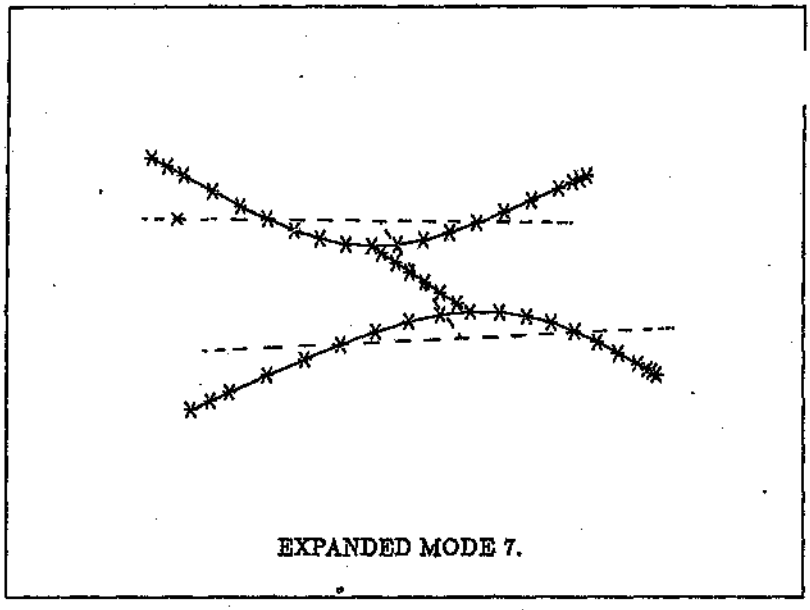

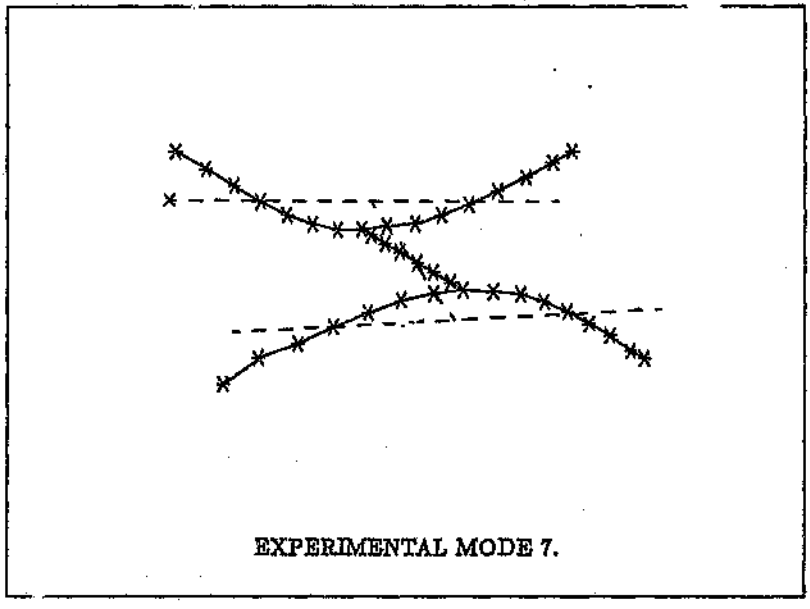

Figure E.17: Expansion of Mode 7

Modified Structure Mode Shapes

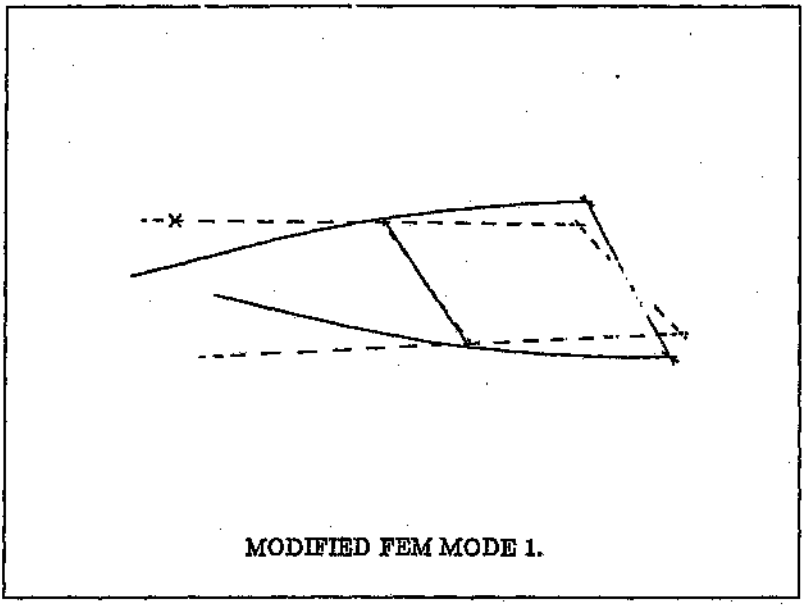

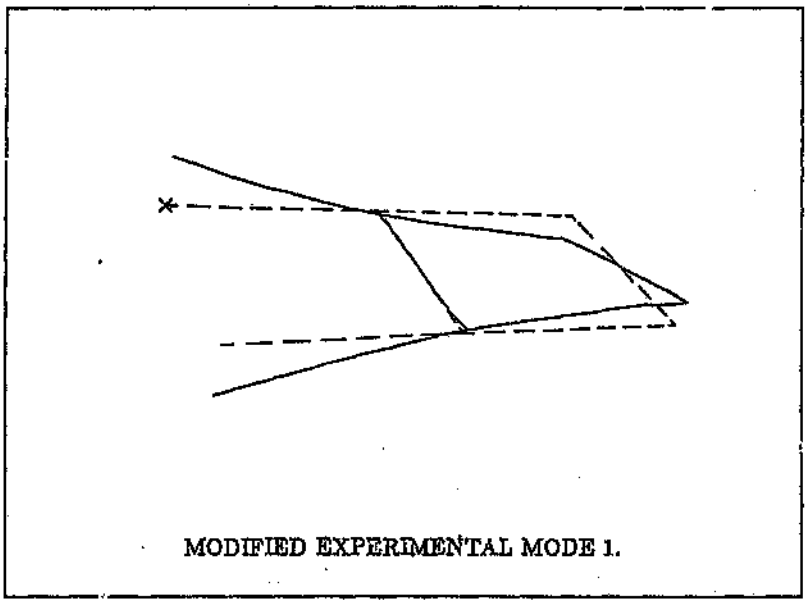

Figure E.18: Modified Structure Mode 1

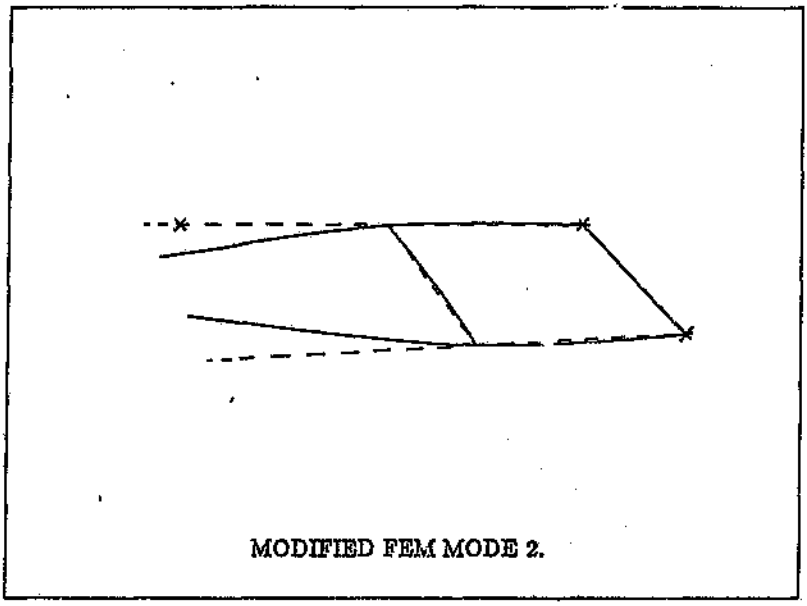

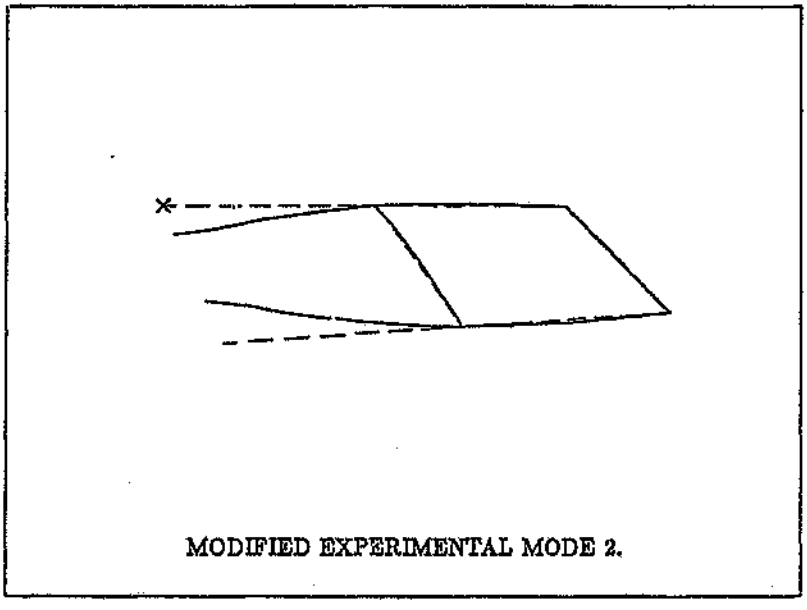

Figure E.19: Modified Structure Mode 2

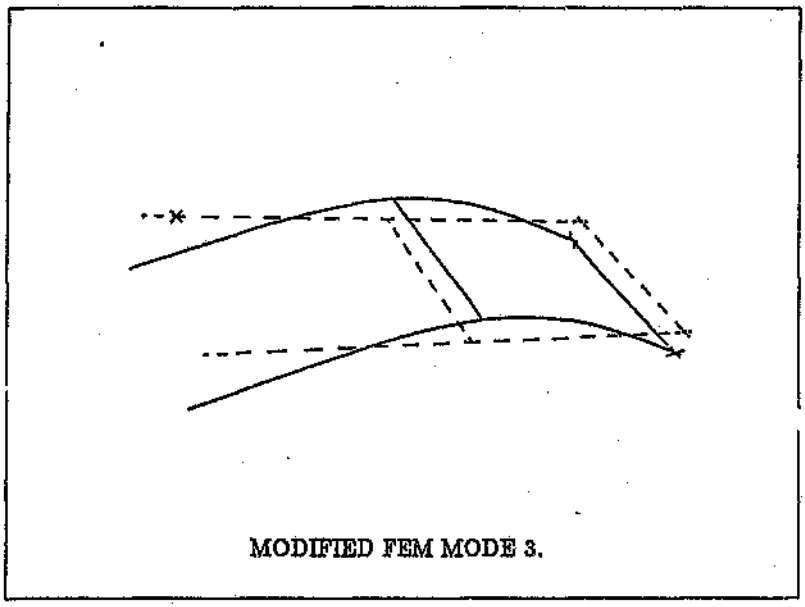

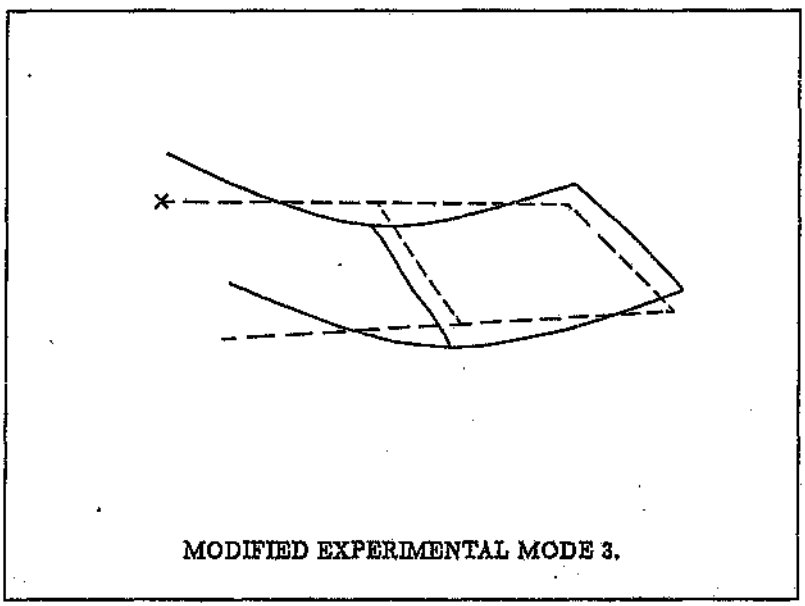

Figure E.20: Modified Structure Mode 3

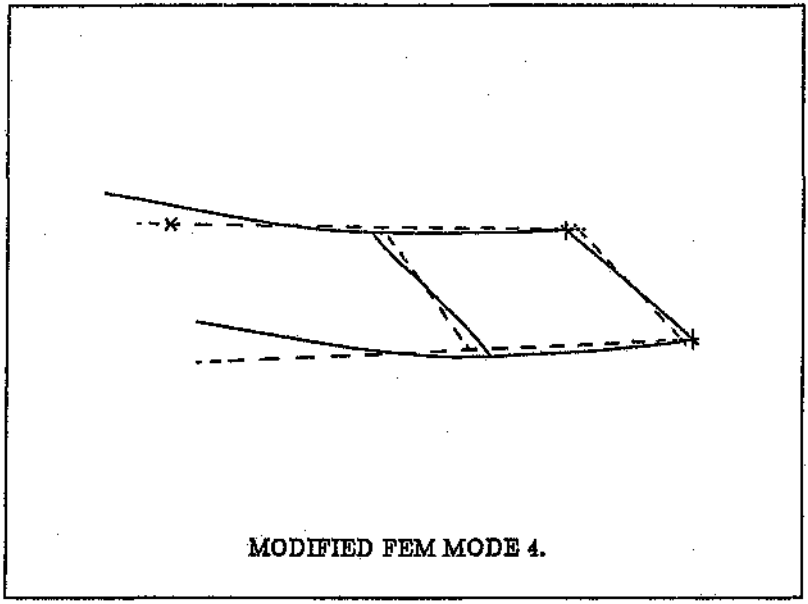

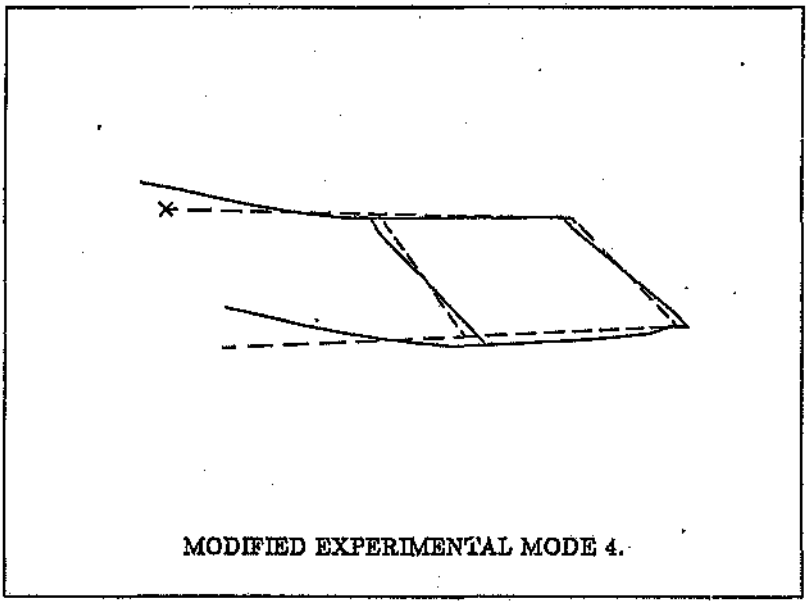

Figure E.21: Modified Structure Mode 4

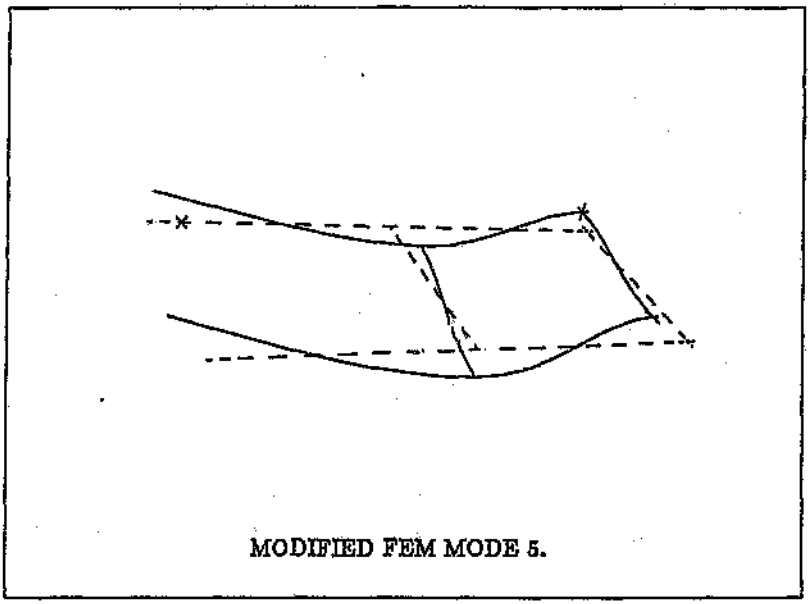

MODIFIED FEM MODE 5.

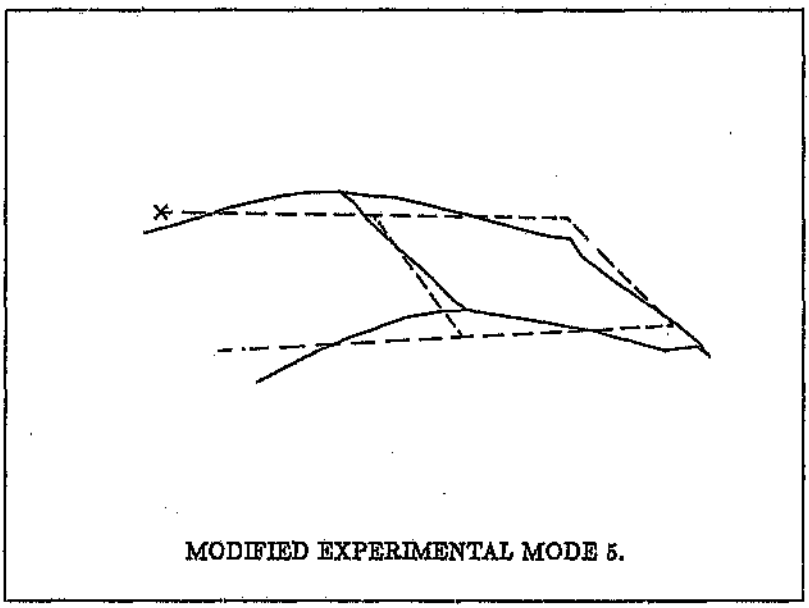

MODIFIED EXPERIMENTAL MODE 5.

Figure E.22: Modified Structure Mode 5

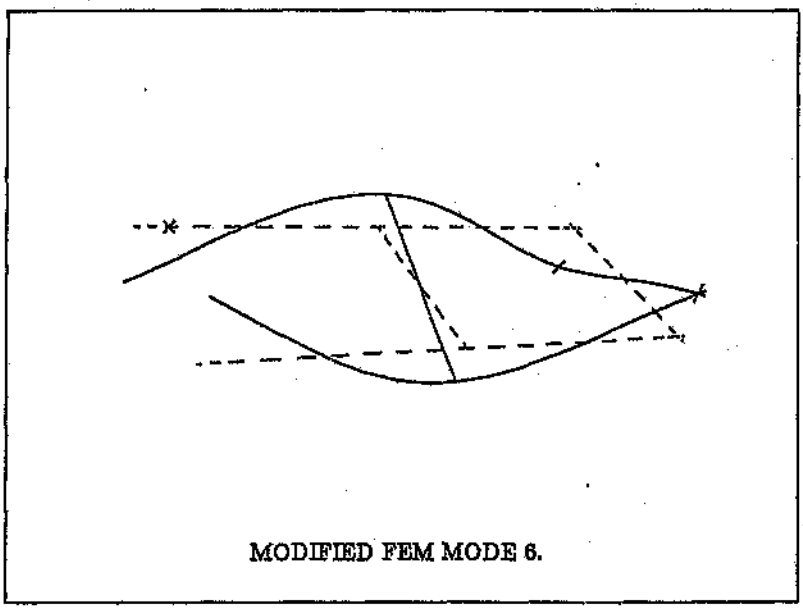

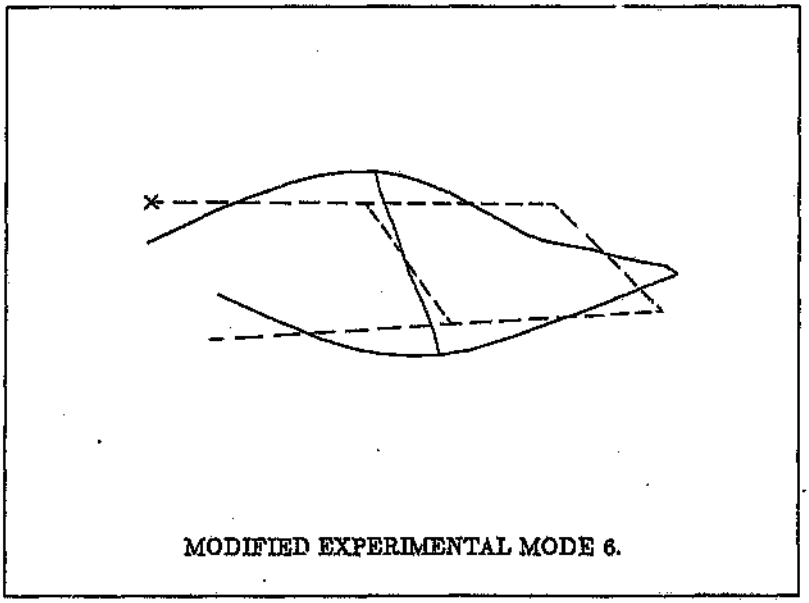

Figure E.23: Modified Structure Mode 6

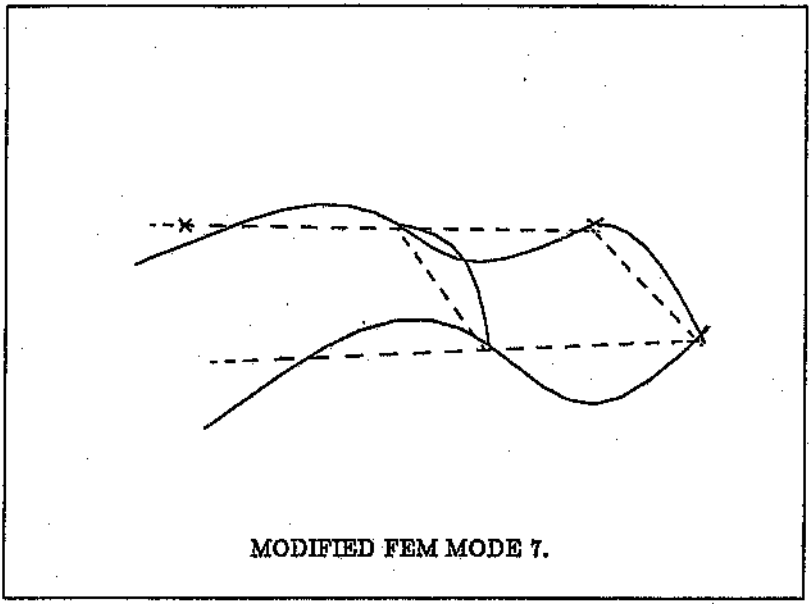

MODIFIED FEM MODE 7.

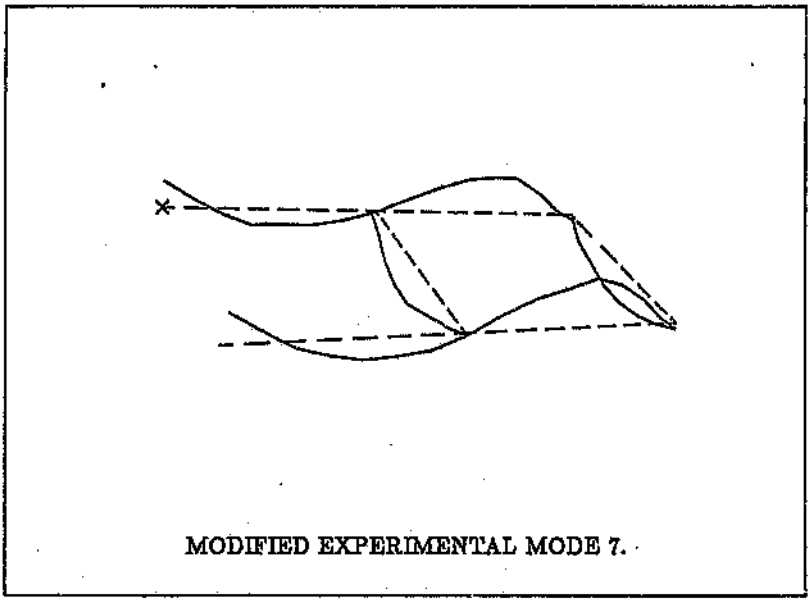

MODIFIED EXPERIMENTAL MODE 7.

Figure E.24: Modified Structure Mode 7

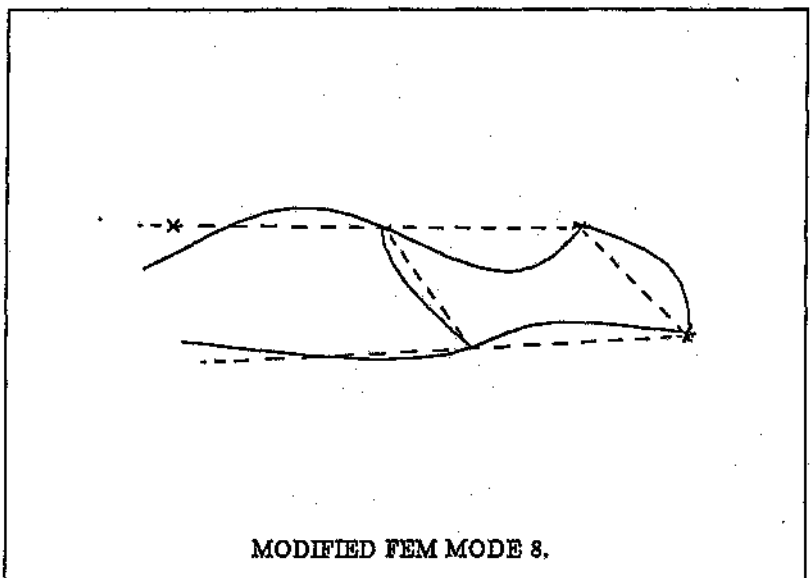

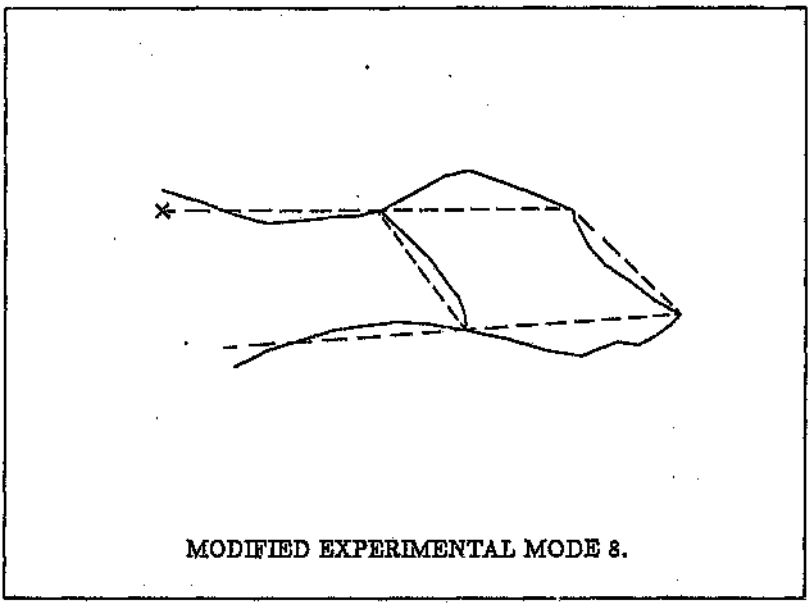

Figure E.25: Modified Structure Mode 8

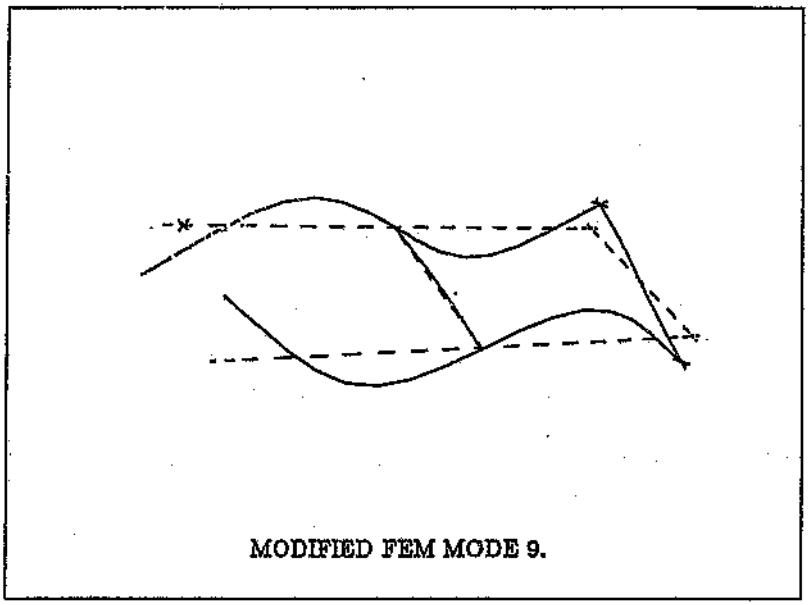

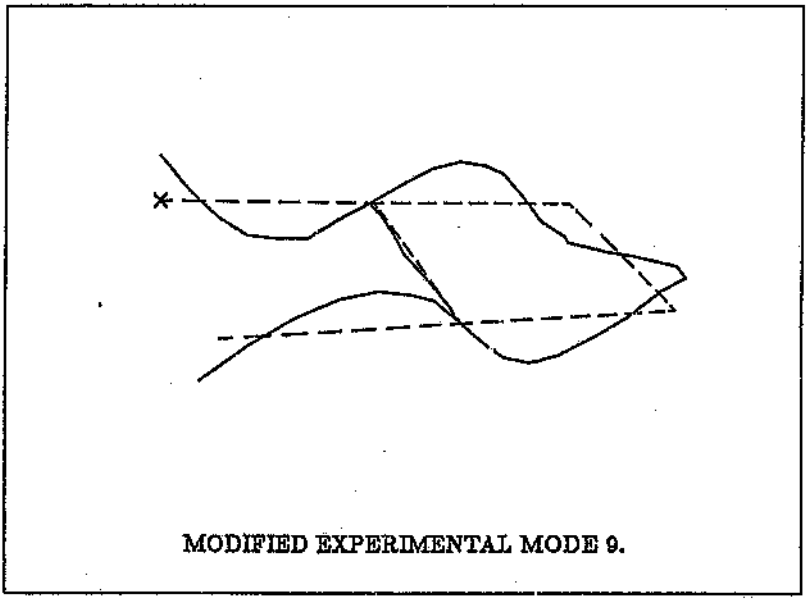

Figure E.26: Modified Structure Mode 9

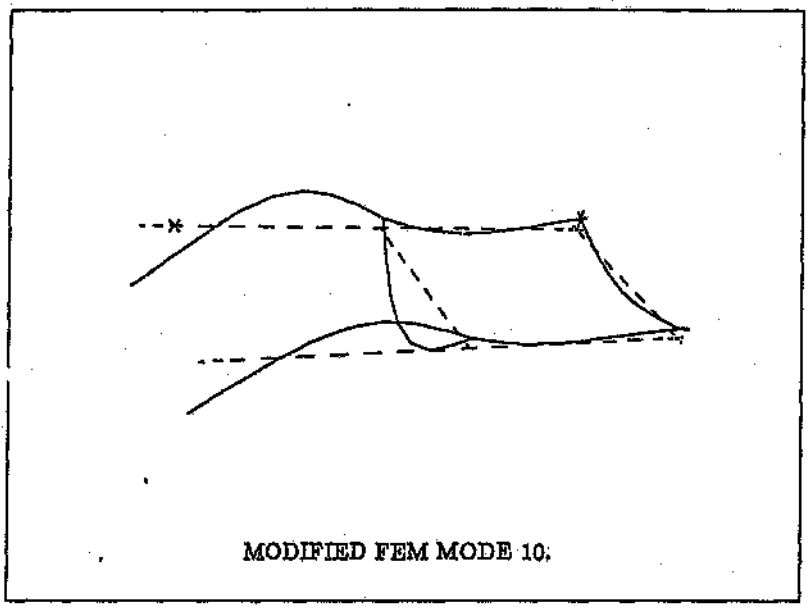

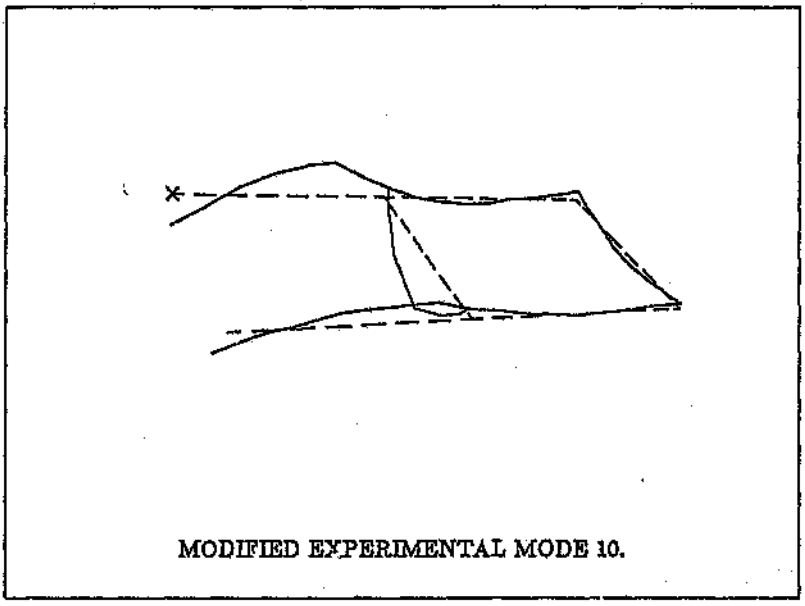

Figure E.27: Modified Structure Mode 10

Joint Characterization

MODE NO.	EXPERIMENTAL	FINITE ELEMENT
1	38.84	40.83
2	148.26	149.58
3	156.95	158.61
4	213.17	215.84
5	218.80	227.16
6	474.64	478.74
7	490.72	488.88
8	567.05	582.66
9	590.83	598.032

Table E.2: Joint Model Frequencies

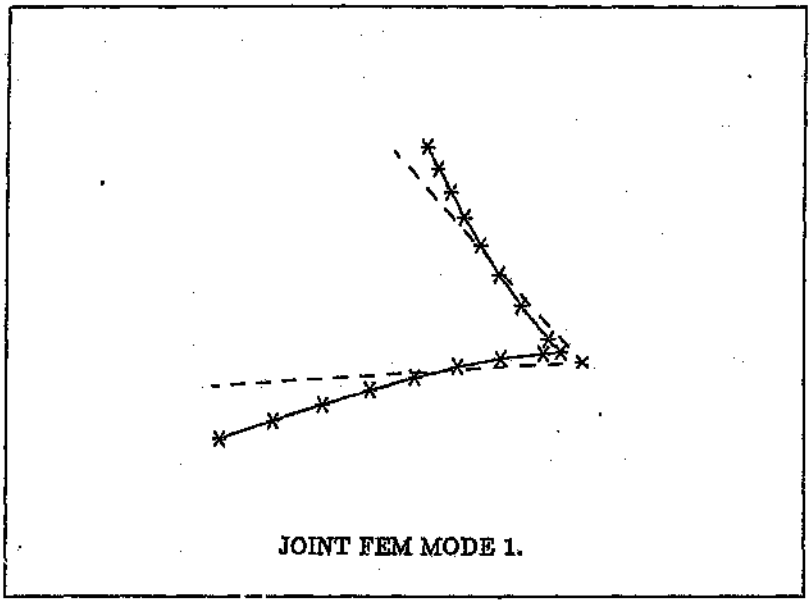

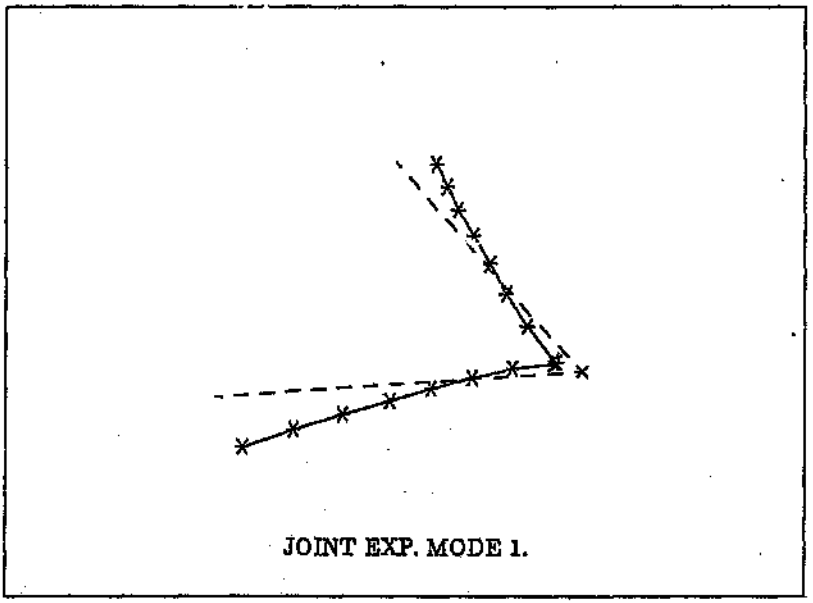

Figure E.28: Joint Mode 1

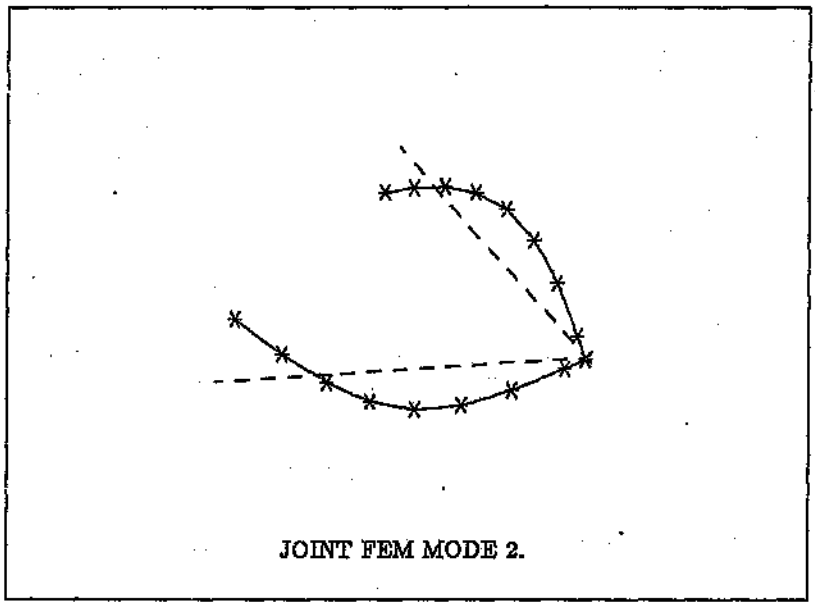

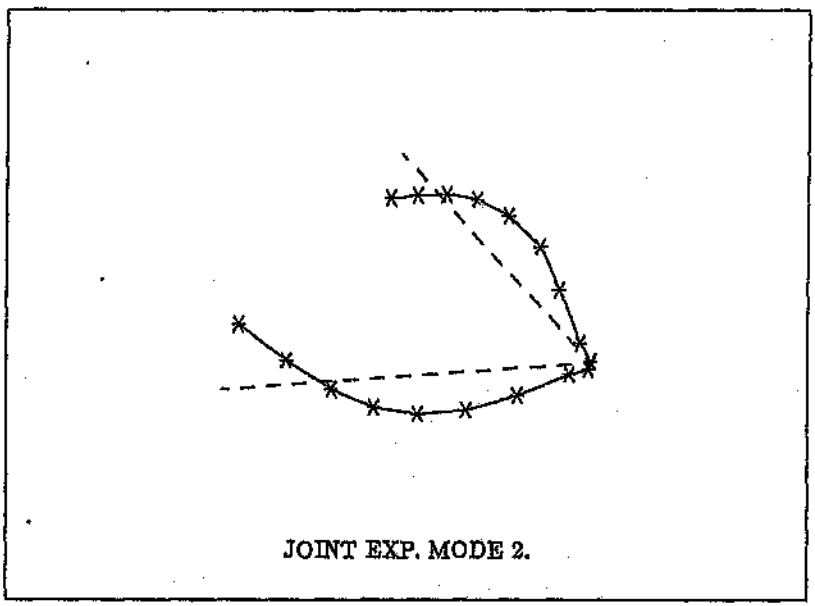

Figure E.29: Joint Mode 2

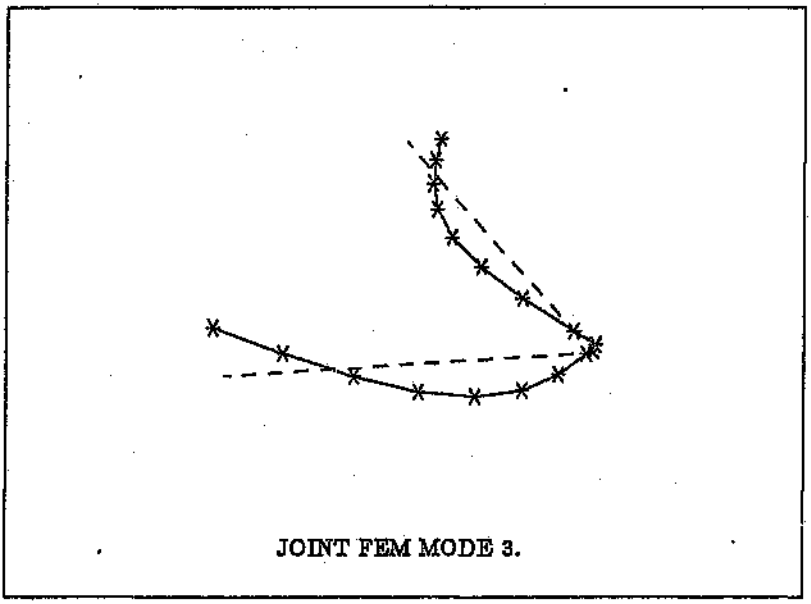

JOINT FEM MODE 3.

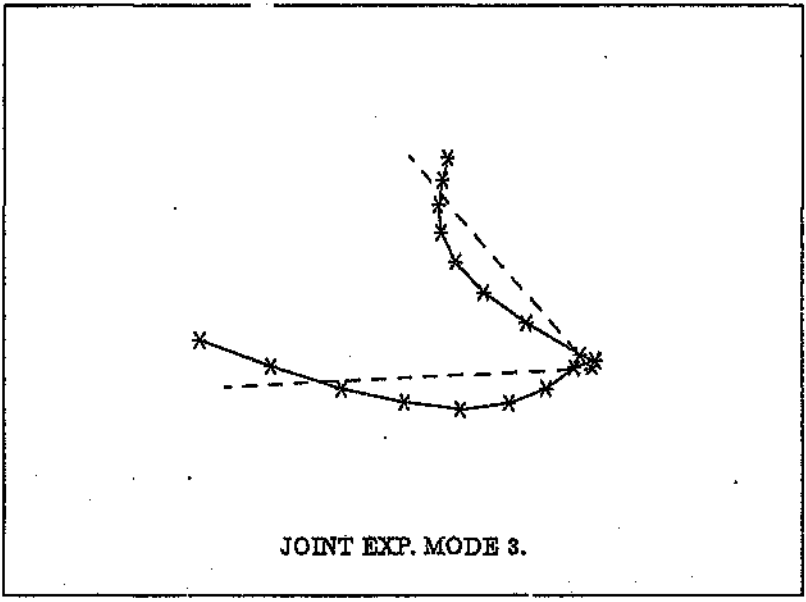

JOINT EXP. MODE 3.

Figure E.30: Joint Mode 3

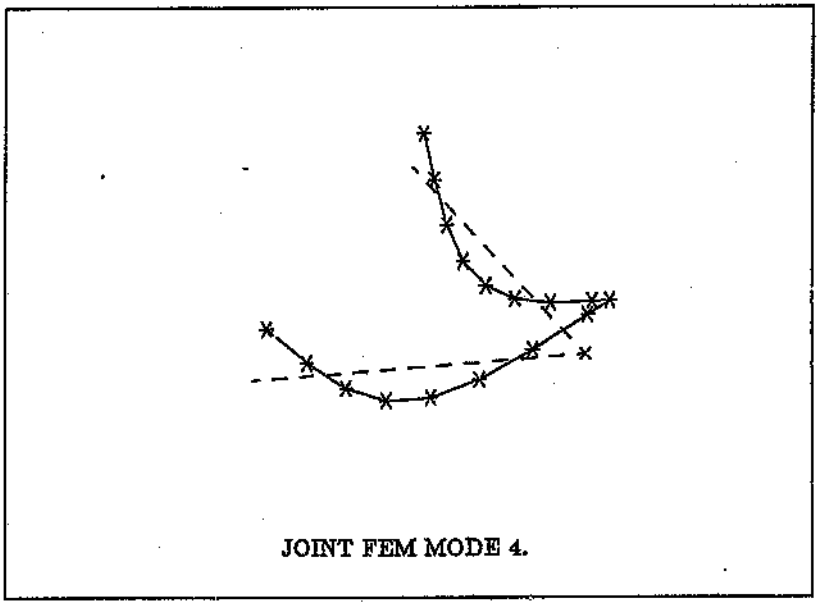

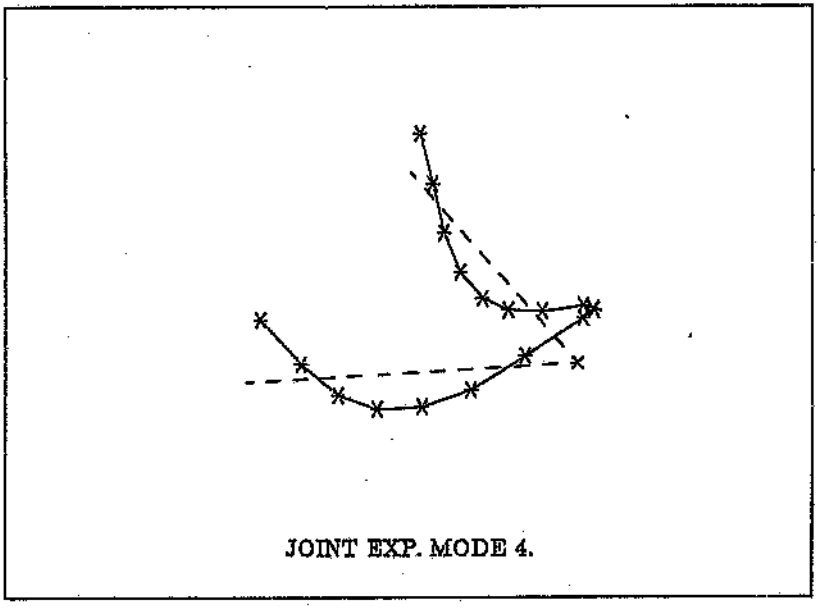

Figure E.31: Joint Mode 4

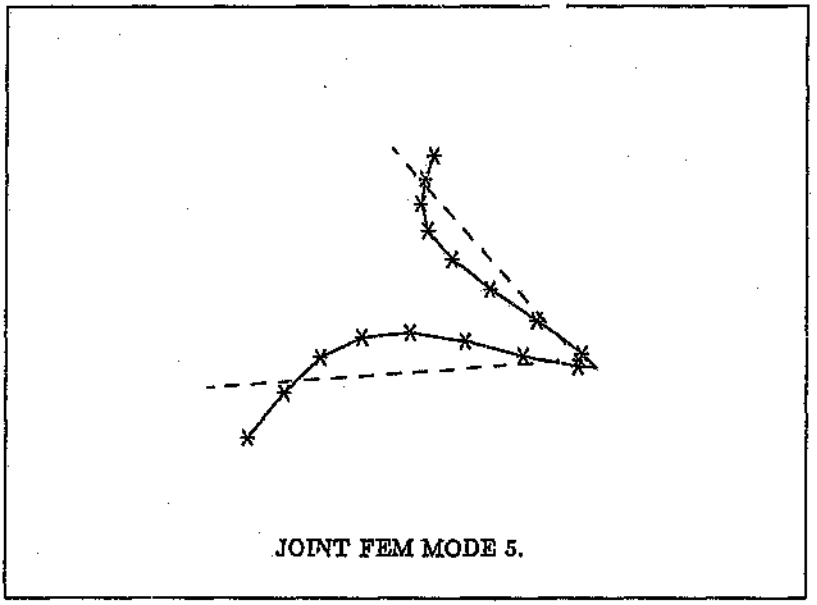

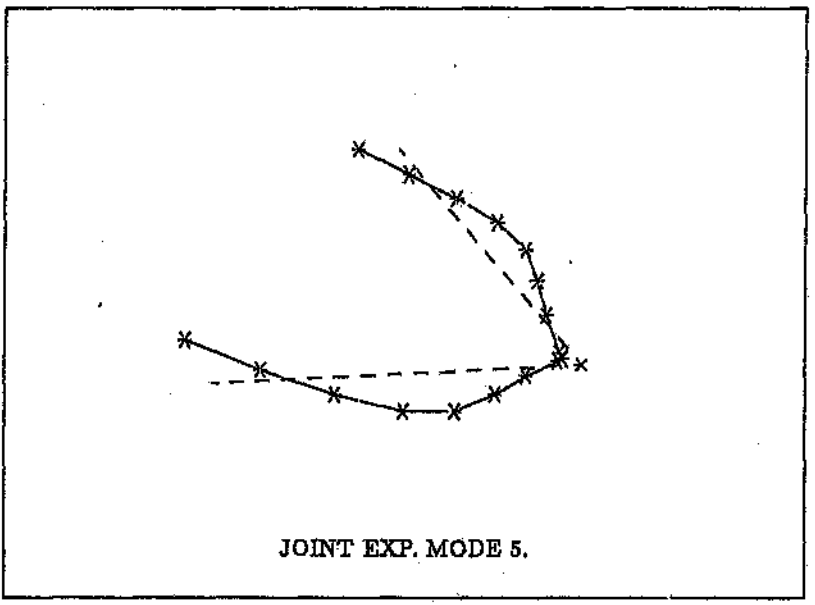

Figure E.32: Joint Mode 5

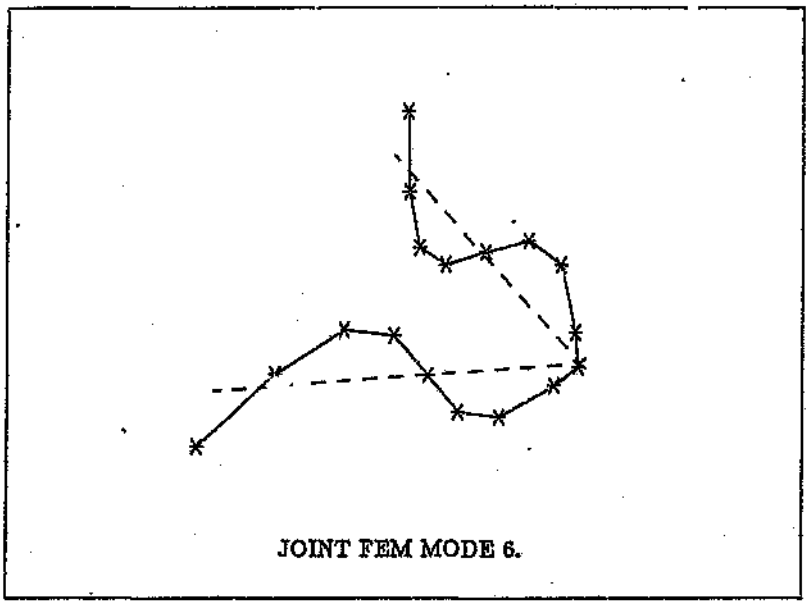

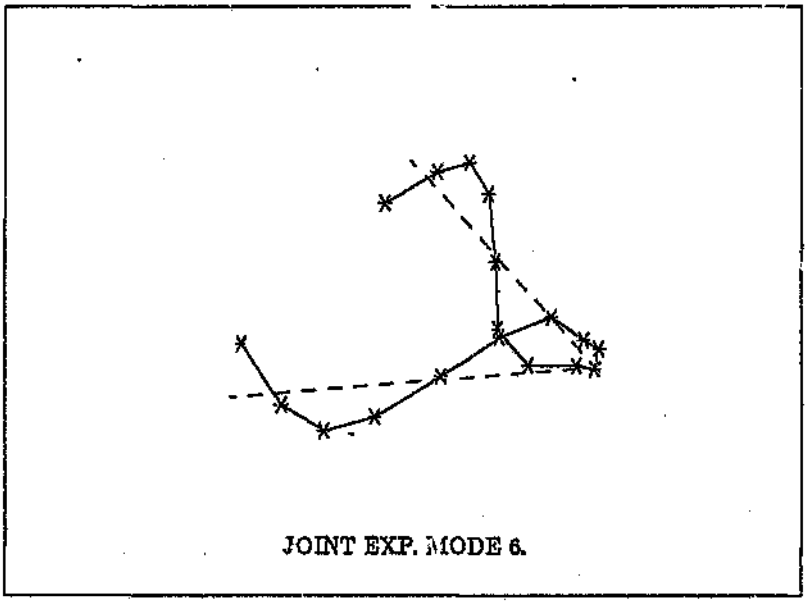

Figure E.33: Joint Mode 6

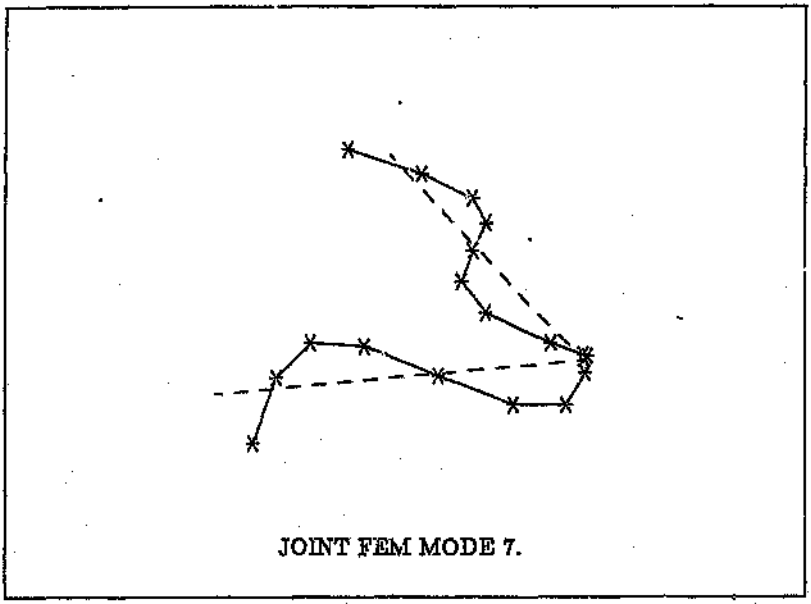

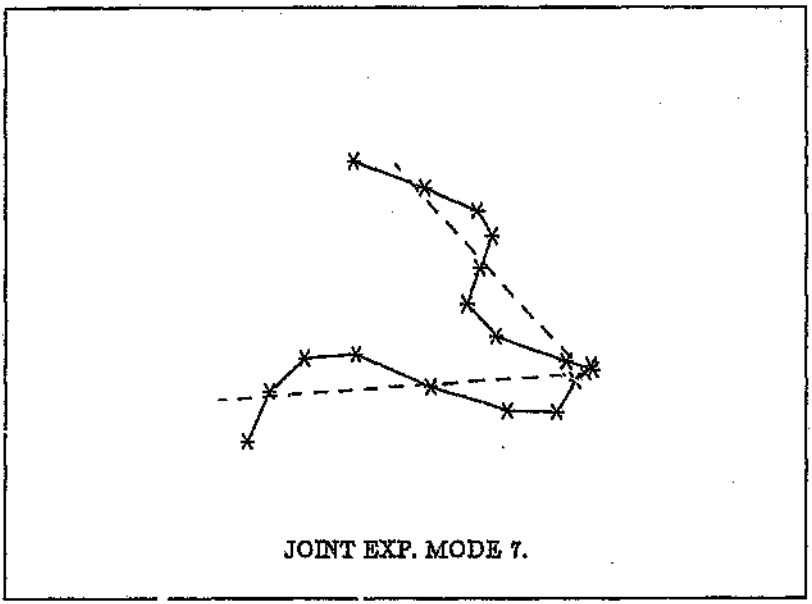

Figure E.34: Joint Mode 7

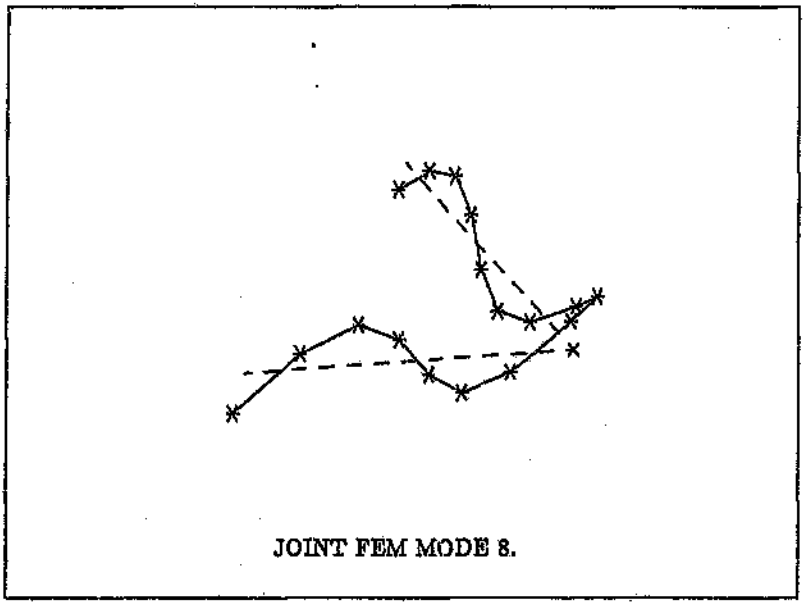

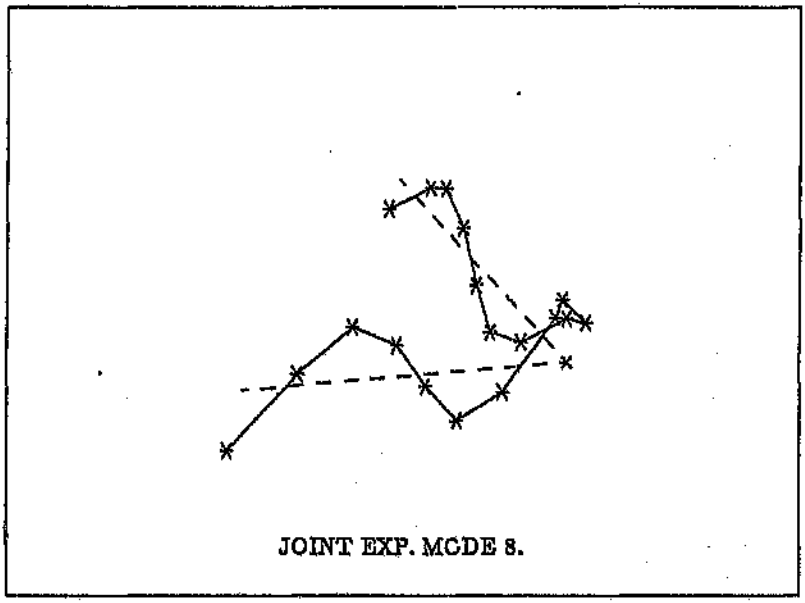

Figure E.35: Joint Mode 8

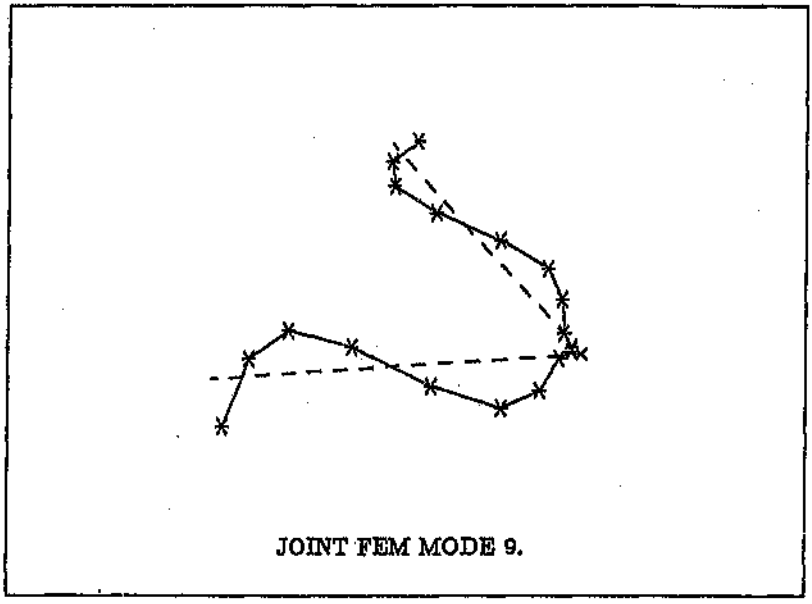

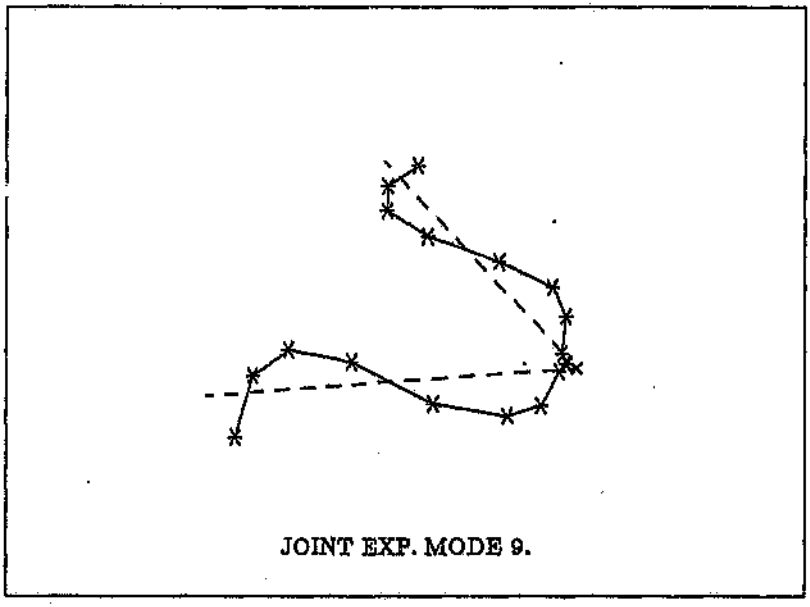

Figure E.36: Joint Mode 9